

ТОНКИЕ ХИМИЧЕСКИЕ ТЕХНОЛОГИИ

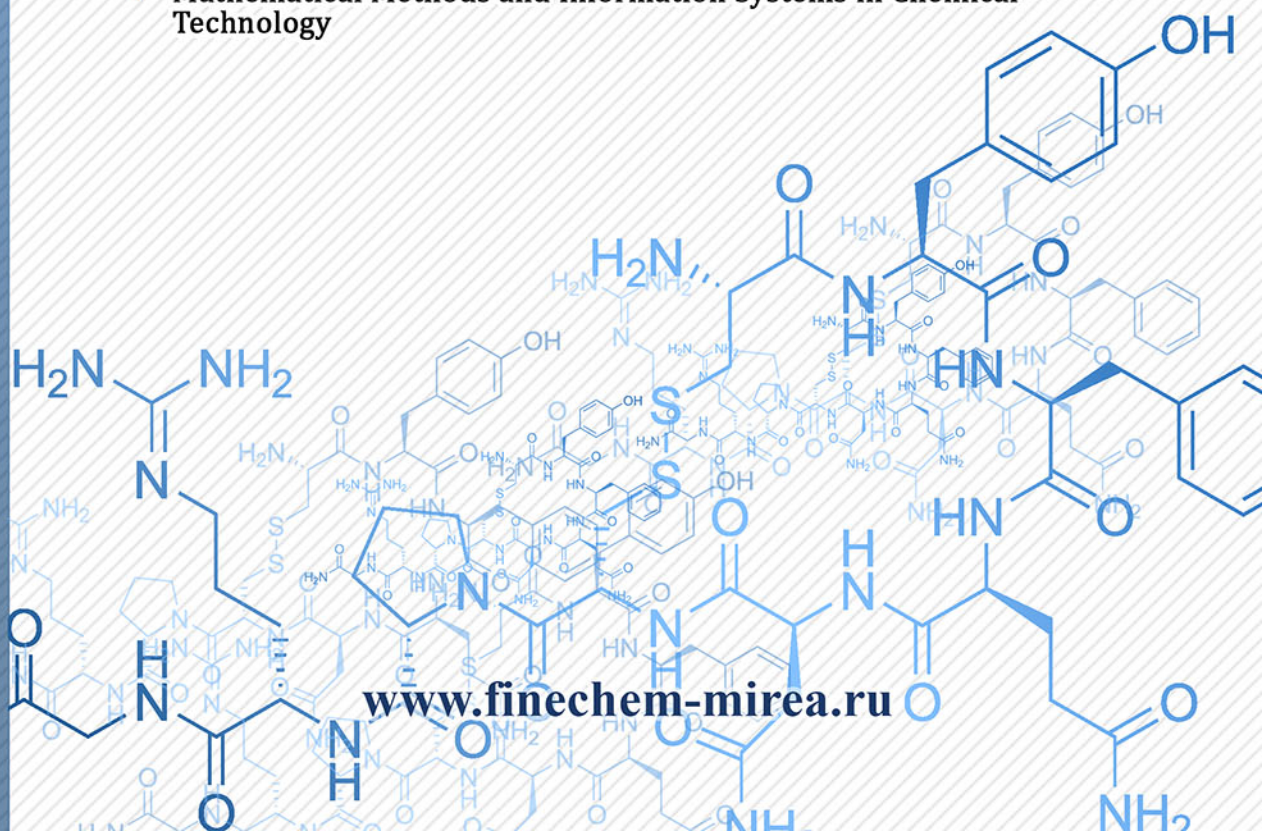
Fine Chemical Technologies

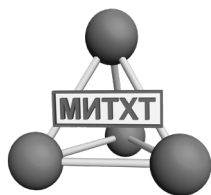
- | Theoretical Bases of Chemical Technology
- | Chemistry and Technology of Organic Substances
- | Chemistry and Technology of Medicinal Compounds and Biologically Active Substances
- | Synthesis and Processing of Polymers and Polymeric Composites
- | Chemistry and Technology of Inorganic Materials
- | Analytical Methods in Chemistry and Chemical Technology
- | Mathematical Methods and Information Systems in Chemical Technology

15(1)

2020

www.finechem-mirea.ru





ISSN 2686-7575 (Online)

ТОНКИЕ ХИМИЧЕСКИЕ ТЕХНОЛОГИИ

Fine Chemical Technologies

- | Theoretical Bases of Chemical Technology
- | Chemistry and Technology of Organic Substances
- | Chemistry and Technology of Medicinal Compounds and Biologically Active Substances
- | Synthesis and Processing of Polymers and Polymeric Composites
- | Chemistry and Technology of Inorganic Materials
- | Analytical Methods in Chemistry and Chemical Technology
- | Mathematical Methods and Information Systems in Chemical Technology

Tonkie Khimicheskie Tekhnologii =
Fine Chemical Technologies
Vol. 15, No. 1, 2020

Тонкие химические технологии =
Fine Chemical Technologies
Том 15, № 1, 2020

<https://doi.org/10.32362/2410-6593-2020-15-1>
www.finechem-mirea.ru

Tonkie Khimicheskie Tekhnologii
= Fine Chemical Technologies
2020, vol. 15, no. 1

The peer-reviewed scientific and technical journal Fine Chemical Technologies highlights the modern achievements of fundamental and applied research in the field of fine chemical technologies, including theoretical bases of chemical technology, chemistry and technology of medicinal compounds and biologically active substances, organic substances and inorganic materials, synthesis and processing of polymers and polymeric composites, analytical and mathematical methods and information systems in chemistry and chemical technology.

Founder and Publisher

Federal State Budget
Educational Institution
of Higher Education

“MIREA – Russian Technological University”
78, Vernadskogo pr., Moscow 119454, Russian Federation.

Six issues a year are published.

The journal was founded in 2006. The name was Vestnik MITHT until 2015 (ISSN 1819-1487).

The journal is included into the List of peer-reviewed science press of the State Commission for Academic Degrees and Titles of the Russian Federation.

The journal is indexed:
DOAJ, Chemical Abstracts, Science Index, RSCI,
Ulrich's International Periodicals Directory

Editor-in-Chief:

Alla K. Frolkova – Dr. of Sci. (Engineering), Professor,
MIREA – Russian Technological University, Moscow, Russian Federation. Scopus Author ID 35617659200, ResearcherID G-7001-2018, <http://orcid.org/0000-0002-9763-4717>,
frolkova@mitht.ru

Deputy Editor-in-Chief:

Valery V. Fomichev – Dr. of Sci. (Chemistry), Professor,
MIREA – Russian Technological University, Moscow, Russian Federation. Scopus Author ID 57196028937,
<http://orcid.org/0000-0003-4840-0655>,
valeryfom@rambler.ru

Editorial staff:

Managing Editor	Cand. Sci (Eng.) Galina D. Seredina
Science editors	Dr. Sci. (Chem.), Prof. Tatyana M. Buslaeva
	Dr. Sci. (Eng.), Prof. Anatolii V. Markov
Desktop publishing	Larisa G. Semernya

86, Vernadskogo pr., Moscow 119571, Russian Federation.

Phone: +7(495) 246-05-55 (#2-88)

E-mail: vestnik@mitht.ru

Registration Certificate ПИ № ФС 77–74580, issued on December 14, 2018 by the Federal Service for Supervision of Communications, Information Technology, and Mass Media of Russia

The subscription index of *Pressa Rossii*: **36924**

Тонкие химические технологии
= Fine Chemical Technologies
2020, том 15, № 1

Научно-технический рецензируемый журнал «Тонкие химические технологии» освещает современные достижения фундаментальных и прикладных исследований в области тонких химических технологий, включая теоретические основы химической технологии, химию и технологию лекарственных препаратов и биологически активных соединений, органических веществ и неорганических материалов, синтез и переработку полимеров и композитов на их основе, аналитические и математические методы и информационные системы в химии и химической технологии.

Учредитель и издатель

федеральное государственное бюджетное
образовательное учреждение
высшего образования

«МИРЭА – Российский технологический университет»
119454, РФ, Москва, пр-кт Вернадского, д. 78.

Периодичность: 6 раз в год.

Журнал основан в 2006 году. До 2015 года издавался под названием «Вестник МИТХТ» (ISSN 1819-1487).

Журнал входит в Перечень ведущих рецензируемых научных журналов ВАК РФ.

Индексируется:
DOAJ, Chemical Abstracts,
РИНЦ (Science Index), RSCI,
Ulrich's International Periodicals Directory

Главный редактор:

Фролкова Алла Константиновна – д.т.н., проф.,
МИРЭА – Российский технологический университет, Москва, Российская Федерация. Scopus Author ID 35617659200, ResearcherID G-7001-2018, <http://orcid.org/0000-0002-9763-4717>,
frolkova@mitht.ru

Заместитель главного редактора:

Фомичёв Валерий Вячеславович – д.х.н., проф.,
МИРЭА – Российский технологический университет, Москва, Российская Федерация. Scopus Author ID 57196028937,
<http://orcid.org/0000-0003-4840-0655>,
valeryfom@rambler.ru

Редакция:

Зав. редакцией	к.т.н. Г.Д. Середина
Научные редакторы	проф., д.х.н. Т.М. Буслаева
	проф., д.т.н. А.В. Марков
Компьютерная верстка	Л.Г. Семерня

119571, Москва, пр. Вернадского, 86, оф. Л-119.

Тел.: +7(495) 246-05-55 (#2-88)

E-mail: vestnik@mitht.ru

Свидетельство о регистрации СМИ: ПИ № ФС 77-74580 от 14.12.2018 г. выдано Федеральной службой по надзору в сфере связи, информационных технологий и массовых коммуникаций (Роскомнадзор)

Индекс по Объединенному каталогу «Пресса России»: **36924**

Editorial Board

Zinesh S. Abisheva – Corresponding Member of the National Academy of Sciences of Kazakhstan, Dr. Sci. (Eng.), Professor, Institute of Metallurgy and Ore Beneficiation, K.I. Satpaev Kazakh National Research Technical University, Almaty, Kazakhstan. Scopus Author ID 6601954283, ResearcherID O-8453-2017, <http://orcid.org/0000-0002-4506-0694>, abisheva_z@mail.ru.

Sergey P. Verevkin – Dr. Sci. (Eng.), Professor, University of Rostock, Rostock, Germany. Scopus Author ID 7006607848, ResearcherID G-3243-2011, Sergey.verevkin@uni-rostock.de.

Dmitry V. Drobot – Dr. Sci. (Chem.), Professor, MIREA – Russian Technological University, Moscow, Russian Federation. Scopus Author ID 35580931100, dvdrobot@mail.ru.

Konstantin Yu. Zhizhin – Corresponding Member of the Russian Academy of Sciences, Dr. Sci. (Chem.), Professor, N.S. Kurnakov Institute of General and Inorganic Chemistry of the RAS, Moscow, Russian Federation. Scopus Author ID 6701495620, ResearcherID C-5681-2013, <http://orcid.org/0000-0002-4475-124X>, kyuzhizhin@igic.ras.ru.

Igor V. Ivanov – Dr. Sci. (Chem.), Professor, MIREA – Russian Technological University, Moscow, Russian Federation. Scopus Author ID 34770109800, ResearcherID I-5606-2016, <http://orcid.org/0000-0003-0543-2067>, ivanov_i@mirea.ru.

Anatolii A. Ischenko – Dr. Sci. (Chem.), Professor, MIREA – Russian Technological University, Moscow, Russian Federation. Scopus Author ID 6701507307, aischenko@yasenevo.ru.

Carlos A. Cardona – PhD (Eng.), Professor, National University of Columbia, Manizales, Colombia. Scopus Author ID 7004278560, ResearcherID G-8554-2016, <http://orcid.org/0000-0002-0237-2313>, ccardonaal@unal.edu.co.

Oskar I. Koifman – Corresponding Member of the Russian Academy of Sciences, Dr. Sci. (Chem.), Professor, Ivanovo University of Chemical Technology, Ivanovo, Russian Federation. Scopus Author ID 6602070468, ResearcherID R-1020-2016, <http://orcid.org/0000-0002-1764-0819>, president@isuct.ru.

Valery F. Korniyushko – Dr. Sci. (Eng.), Professor, MIREA – Russian Technological University, Moscow, Russian Federation, vfk256@mail.ru.

Elvira T. Krut'ko – Dr. Sci. (Eng.), Professor, Belarusian State Technological University, Minsk, Belarus. Scopus Author ID 6602297257, ela_krutko@mail.ru.

Anatolii I. Miroshnikov – Academician of the Russian Academy of Sciences, Dr. Sci. (Chem.), Professor, M.M. Shemyakin and Yu.A. Ovchinnikov Institute of Bioorganic Chemistry of the RAS, Member of the Presidium of the RAS, Chairman of the Presidium of the RAS Pushchino Research Center, Moscow, Russian Federation. Scopus Author ID 7006592304, ResearcherID G-5017-2017, aiv@ibch.ru.

Yuri P. Miroshnikov – Dr. Sci. (Chem.), Professor, MIREA – Russian Technological University, Moscow, Russian Federation. Scopus Author ID, 6603349573, miroshnikov@mirea.ru.

Редакционная коллегия

Абишева Зинеш Садыровна – член-корр. Национальной Академии Наук Республики Казахстан, д.т.н., профессор, Институт металлургии и обогащения, Казахский национальный технический университет имени К. И. Сатпаева, Алматы, Казахстан. Scopus Author ID 6601954283, ResearcherID O-8453-2017, <http://orcid.org/0000-0002-4506-0694>, abisheva_z@mail.ru.

Верёвкин Сергей Петрович – д.т.н., профессор Университета г. Росток, Росток, Германия. Scopus Author ID 7006607848, ResearcherID G-3243-2011, Sergey.verevkin@uni-rostock.de.

Дробот Дмитрий Васильевич – д.х.н., профессор, МИРЭА – Российский технологический университет, Москва, Российская Федерация. Scopus Author ID 35580931100, dvdrobot@mail.ru.

Жижин Константин Юрьевич – член-корр. Российской академии наук, д.х.н., профессор, Институт общей и неорганической химии им. Н.С. Курнакова РАН, Москва, Российская Федерация. Scopus Author ID 6701495620, ResearcherID C-5681-2013, <http://orcid.org/0000-0002-4475-124X>, kyuzhizhin@igic.ras.ru.

Иванов Игорь Владимирович – д.х.н., профессор, МИРЭА – Российский технологический университет, Москва, Российская Федерация. Scopus Author ID 34770109800, ResearcherID I-5606-2016, <http://orcid.org/0000-0003-0543-2067>, ivanov_i@mirea.ru.

Ищенко Анатолий Александрович – д.х.н., профессор, МИРЭА – Российский технологический университет, Москва, Российская Федерация. Scopus Author ID 6701507307, aischenko@yasenevo.ru.

Кардона Карлос Ариэль – профессор Национального университета Колумбии, Манизалес, Колумбия. Scopus Author ID 7004278560, ResearcherID G-8554-2016, <http://orcid.org/0000-0002-0237-2313>, ccardonaal@unal.edu.co.

Койфман Оскар Иосифович – член-корр. Российской академии наук, д.х.н., профессор, Ивановский химико-технологический университет, Иваново, Российская Федерация. Scopus Author ID 6602070468, ResearcherID R-1020-2016, <http://orcid.org/0000-0002-1764-0819>, president@isuct.ru.

Корнюшко Валерий Федорович – д.т.н., профессор, МИРЭА – Российский технологический университет, Москва, Российская Федерация, vfk256@mail.ru.

Крутько Эльвира Тихоновна – д.т.н., профессор Белорусского государственного технологического университета, Минск, Беларусь. Scopus Author ID 6602297257, ela_krutko@mail.ru.

Мирошников Анатолий Иванович – академик Российской академии наук, д.х.н., профессор, Институт биоорганической химии им. академиков М.М. Шемякина и Ю.А. Овчинникова РАН, член Президиума РАН, председатель Президиума Пушкинского научного центра РАН, Москва, Российская Федерация. Scopus Author ID 7006592304, ResearcherID G-5017-2017, aiv@ibch.ru.

Мирошников Юрий Петрович – д.х.н., профессор, МИРЭА – Российский технологический университет, Москва, Российская Федерация. Scopus Author ID 6603349573, miroshnikov@mirea.ru.

Aziz M. Muzafarov – Academician of the Russian Academy of Sciences, Dr. Sci. (Chem.), Professor, A.N. Nesmeyanov Institute of Organoelement Compounds of the RAS, Moscow, Russian Federation. ResearcherID G-1644-2011, <https://orcid.org/0000-0002-3050-3253>, aziz@ineos.ac.ru.

Ivan A. Novakov – Academician of the Russian Academy of Sciences, Dr. Sci. (Chem.), Professor, Volgograd State Technical University, Volgograd, Russian Federation. Scopus Author ID 7003436556, ResearcherID I-4668-2015, <http://orcid.org/0000-0002-0980-6591>, president@vstu.ru.

Alexander N. Ozerin – Corresponding Member of the Russian Academy of Sciences, Dr. Sci. (Chem.), Professor, Enikolopov Institute of Synthetic Polymeric Materials of the RAS, Moscow, Russian Federation. Scopus Author ID 7006188944, ResearcherID J-1866-2018, <https://orcid.org/0000-0001-7505-6090>, ozerin@ispm.ru.

Tapani A. Pakkanen – PhD, Professor, Head of Department of Chemistry, University of Eastern Finland, Joensuu, Finland. Scopus Author ID 7102310323, tapani.pakkanen@uef.fi.

Armando J.L. Pombeiro – Academician of the Academy of Sciences of Lisbon, PhD, Professor, Higher Technical Institute of the University of Lisbon, Lisbon, Portugal. Scopus Author ID 7006067269; ResearcherID I-5945-2012, <https://orcid.org/0000-0001-8323-888X>, pombeiro@ist.utl.pt.

Dmitrii V. Pyshnyi – Corresponding Member of the Russian Academy of Sciences, Dr. Sci. (Chem.), Professor, Institute of Chemical Biology and Fundamental Medicine, Siberian Branch of the Russian Academy of Sciences, Novosibirsk, Russian Federation. Scopus Author ID 7006677629, ResearcherID F-4729-2013, <https://orcid.org/0000-0002-2587-3719>, pyshnyi@niboch.nsc.ru.

Alexander S. Sigov – Academician of the Russian Academy of Sciences, Dr. Sci. (Phys. and Math.), Professor, President of MIREA – Russian Technological University, Moscow, Russian Federation. Scopus Author ID 35557510600, ResearcherID L-4103-2017, sigov@mirea.ru.

Vladimir A. Tverskoy – Dr. Sci. (Chem.), Professor, MIREA – Russian Technological University, Moscow, Russian Federation. Scopus Author ID 6604012434, 29567701900, ResearcherID H-8042-2017, <https://orcid.org/0000-0003-4348-8854>, tverskoy@mitht.ru.

Alexander M. Toikka – Dr. Sci. (Chem.), Professor, Institute of Chemistry, Saint Petersburg State University, St. Petersburg, Russian Federation. Scopus Author ID 6603464176, ResearcherID A-5698-2010, <http://orcid.org/0000-0002-1863-5528>, a.toikka@spbu.ru.

Andrzej W. Trochimczuk – Dr. Sci. (Chem.), Professor, Faculty of Chemistry, Wrocław University of Science and Technology, Wrocław, Poland. Scopus Author ID 7003604847, andrzej.trochimczuk@pwr.edu.pl.

Aslan Yu. Tsivadze – Academician of the Russian Academy of Sciences, Dr. Sci. (Chem.), Professor, A.N. Frumkin Institute of Physical Chemistry and Electrochemistry of the RAS, Moscow, Russian Federation. Scopus Author ID 7004245066, ResearcherID G-7422-2014, tsiv@phyche.ac.ru.

Музафаров Азиз Мансурович – академик Российской академии наук, д.х.н., профессор, Институт элементоорганических соединений им. А.Н. Несмеянова РАН, Москва, Российская Федерация. ResearcherID G-1644-2011, <https://orcid.org/0000-0002-3050-3253>, aziz@ineos.ac.ru.

Новиков Иван Александрович – академик Российской академии наук, д.х.н., профессор, президент Волгоградского государственного технического университета, Волгоград, Российская Федерация. Scopus Author ID 7003436556, ResearcherID I-4668-2015, <http://orcid.org/0000-0002-0980-6591>, president@vstu.ru.

Озерин Александр Никифорович – член-корр. Российской академии наук, д.х.н., профессор, Институт синтетических полимерных материалов им. Н.С. Ениколопова РАН, Москва, Российская Федерация. Scopus Author ID 7006188944, ResearcherID J-1866-2018, <https://orcid.org/0000-0001-7505-6090>, ozerin@ispm.ru.

Пакканен Тапани – PhD, профессор, руководитель Департамента химии Университета Восточной Финляндии, Йоенсуу, Финляндия. Scopus Author ID 7102310323, tapani.pakkanen@uef.fi.

Помбейро Армандо – академик АН Лиссабона, PhD, профессор, президент Центра структурной химии Высшего технического института Университета Лиссабона, Португалия. Scopus Author ID 7006067269; ResearcherID I-5945-2012, <https://orcid.org/0000-0001-8323-888X>, pombeiro@ist.utl.pt.

Пышный Дмитрий Владимирович – член-корр. Российской академии наук, д.х.н., профессор, Институт химической биологии и фундаментальной медицины Сибирского отделения РАН, Новосибирск, Российская Федерация. Scopus Author ID 7006677629, ResearcherID F-4729-2013, <https://orcid.org/0000-0002-2587-3719>, pyshnyi@niboch.nsc.ru.

Сигов Александр Сергеевич – академик Российской академии наук, д.ф.-м.н., профессор, президент МИРЭА – Российского технологического университета, Москва, Российская Федерация. Scopus Author ID 35557510600, ResearcherID L-4103-2017, sigov@mirea.ru.

Тверской Владимир Аркадьевич – д.х.н., профессор, МИРЭА – Российский технологический университет, Москва, Российская Федерация. Scopus Author ID 6604012434, 29567701900, ResearcherID H-8042-2017, <https://orcid.org/0000-0003-4348-8854>, tverskoy@mitht.ru.

Тойкка Александр Матвеевич – д.х.н., профессор, Институт химии, Санкт-Петербургский государственный университет, Санкт-Петербург, Российская Федерация. Scopus Author ID 6603464176, ResearcherID A-5698-2010, <http://orcid.org/0000-0002-1863-5528>, a.toikka@spbu.ru.

Трохимчук Андржей – д.х.н., профессор, Химический факультет Вроцлавского политехнического университета, Вроцлав, Польша. Scopus Author ID 7003604847, andrzej.trochimczuk@pwr.edu.pl.

Цивадзе Аслан Юсупович – академик Российской академии наук, д.х.н., профессор, Институт физической химии и электрохимии им. А.Н. Фрумкина РАН, Москва, Российская Федерация. Scopus Author ID 7004245066, ResearcherID G-7422-2014, tsiv@phyche.ac.ru.

CONTENTS

Review Articles

*Mikheev A.A., Shmendel E.V., Zhestovskaya E.S.,
Nazarov G.V., Maslov M.A.*

Cationic liposomes as delivery systems
for nucleic acids

**Theoretical Bases of Chemical
Technology**

Blokhin A.V., Yurkshtovich Y.N.
Thermodynamic properties of L-menthol
in crystalline and gaseous states

*Rodin S.S., Zotov Yu.L., Moroshkin V.Yu.,
Fedyanov E.A., Shishkin E.V.*
Improvement of high-viscosity oil production
technology via the effective redistribution
of energy resources

Toro L.A.
Drawing PT-phase envelopes and calculating
critical points for multicomponent systems
using flash calculations

**Chemistry and Technology
of Organic Substances**

*Sulimov A.V., Ovcharova A.V., Kravchenko G.M.,
Sulimova Yu.K.*

Investigation of propylene carbonate synthesis
regularities by the interaction of propylene glycol
with carbamide

СОДЕРЖАНИЕ

Обзорные статьи

- 7 *Михеев А.А., Шмендель Е.В.,
Жестовская Е.С., Назаров Г.В., Маслов М.А.*
Катионные липосомы как средства доставки
нуклеиновых кислот

**Теоретические основы
химической технологии**

- 28 *Блохин А.В., Юркиштович Я.Н.*
Термодинамические свойства L-ментола
в кристаллическом и газообразном состояниях
- 37 *Родин С.С., Зотов Ю.Л., Морошкин В.Ю.,
Федянов Е.А., Шишкин Е.В.*
Совершенствование технологии получения
высоковязких масел с помощью эффективного
перераспределения энергетических ресурсов
- 46 *Toro L.A.*
Drawing PT-phase envelopes and calculating
critical points for multicomponent systems
using flash calculations

**Химия и технология органических
веществ**

- 55 *Сулимов А.В., Овчарова А.В., Кравченко Г.М.,
Сулимова Ю.К.*
Изучение закономерностей синтеза
пропиленкарбоната взаимодействием
пропиленгликоля с карбамидом

Synthesis and Processing of Polymers and Polymeric Composites

*Nguyen C.N., Sanyarova M.V.,
Simonov-Emel'yanov I.D.*

Calculating the composition
of dispersion-filled polymer composite materials
of various structures

Analytical Methods in Chemistry and Chemical Technology

Karpova A.S.

Development of a nasal spray containing aminocaproic
acid and a copolymer of *N*-vinylpyrrolidone
and 2-methyl-5-vinylpyridine for use in the prevention
of influenza and other viral respiratory infections

*Kostoev R.K., Tochiev D.S., Nilkho E.I., Sultigova
Z.H., Archakova R.D., Temirkhanov B.A.,
Uzhakhova L.Ya.*

Application of the mercury porosimetry method
in the analysis of sorption materials

Синтез и переработка полимеров и композитов на их основе

*Нгуен Ч.Н., Саньярова М.В.,
Симонов-Емельянов И.Д.*

- 62 Расчет составов дисперсных наполненных
полимерных композиционных материалов
с разной структурой

Аналитические методы в химии и химической технологии

Карпова А.С.

- 67 Создание назального спрея на основе
аминокапроновой кислоты и сополимера
N-винилпирролидона и 2-метил-5-винилпиридина
для профилактики гриппа и ОРВИ

*Костоев Р.К., Точиев Д.С., Нилхо Э.И.,
Султыгова З.Х., Арчакова Р.Д., Темирханов Б.А.,
Ужахова Л.Я.*

- 76 Применение метода ртутной порозиметрии
в анализе сорбционных материалов

ISSN 2686-7575 (Online)

<https://doi.org/10.32362/2410-6593-2020-15-1-7-27>

UDC 577.1:577.352.3:547.963.32



Cationic liposomes as delivery systems for nucleic acids

Aleksey A. Mikheev¹, Elena V. Shmendel², Elizaveta S. Zhestovskaya¹,
Georgy V. Nazarov¹, Mikhail A. Maslov^{2,@}

¹Scientific Center "Signal," Moscow, 107014 Russia

²MIREA – Russian Technological University (M.V. Lomonosov Institute of Fine Chemical Technologies), Moscow 119571, Russia

@Corresponding author, e-mail: mamaslov@mail.ru

Objectives. Gene therapy is based on the introduction of genetic material into cells, tissues, or organs for the treatment of hereditary or acquired diseases. A key factor in the success of gene therapy is the development of delivery systems that can efficiently transfer genetic material to the place of their therapeutic action without causing any associated side effects. Over the past 10 years, significant effort has been directed toward creating more efficient and biocompatible vectors capable of transferring nucleic acids (NAs) into cells without inducing an immune response. Cationic liposomes are among the most versatile tools for delivering NAs into cells; however, the use of liposomes for gene therapy is limited by their low specificity. This is due to the presence of various biological barriers to the complex of liposomes with NA, including instability in biological fluids, interaction with serum proteins, plasma and nuclear membranes, and endosomal degradation. This review summarizes the results of research in recent years on the development of cationic liposomes that are effective *in vitro* and *in vivo*. Particular attention is paid to the individual structural elements of cationic liposomes that determine the transfection efficiency and cytotoxicity. The purpose of this review was to provide a theoretical justification of the most promising choice of cationic liposomes for the delivery of NAs into eukaryotic cells and study the effect of the composition of cationic lipids (CLs) on the transfection efficiency *in vitro*.

Results. As a result of the analysis of the related literature, it can be argued that one of the most promising delivery systems of NAs is CL based on cholesterol and spermine with the addition of a helper lipid DOPE. In addition, it was found that varying the composition of cationic liposomes, the ratio of CL to NA, or the size and zeta potential of liposomes has a significant effect on the transfection efficiency.

Conclusions. Further studies in this direction should include optimization of the conditions for obtaining cationic liposomes, taking into account the physicochemical properties and established laws. It is necessary to identify mechanisms that increase the efficiency of NA delivery *in vitro* by searching for optimal structures of cationic liposomes, determining the ratio of lipoplex components, and studying the delivery efficiency and properties of multicomponent liposomes.

Keywords: liposomes, nucleic acids, gene therapy, lipids, delivery.

For citation: Mikheev A.A., Shmendel E.V., Zhestovskaya E.S., Nazarov G.V., Maslov M.A. Cationic liposomes as delivery systems for nucleic acids. *Tonk. Khim. Tekhnol. = Fine Chem. Technol.* 2020;15(1):7-27. <https://doi.org/10.32362/2410-6593-2020-15-1-7-27>

Катионные липосомы как средства доставки нуклеиновых кислот

А.А. Михеев¹, Е.В. Шмендель², Е.С. Жестовская¹, Г.В. Назаров¹, М.А. Маслов^{2,@}

¹Научный центр «Сигнал», Москва, 107014 Россия

²МИРЭА – Российский технологический университет (Институт тонких химических технологий имени М.В. Ломоносова), Москва, 119571 Россия

@Автор для переписки, e-mail: mamaslov@mail.ru

Цели. Генная терапия основана на введении генетического материала в клетки, ткани или органы с целью лечения наследственных или приобретенных заболеваний. Ключевым фактором успеха генной терапии является развитие систем доставки, способных эффективно переносить генетический материал к месту их терапевтического действия, не вызывая каких-либо связанных с ними побочных эффектов. За последнее десятилетие много усилий было направлено на создание более эффективных и биосовместимых векторов, способных переносить нуклеиновые кислоты в клетки, не вызывая иммунного ответа. Катионные липосомы являются одним из самых универсальных инструментов для доставки нуклеиновых кислот в клетки, однако применение липосом для целей генной терапии ограничено неспецифичностью такой доставки. Это связано с наличием различных биологических барьеров на пути комплекса липосом с нуклеиновыми кислотами; например, с нестабильностью в биологических жидкостях; взаимодействиями с белками сыворотки крови, плазматической и ядерной мембранами; а также с эндосомной деградацией. В этом обзоре обобщены результаты исследований за последние годы по разработкам катионных липосом, эффективных *in vitro* и *in vivo*. Особое внимание уделено отдельным структурным элементам катионных липосом, определяющим эффективность трансфекции и цитотоксичность. Целью данного обзора являлось теоретическое обоснование выбора катионных липосом, наиболее перспективных для доставки нуклеиновых кислот в эукариотические клетки, а также изучение влияния состава катионных липидов на эффективность трансфекции *in vitro*.

Результаты. В результате проведенного анализа литературы можно утверждать, что одними из наиболее перспективных систем доставки нуклеиновых кислот являются катионные липиды на основе холестерина и спермина с добавлением липида-хелпера DOPE. Кроме того, было установлено, что варьирование состава катионных липосом, соотношения катионных липидов и нуклеиновых кислот, а также размера и дзета-потенциала липосом оказывают значительное влияние на эффективность трансфекции.

Выводы. Дальнейшие исследования в данном направлении должны включать в себя оптимизацию условий получения катионных липосом с учетом установленных закономерностей, а также физико-химических свойств. Необходимо исследовать возможности повышения эффективности доставки нуклеиновых кислот путем поиска оптимальных структур катионных липосом, определения соотношения компонентов липоплексом и изучения свойств и эффективности доставки многокомпонентных липосом *in vitro*.

Ключевые слова: липосомы, нуклеиновые кислоты, генная терапия, липиды, доставка.

Для цитирования: Михеев А.А., Шмендель Е.В., Жестовская Е.С., Назаров Г.В., Маслов М.А. Катионные липосомы как средства доставки нуклеиновых кислот. *Тонкие химические технологии*. 2020;15(1):7-27. <https://doi.org/10.32362/2410-6593-2020-15-1-7-27>

INTRODUCTION

Gene therapy is one of the more promising methods for the treatment of a wide range of diseases. This method is based on the administration of therapeutic nucleic acids (NA) into the organism, which results in either the expression of the genetic construction or the partial/complete suppression of the defective

gene [1]. Unlike drug compounds of low molecular weight whose therapeutic effect is based on binding to target proteins, therapeutic NAs could regulate the expression of specific genes by controlling the expression levels of functional proteins.

Therapeutic NAs include small interfering RNAs (siRNA), antisense, antigenic or immunostimulatory oligodeoxynucleotides (ODNs), plasmid DNA

(pDNA), and ribozymes. One of the first NAs considered as an object of cargo delivery was pDNA [2].

The low efficiency of NA delivery into target cells and the need to create conditions for their long-term functioning are the main challenges associated with gene therapy [1–3]. The therapeutic effect of NA molecules is determined by their physicochemical properties to a much greater extent than that of low molecular weight compounds. Thus, NAs are negatively charged, can be degraded by serum nucleases, and are rapidly excreted by the kidneys [4–6]. Eukaryotic cells do not have a specialized pathway for the uptake of NA. In this regard, there are many limitations to the use of NA as drugs, including low stability, short half-life, and low delivery efficiency. To address these issues, the development of effective systems for the delivery of NA into eukaryotic cells is essential.

The vast majority of studies on the systemic delivery of NA into cells use viral vectors (retroviruses, lentiviruses, adenoviruses, and adeno-associated viruses), which are characterized by a high transfection efficiency (TE) of cells and provide a high level of gene expression [7–9]. However, these vectors have a number of disadvantages: carcinogenicity [10], immunogenicity [11], tropism for a wide range of cells [12], and difficult production [13]. In addition, some viral systems are rapidly cleared from the organism [14].

The use of nonviral vectors, such as liposomes, polymers, and dendrimers, for the delivery of NA addresses some of the problems mentioned above because they have low immunogenicity and usually do not cause an immune response [15]. The absence of limitations on the size of transferred therapeutic NA, the simplicity of synthesis, and the possibility of modifying the structure make nonviral vectors a promising NA delivery system [16, 17]. The biggest limitation to the use of nonviral vectors is the low TE. One potential solution to this problem is the use of liposomes as nonviral vectors because of their diverse morphology, composition, and ability to include various therapeutic biomolecules.

Liposomes based on cationic lipids (CLs) have attracted particular attention as nonviral delivery systems. By adjusting the surface charge of liposomes by changing the lipid composition, one can control the degree of interaction of liposomes with negatively charged NAs. Liposomes consisting of CLs are biodegradable because endogenous enzymes are capable of breaking down the lipid components of liposomes after being administered into the body. Furthermore, the surface of cationic liposomes can be modified by the addition of polyethylene glycol residues or targeted ligands [18, 19], and the incorporation of lipophilic chemotherapeutic drugs in the lipid bilayer can ensure the co-delivery of the drug and therapeutic NA [20, 21].

The formation of lipoplexes, which are complexes of negatively charged NAs and positively charged lipids/liposomes, occurs as a result of electrostatic interactions. The size of the formed lipoplexes mainly depends on the type of CL used and the quantitative ratio of positively charged CL nitrogen atoms and negatively charged NA phosphate groups (N/P ratio). By modifying the conditions for producing lipoplexes (NA concentration, pH, and the composition of the buffer solution), their size can also be controlled. As a rule, lipoplexes are formed, with a slight excess of a positive charge so that they can interact with negatively charged components of the cell membrane.

EXTRACELLULAR AND INTRACELLULAR BARRIERS

Most lipoplexes undergo structural changes and can be broken down by endogenous factors *in vivo* due to the presence of a number of extracellular (interactions with blood components, endothelial barriers, and cell membrane) and intracellular (cell uptake, release from endosomes, intracellular transfer, and delivery to the nucleus) barriers [22, 23].

The interaction of lipoplexes with blood components plays a significant role in their biological distribution [24–26] and can provoke the rapid elimination of lipoplexes from the bloodstream due to the reticuloendothelial system of the body and being captured by tissue macrophages [27]. It is known that serum proteins, such as albumin and high- and low-density lipoproteins, can bind to the surface of lipoplexes. In addition, the balance of adsorbed opsonins, which are differently recognized by receptors on the surface of macrophages, affects the clearance of lipoplexes [28–30]. The positive charge of lipoplexes activates the complement system, which accelerates the process of their elimination [31]. In general, larger lipoplexes are more rapidly excreted from the body compared with smaller particles [32].

It was shown that the absorption of cationic liposome–siRNA complexes can lead to the activation of innate immunity [33–35] by acting on RNA-sensitive Toll-like receptors and inducing inflammatory cytokines; in this case, a response occurs in the interferon production [35]. An immune response can also be caused by cationic liposomes themselves, even in the absence of siRNAs [36].

Lipoplexes that avoid clearance are delivered to the target tissue, but an endothelial barrier arises in their path. The endothelial barrier is a dense network of intracellular matrix that blocks the diffusion of liposome–NA complexes into target cells [37].

It is generally accepted that the penetration of lipoplexes through the cell membrane is due to the electrostatic interaction between the CL of lipoplexes and the negatively charged surface of the cell [38]. Endocytosis is the most common pathway for lipoplex

uptake and includes many mechanisms, such as clathrin- and caveolin-mediated endocytosis, macropinocytosis, and clathrin- and caveolin-independent pathways. An additional mechanism of lipoplex uptake, phagocytosis, only occurs in specialized cells, such as macrophages and dendritic cells [38]. The “choice” of the uptake mechanism is determined by the size of the absorbed lipoplexes, the type of transfected cells, and the composition of cationic liposomes.

After penetration into the cells, an important step in the transport pathway of lipoplexes is their escape from endosomes. There are several mechanisms for the release of NAs. Advantageously, monocationic lipid-based liposomes release their contents into the cytosol via lipid mixing. The basis of this mechanism is the fusion of lipoplex and endosome membranes, while CLs stimulate the translocation of negatively charged phospholipids of the membrane to the inner surface of endosomes. As a result, endosomal membrane destabilization and NA release into the cytoplasm occur [39]. Of note, the presence of special helper lipids in the composition of liposomes (see Section “Helper Lipids”) promotes the fusion of lipoplexes with the endosomal membrane and its destabilization.

The second mechanism of NA release from lipoplexes is called the “proton sponge effect.” It is characteristic of CLs containing a large number of secondary or tertiary amino groups, which have pKa values between physiological and lysosomal pH (usually from 5.5 to 6). When the medium is acidified inside the endosomes, the amino groups of CLs are protonated, which contributes to an additional influx of unbound chloride anions. To compensate for the increase in anions, additional water molecules enter the endosomes, causing osmotic swelling and rupture [39].

After their release from endosomes and entering the cytoplasm, NAs need to be delivered to the target compartment of the cell to achieve the desired biological effect. For NAs whose activity is in the cytoplasm, such as ODNs and siRNAs, this barrier is not important, but for pDNA, the target compartment is the nucleus. The mobility of large molecules, such as pDNA, in the cytoplasm is extremely low, which makes them susceptible to degradation by cytoplasmic nucleases [40].

The determining factors for the movement speed of pDNA through the cytoplasm are the size and structure of the pDNA molecule; cyclic pDNA moves faster than linear pDNA [41]. The effect of pDNA packing density on delivery efficiency is not well understood. However, tight packing increases the mobility and resistance of pDNA to cytoplasmic nucleases.

Finally, the expression of pDNA requires overcoming the last intracellular barrier, which is the nuclear membrane. During cell division, pDNA can

penetrate the nucleus due to a transient loss of the integrity of the nuclear membrane; however, in nondividing cells, pDNAs pass through the membrane through a nuclear pore complex that can transfer molecules up to 9 nm in size and weighing less than 40 kDa by free diffusion [42]. The incorporation of peptide sequences termed nuclear localization signals into the composition of lipoplexes promotes a more efficient transfer of pDNA across the nuclear membrane [39].

Thus, when transfecting cells with lipoplexes, it is necessary to take into account not only their characteristics but also the existence of extracellular and intracellular barriers.

CATIONIC LIPIDS

Among nonviral vectors, the use of cationic liposomes as an NA delivery system has attracted the attention of drug developers owing to their obvious advantages, such as their ease of preparation, reproducibility, biodegradability, and commercial availability [43]. The main structural components of liposomes are CLs, which are amphiphilic molecules that can be easily obtained during chemical synthesis and used to study the relationship between structure and TE.

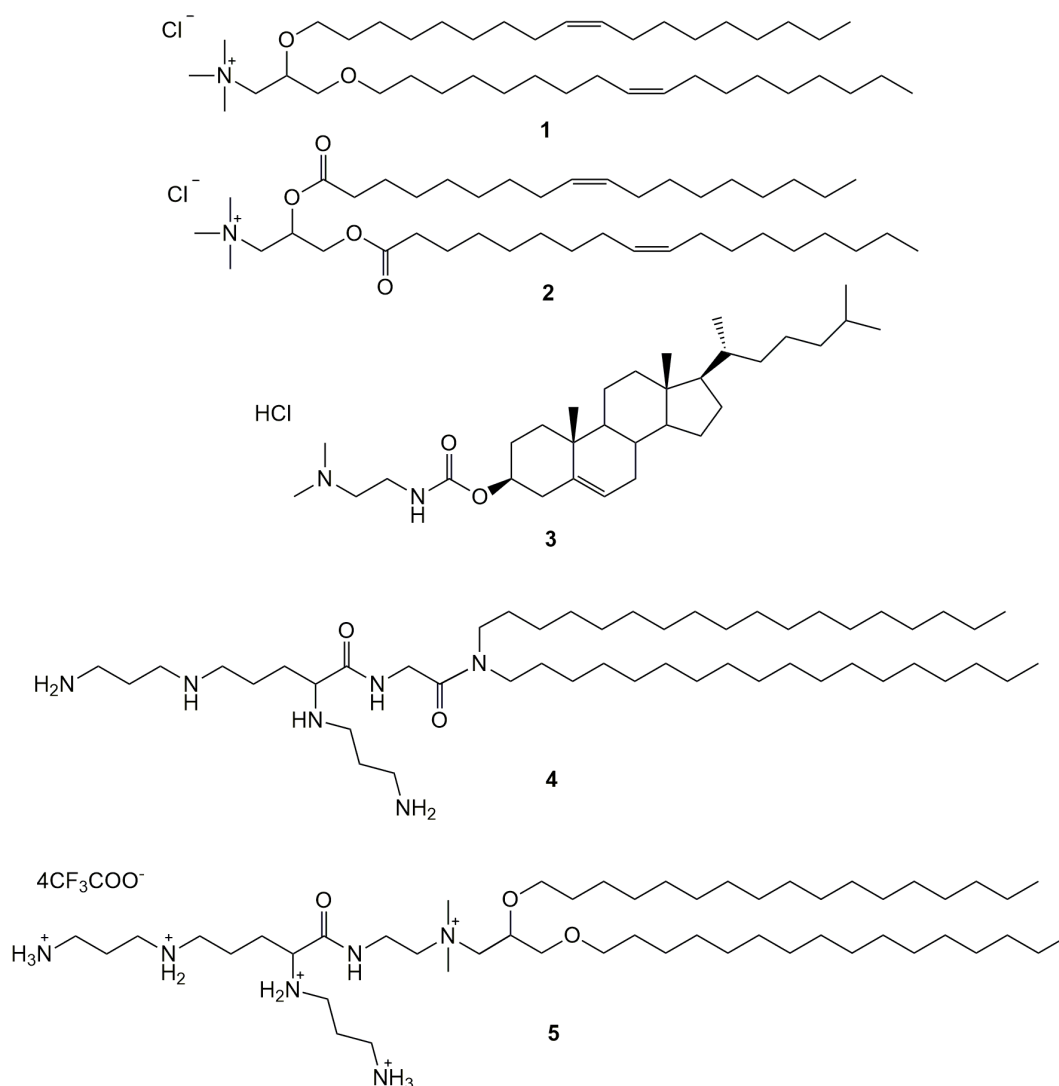
Among CLs for the construction of cationic liposomes, the most widely used are *N*-(1-(2,3-dioleoyloxy)propyl)-*N,N,N*-trimethylammonium chloride (**1**, DOTMA) [17], *N*-[1-(2,3-dioleoyloxy)propyl]-*N,N,N*-trimethylammonium chloride (**2**, DOTAP) [17], 3 β -[*N*-(*N'*,*N'*-dimethylaminoethyl)carbamoyl]cholesterol hydrochloride (**3**, DC-Chol) [8], dioctadecylamidoglycyl spermine (**4**, DOGS) [3], and 2,3-dioleoyloxy-*N*-[2-(sperminecarboxamido)ethyl]-*N,N*-dimethyl-1-propylammonium tetrafluoroacetate (**5**, DOSPA) [3].

CLs consist of four main structural units:

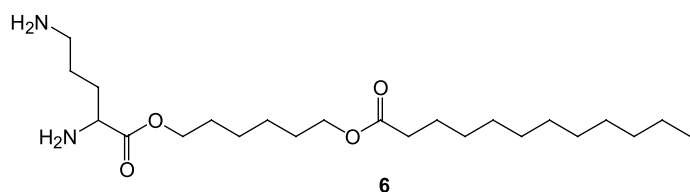
- Hydrophilic cationic group (HCG);
- Spacer group (SG);
- Linker group (LG);
- Hydrophobic domain (HD).

The cationic nature of a lipid is determined by the structure of its hydrophilic group, which is formed by primary, secondary, tertiary amines, quaternary ammonium groups, amino acids, short peptides, or heterocyclic bases [43]. It has been experimentally demonstrated that CLs based on quaternary ammonium salts are more toxic compared with analogs containing tertiary amino groups [44]. For the binding and delivery of NA, CLs containing charged phosphorus or arsenic atoms can be used, which increases the TE and decreases toxicity [45].

The hydrophobic CL domain is most often formed by long-chain hydrocarbon substituents (from 12 to 20 carbon atoms) or cholesterol. It was found that CL with a single hydrocarbon chain exhibited greater



toxicity and a lower TE compared with CL with two chains [46]. However, it was shown that compound **6**, containing one dodecanoic acid residue as the HD, was not only more effective but also less toxic than DOTAP (**2**) [47]. Given the different dependence of TE and CL toxicity, as well as the structure of their HDs, the HD should be specifically selected.



The LG (ester, ether, carbamoyl, or disulfide) binds to the HD and HCG and determines the stability and biodegradability of CL, which also affects the TE. DOTMA (**1**) with an ether linker exhibits a high TE but is too stable to be biodegraded in the body, which explains its high toxicity. Lipids with ester linkers,

such as compound **2**, are more readily biodegradable after systemic administration [48]. When using a carbamoyl bond as a linker (lipid **3**), a decrease in pH will trigger the separation of the hydrophobic and hydrophilic parts of CL and, thus, promote the release of NA after penetration into the cell and endosomal uptake [49, 50]. Compounds containing disulfide bonds sensitive to the action of reducing agents as an LG are stable in the bloodstream but are broken down after penetration into the cytosol by the action of glutathione and/or reductases, which can be used to improve the TE [51]. However, the presence of a disulfide bond as an LG in compound **7** led to a complete loss of luciferase gene expression in HepG2 and HeLa cells [52].

The SG (glycerin, amino acids, oligomethylene groups, and polyethylene glycols) separates the HD and HCG. The length of the SG affects the toxicity and TE of cationic liposomes. For example, for CL **8** based on cholesterol, an increase in the length of the SG to three carbon atoms decreases the cytotoxicity of CL *in vitro* and *in vivo* [53].

When using spacers of the same length, but an HCG with a different structure, it was shown that the replacement of the methyl group in compound **9** with the ethyl in compound **10** increased both the toxicity and TE *in vitro* [53].

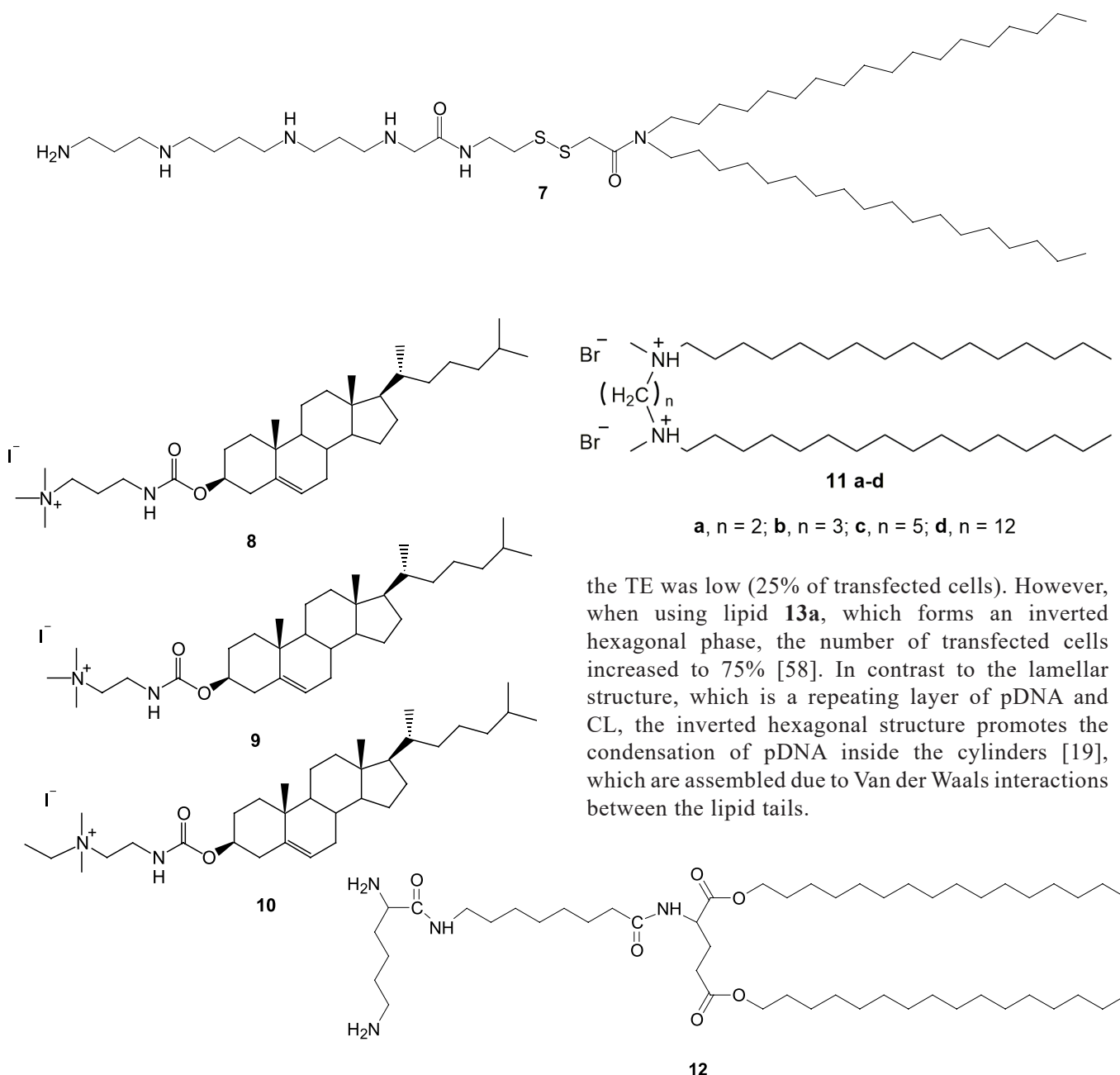
Cationic gemini amphiphiles **11a,b** with short SGs exhibited an increased TE compared with their analogs **11c,d** with long spacers [54].

In addition to length, the hydrophobicity of SGs plays an important role in the delivery of NA. When comparing the TE of CL based liposomes with hydrophobic oligomethylene spacers ($n = 3, 5, 7, 11$) and a hydrophilic trioxyethylene spacer, the maximum expression level was achieved using lipid **12** with a heptamethylene spacer [55].

HELPER LIPIDS

Cationic liposomes can form only from one CL; however, the addition of a neutral helper lipid to their composition can increase the TE [56]. Among the helper lipids, 1,2-dioleoyl-*sn*-glycero-3-phosphoethanolamine (**13a**, DOPE) [19] and phosphatidylcholine (**14**, PC) are the most widely used [57].

Two different helper lipids **13a** (DOPE) and 1,2-dipalmitoyl-*sn*-glycero-3-phosphoethanolamine (**13b**, DPPE) were used as component liposomes to study the efficiency of the endosomal release of NA into the cytosol and its further transport to the nucleus. In the case of helper lipid **13b**, which promotes the formation of lipoplexes with a lamellar structure,



the TE was low (25% of transfected cells). However, when using lipid **13a**, which forms an inverted hexagonal phase, the number of transfected cells increased to 75% [58]. In contrast to the lamellar structure, which is a repeating layer of pDNA and CL, the inverted hexagonal structure promotes the condensation of pDNA inside the cylinders [19], which are assembled due to Van der Waals interactions between the lipid tails.

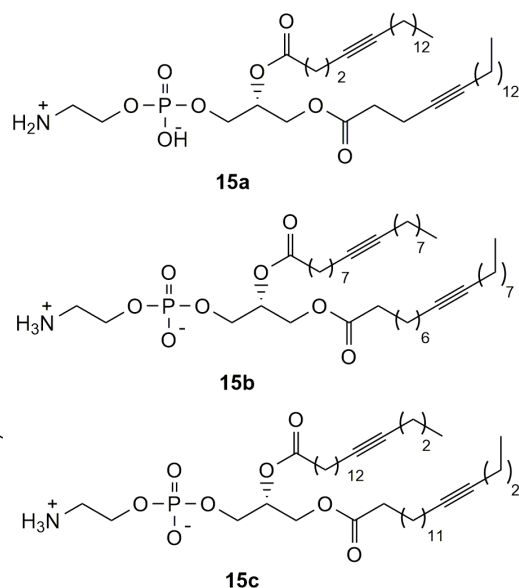
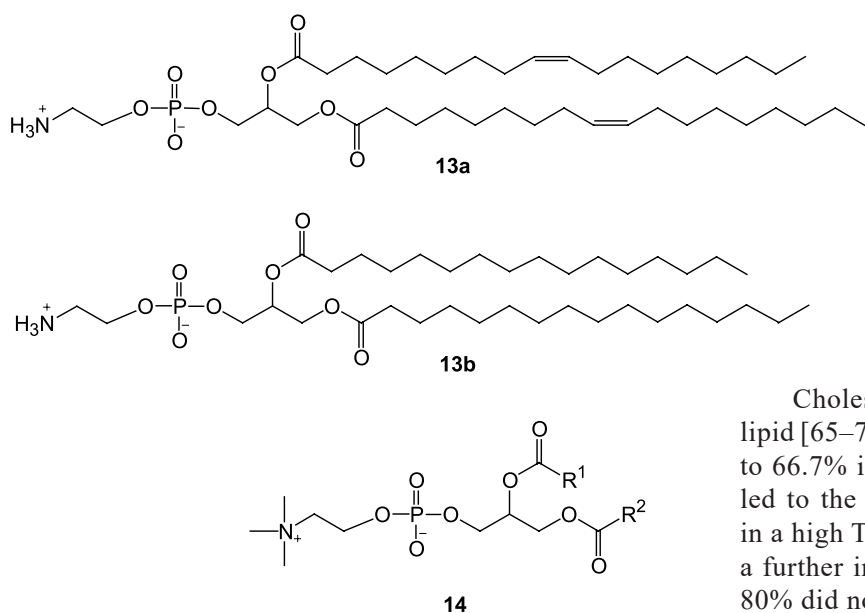
The use of DOPE as a helper lipid in various cationic liposomes increases the TE of numerous cell lines [19, 56, 59], because under the conditions of endosomal acidification, it can form an inverted hexagonal phase with a decrease in pH and thereby destabilize the endosomal membrane. Thus, a study of micelles formed by DOPE revealed that with a decrease in pH from 10.8 to 7.0, the transition of spherical micelles to hexagonal packed cylinders occurred [60]. The optimal range for this transition is a pH value from 9 to 7. This transition is associated with the zwitterionic nature of the DOPE polar head group. At high pH values, the phosphate group is negatively charged, which causes the repulsion of the hydrophilic groups of neighboring molecules. With a decrease in pH, hydrogen bonds form, which, together with the electrostatic interaction, causes the formation of hexagonally packed aggregates.

Liposomes based on CL **2** efficiently formed lipoplexes with pDNA starting from the N/P ratio of 2:1 and higher [59]. The incorporation of DOPE into the liposomal composition and further incubation with pDNA leads to the formation of a negatively charged lipoplex. The formation of salt bridges between the positively charged hydrophilic group of the CL **2** and the phosphate groups of the DOPE lipid allows the primary amino group of DOPE to stabilize near the surface of liposomes and interact more closely with negatively charged phosphate groups of DNA. It should be noted that at the N/P ratio of 6:1 and higher, compact, and homogeneous lipoplexes with a high positive charge were formed. DOPE can also provide the availability of HCG of the CL for DNA binding, thereby decreasing the interaction energy [59].

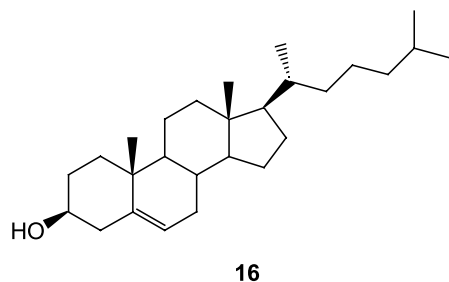
Thus, the use of DOPE provides an efficient release of compacted NA from endosomes by destabilizing the endosomal membrane [58, 61] and favors the more compact packing of DNA [62, 63].

Phosphatidylcholine **14** (PC) is a phospholipid consisting of a choline residue as a hydrophilic group and a phosphatidic acid with various acyl residues as an HD [57]. However, when using PC as a helper lipid, which forms lamellar cationic liposomes, the TE was lower than DOPE [56].

The low-DOPE phase transition temperature (10°C) reduces the stability of cationic liposomes and lipoplexes *in vivo*. One approach to solving this problem is the synthesis of DOPE analogs, the phase transition of which is near the temperature of the human body (~37°C). DOPE analogs (**15a–c**) were synthesized, in which the *cis* double bond in two acyl residues was replaced by a triple bond located at different positions of hydrocarbon substituents [64]. This chemical modification made it possible to form a new intermolecular package, which contributes to an increase in the phase transition temperature under physiological conditions.

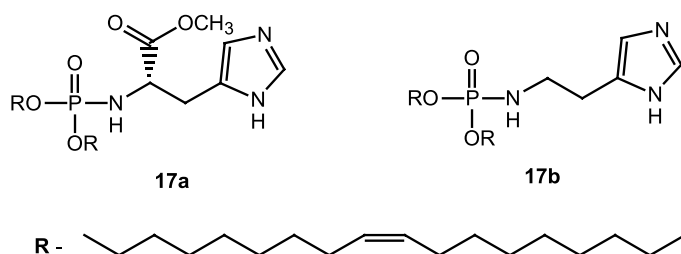


Cholesterol (**16**, Chol) is another common helper lipid [65–72]. An increase in the amount of cholesterol to 66.7% in the composition of liposomes with CL **3** led to the formation of stable particles that resulted in a high TE in the presence of blood serum. Of note, a further increase in the amount of cholesterol up to 80% did not change the TE [66].



It was found that some CLs have a high affinity for the helper lipid and are only active in the presence of cholesterol or DOPE. Liposomes containing a helper lipid are often more effective at transfecting cells than those with phospholipids, which may be related to the endogenous nature of cholesterol [73].

Another approach to identifying more efficient helper lipids was the synthesis of new lipids **17a** and **17b** with an imidazole-based polar group, which are not charged at a physiological pH. Their protonation in endosomes induces the fusion of lipoplexes with the endosomal membrane and promotes the release of NA into the cytosol. Of note, adding the new helper lipids **17a** and **17b** to the composition of cationic liposomes can improve transfection by 100 times compared with DOPE [74].



Thus, the efficiency of NA delivery can be optimized by adding helper lipids to the composition of cationic liposomes.

COMMERCIAL TRANSFECTANTS BASED ON CL

To date, there are a number of commercial transfectants based on CL: Lipofectamine (Lipofectamine 2000, Lipofectamine 3000, Lipofectamine RNAiMAX, Lipofectamine MessengerMAX, Lipofectamine CRISPRMAX, Lipofectamine LTX, Lipofectamine Stem), Lipofectin, LipofectACE, Transfect, Transfectam, Cellfectin, Cellfectin II, and others [75–79].

Since it was launched into large-scale production in 1993, lipofectamine and its analogs have been

mainly used for cell transfection [80]. Achieving a high TE of a wide range of cell lines and the ability to transfer various types of NA, lipofectamines are considered the “gold standard” among transfection reagents and are most often used for the comparative evaluation of efficacy both in the development of new CLs and alternative transfection methods.

Lipofectamine 2000 (Lf 2000) is a mixture of a polycationic lipid **5** and a neutral lipid DOPE at a ratio of 3:1 mol [78]. When choosing the appropriate transfection agent, it is necessary to consider the type of NA being delivered. Universal reagents, such as Lf 2000 and Lf 3000, are used for both DNA and RNA delivery. Lipofectamine RNAiMAX [81, 82] and Lipofectamine MessengerMAX™ were developed specifically for the transfection of siRNA and miRNA cells, respectively.

Lf 2000 successfully transfects neonate hamster kidney cells (BHK-21), mouse embryonic fibroblasts (NIH 3T3), African green monkey cells (COS-1), human colonic epithelial cells (HT-29), human diploid cells (MRC-5), and breast cancer cells (SK-BR3). Lf 3000 is an improved version of Lf 2000 and successfully transfects a wide variety of biologically relevant cell types [78, 83–85]. Its distinguishing feature is its high TE in the presence of blood serum, and therefore, there is no need to change the culture medium after transfection, as well as the presence of the second component, which is only used for the delivery of pDNA. Lipofectamine LTX can effectively transfect cells that are usually difficult to transfect, sensitive cells, and primary cell cultures. In turn, Lipofectamine Stem was developed specifically for the transfection of stem cells. Invivolectamine 3.0 is suitable for the *in vivo* delivery of NA [86–88] and, in particular, for the delivery of siRNA and duplex miRNA in mouse liver cells by the injection of lipoplexes into the tail vein.

The transfection agent Lipofectin is a mixture of lipid **1** and DOPE at a ratio of 1:1 mol and is used for the transfection of a wide range of cells [89, 90]. It is believed that DNA spontaneously interacts with lipid **1** according to the same principle as with lipid **5**, while 100% of the DNA binds into lipoplexes.

Based on lipopolyamine **4**, the commercial transfectant Transfectam was created, which effectively delivers NAs into corticotropic tumor cells (AtT20) and NIH 3T3 cells [91, 92].

A study based on identifying the simplest surfactants for the transfection of eukaryotic cells revealed that liposomes based on dimethyldioctadecylammonium bromide (**18**, DDAB) and DOPE were more effective than Lipofectin [93, 94], and therefore, TransfectACE (or LipofectACE) containing compound **18** and DOPE in a ratio of 1:2.5 mol was patented.

Transfecting agents Cellfectin and Cellfectin II are a mixture of *N,N,N,N*-tetramethyl-*N,N,N,N*-tetra(hexadecyl)spermine (**19**, TM-TPS) and DOPE at a ratio of 1:1.5 mol that are suitable for the transfection of both mammalian and insect cells (Sf9, Sf21, and S2) [78, 79, 94].

The DMRIE-C transfection agent, consisting of 1,2-di(tetradecyloxy)propyl-3-*N*-2-hydroxyethyl-*N,N*-dimethylammonium bromide **20** and cholesterol in a ratio of 1:1 mol, is suitable for the transfection of eukaryotic cells and is especially effective for the transfection of suspension cultures (human T-lymphoblastic leukemia cells or Jurkat cells), as well as other cell lines derived from lymphoid cells [95, 96].

Oligofectamine is a proprietary composition for ODN and siRNA delivery into eukaryotic cells. Due to the formation of stable complexes with ODNs, it efficiently transfects eukaryotic cells, including Chinese hamster ovary cells, human kidney embryo cells (HEK 293), NIH 3T3, and human cervical cancer cells (HeLa) [97].

Despite the wide variety of existing transfection agents, the development of new delivery systems that can efficiently transfer various types of NA *in vitro* and *in vivo* without having a toxic effect on cell viability will lead to the appearance of more and more liposomes.

LIPOSOMES BASED ON NEW SYNTHETIC CL

Over the past two decades, a large number of studies have been published, in which cationic liposomes are used as carriers for NA delivery *in vitro* and *in vivo*. The formation of liposome-NA complexes (lipoplexes) and their ability to transfect eukaryotic cells depends on both the composition of liposomes and the structural features of CL. In addition, the ratio of the lipoplex components (defined by the N/P ratio) and their physicochemical characteristics (size and zeta potential) also determine the efficiency of cell transfection.

Recently, it has been suggested that the penetration of lipoplexes into the cell is mediated by special cholesterol transporters. The cholesterol presented in cell membranes disrupts the dense packing of phospholipids and reduces their membrane fluidity, as well as their permeability to small water-soluble molecules. Since the energy barrier for the flip-flop translocation of cholesterol molecules is low, its redistribution between layers occurs quickly, which affects the cellular uptake of complexes, as well as the formation and degradation of endosomes [98].

The use of cholesterol-containing CL or cholesterol as a helper lipid increases the TE [66]. This may be due to the formation of cholesterol nanodomains in lipoplexes, which mediate endocytosis, and/or intracellular transport of complexes. In addition, cholesterol in liposomes protects NA from degradation by nucleases in the body and reduces the binding of lipoplexes to serum proteins, thereby improving the delivery of NA. Thus, the use of cholesterol-based CL can significantly increase the efficiency of NA delivery and expression [59, 66, 67, 99–105].

One of the most widely used cholesterol-based CL (**3**, DC-Chol) effectively delivered NAs either alone or in combination with other lipids into various eukaryotic cells [59, 66, 68, 99, 100]. In addition, other cholesterol-based CLs (**21–26**) were synthesized (Table 1) for the delivery of various types of NA.

A comparative study of the effectiveness of liposomes consisting of monomeric **21** or dimeric CL **22a–e** and DOPE, which was conducted both in the presence (+FBS) and absence of serum (–FBS) (Table 1), revealed that in the absence of serum, CL **21** transfected about 70% of cells with a mean fluorescence intensity (MFI) of 20 relative units, whereas CL **22a–e** transfected 45–70% of cells with an AFI of 20–75 relative units. In the presence of blood serum, the TE of monomeric CL and dimeric CL decreased to ~20 and 40%, respectively. Liposomes based on CL **22d–e** were toxic in the absence of serum in the culture medium [101].

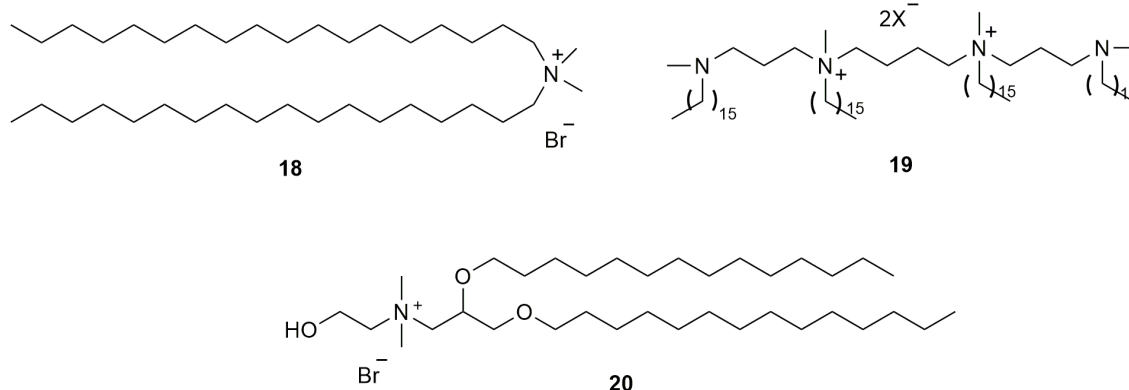


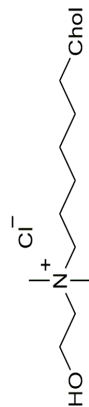

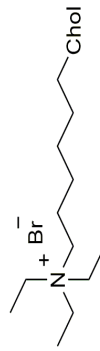



Table 1. CL based on cholesterol

	CL structure	CL:helper lipid, molar ratio	Transferred NA	Cell type	FBS (-) / FBS (+) ⁴			Source
					IC ₅₀ , μ M	TC ² , %	MFT ³ , rel. unit	
21		21-DOPE, 1:1	pEGFP-C3 ⁵	HeLa ⁶	>80 / >80	70 / 20	20 / 20	[101]
22a		22a-DOPE, 1:1				60 / 40	20 / 30	
22b		22b-DOPE, 1:1				70 / 70	25 / 30	
22c		22c-DOPE, 1:2				70 / 50	75 / 60	
22d		22d-DOPE, 1:2			40 / >80	55 / 45	55 / 55	
22e		22e-DOPE, 1:2				45 / 40	30 / 55	
23a		23a-DOPE, 1:1	pEGFP-C2	HEK 293 ⁷	36.0 / 35.0	55 / 29.6	30 / 21.4	[59]
23b		23b-DOPE, 1:1			37.2 / 37.3	68 / 44.2	55 / 42.1	
23c		23c-DOPE, 1:1			38.8 / 35.5	45 / 18.9	18 / 9.1	
24a		24a-DOPE, 1:1	pEGFP-C2	HEK 293	>80	35 / 21.5	12 / 5.9	[59]
24b		24b-DOPE, 1:1			>80 / 71.9	35 / 21.8	10 / 3.3	
24c		24c-DOPE, 1:1			40.5 / 37.1	70 / 75.7	29 / 42	
25a		2-16-25a	pEGFP	SKOV-3 ⁸	100 / n.d. ¹⁰	20 / n.d.	n.d.	[102]
25b		2-16-25b		A549 ⁹	n.d.	17 / n.d.		
25c		2-16-25c		SKOV-3	143 / n.d.	7 / n.d.		
				A549	n.d.	15 / n.d.		
				SKOV-3	302 / n.d.	9 / n.d.		
				A549	n.d.	12 / n.d.		

Table 1. Continued

	CL structure	CL:helper lipid, molar ratio	Transferred NA	Cell type	IC ₅₀ ¹ , μM	TC ² , %	MFI ³ , rel. unit	Source
					FBS (–) / FBS (+) ⁴			
26a		26a -DOPE, 2:1	pEGFP-N1	293T ¹¹	100 / n.d.	43 / 41	300 / 290	[103]
				HeLa		15 / 16	20 / 23	
26b		26b -DOPE, 2:1		293T	50 / n.d.	22 / 25	150 / 155	
26c		26c -DOPE, 2:1		293T	30 / n.d.	3 / 5	40 / 50	
26d		26d -DOPE, 1:0.5		293T	50 / n.d.	23 / 25	150 / 153	
26e		26e -DOPE, 1:0.5		293T	30 / n.d.	5 / 4	3 / 2	
26f		26f -DOPE, 1:0.5		293T	100 / n.d.	37 / 53	240 / 250	
				HeLa		80 / 77	110 / 100	

¹IC₅₀ – liposome concentration at which cell growth is inhibited by 50%.

²TC – transfected cells.

³MFI – mean fluorescence intensity.

⁴FBS (–) / FBS (+) – absence / presence of fetal bovine serum (10%).

⁵EGFP – enhanced green fluorescent protein.

⁶HeLa – cervical cancer cell line.

⁷HEK 293 – human embryonic kidney cells.

⁸SKOV-3 – human ovarian adenocarcinoma cell line.

⁹A549 – human lung carcinoma cells.

¹⁰n.d. – no data.

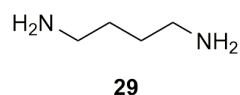
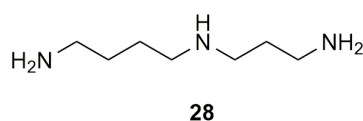
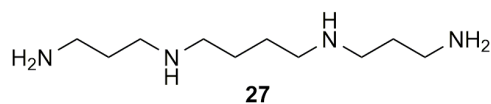
¹¹293T – human embryonic kidney cells transfected by adenovirus type 5 and SV40 virus.

The transfection activity of liposomes formed by polycationic lipids depends on the type of linker, the length of the spacer, and the amount of cholesterol residues. Liposomes prepared from CL **24c** (Table 1), consisting of two cholesterol residues, a carbamoyl linker, and a hexamethylene SG and DOPE revealed the best *in vitro* TE among other tested analogs with CL **23a–c** and **24a,b** [59]. In the absence of blood serum, an increase in TE was observed with an increase in the N/P ratio for all liposome compositions, whereas the **23a**-DOPE, **23b**-DOPE, or **24c**-DOPE liposomes transferred pDNA efficiently at an N/P ratio of 6:1. Lf 2000 provided less efficient delivery of NA. The presence of blood serum decreased the TE by 20–30% for all cationic liposomes, except for the **24c**-DOPE composition (Table 1).

Cationic liposomes based on CL **2**, helper lipid **16**, and cholesterol-containing PEG derivatives **25a–c** efficiently delivered pDNA encoding a green fluorescent protein into 7–20% of SKOV-3 cells and 12–17% of A549 cells (Table 1) [102].

A number of liposomes based on lipids **26a–f** (Table 1), in which cholesterol was used as an HD, and primary, tertiary, or quaternary amino groups served as hydrophilic cationic heads were also studied. The hydrophobic and hydrophilic domains were linked via ether or ester bonds. Among the six studied compositions, the highest TEs were demonstrated by liposomes with CL **26a** and **26f** containing primary amino groups in their structure. Specifically, they delivered pEGFP pDNA into 293T cells more efficiently than the commercial agent Lf 2000 [103].

Another structural element that has a strong effect on TE is the cationic group, which is necessary for the binding and compaction of NA. It is known that mammalian polyamines, such as spermine (**27**), spermidine (**28**), and putrescine (**29**), not only have the ability to bind NA but also affect the fusion of liposomes with the cell membrane [104]. Liposomes based on CL **30a–c** were used to deliver siRNA into HeLa cells (Table 2) [105]. The maximum number of



transfected cells (62%) was achieved using spermine-based liposomes with CL **30a**.

The important role of spermine in the formation of lipoplexes has been presented in a number of studies [105–111]. In [106], the prospects of using cationic liposomes consisting of spermine-containing CL **31a–c** with acyl substituents of various lengths and a helper lipid **14** were considered (Table 2). Among them, liposomes containing CL **31a** with a myristoyl substituent revealed the highest level of transfection and the lowest cytotoxicity. The same pattern was observed when using these lipids in the composition of niosomes (nonionic surfactant vesicles) [107].

Liposomes based on *N*⁴,*N*⁹-diacylated spermine derivatives **32a–j** (Table 2) containing two fatty acid residues from 18 to 24 hydrocarbon chains protect NA from nucleases and promote efficient NA transport. In the absence of serum, liposomes based on asymmetric CL **32d** with oleic and arachidonic acid residues were found to transfect the highest number of cells (68%), and CL **32c** with two linoleic acid residues produced the highest MFI (15 relative units) [108]. In the presence of serum, liposomes with CL **32e–j** have demonstrated a TE comparable or superior to Lf 2000 [70, 109]. The most promising CL (**32g**) containing unsaturated oleic and saturated lignoceric acids transfected 85% of HeLa cells with a MFI of 50 relative units.

In [110, 111], the authors studied the transfection ability of liposomes based on spermine-containing CL with different LGs (di(hydroxyethyl)amino (**33**), di(hydroxyethyl)aminocarboxy (**34a–c**), 3-amino-1,2-dioxipropyl (**35a–c**), and 2-amino-1,3-dioxipropyl (**36a–c**)) and three HDs (lauric, myristic, and palmitic acids). All obtained liposomes and their complexes with pDNA were found to be slightly toxic for cells (Table 2). Among liposomes containing CL **33–36**, lipids **35b** and **35c** with myristoyl and palmitoyl residues were the most effective for cell transfection, although CL **36a**, with a shorter hydrocarbon chain, also facilitated efficient delivery of pDNA in the absence of blood serum. The addition of serum to the culture medium decreased the TE of liposomes based on CL **35b** and **35c** with a 3-amino-1,2-dioxipropyl linker, whereas the efficiency of liposomes based on CL **36a** with a 2-amino-1,3-dioxipropyl linker did not change (93% of cells).

CONCLUSIONS

The development of cationic liposomes capable of efficiently delivering NA to target cells with minimal toxic effects is the ultimate goal of any transfection related research field. Despite numerous studies on the development of optimal systems for the delivery of NA into eukaryotic cells, the question

Table 2. CL based on spermine

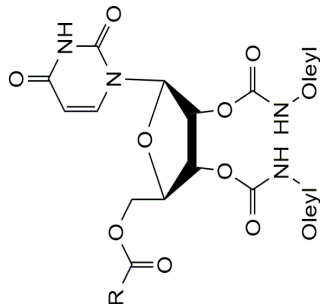
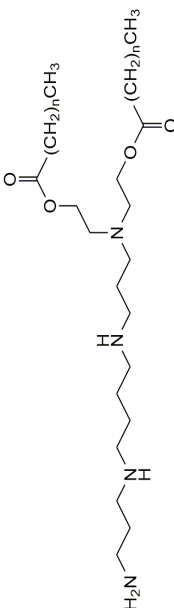
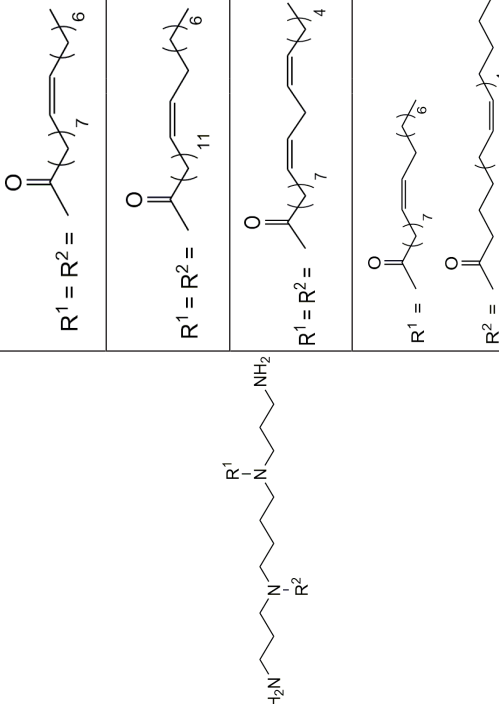
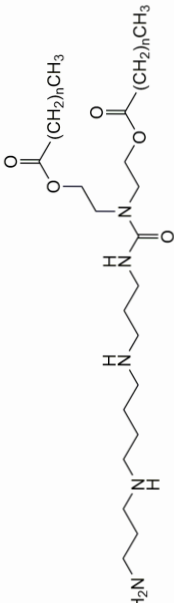
	CL structure	CL:helper lipid, molar ratio	Transferred NA	Cell type	IC ₅₀ ¹ , μM	TC ² , %	MFI ³ , rel. unit	Source		
					FBS (-) / FBS (+) ⁴					
30a		R = 27	siRNA	HeLa ⁵	50 / n.d. ⁶	62 / n.d.		n.d.	[105]	
30b		R = 28				43 / n.d.				
30c		R = 29				15 / n.d.				
31a		n = 12	pEGFP-C2 ⁷	HeLa	30 / n.d.	15 / n.d.		n.d.	[106], [107]	
31b		n = 14				12.5 / n.d.				
31c		n = 16				10 / n.d.				
32a		32a	siEGFP-AF	HeLa	n.d. / 100	50 / n.d.		17 / n.d.	[108]	
32b		32b				30 / n.d.				10 / n.d.
32c		32c				25 / n.d.				
32d		32d				68 / n.d.				10 / n.d.

Table 2. Continued

	CL structure	CL:helper lipid, molar ratio	Transferred NA	Cell type	IC ₅₀ ¹ , μM	TC ² , %	MFI ³ , rel. unit	Source
					FBS (-) / FBS (+) ⁴			
32e		32e	siEGFP-AF	HeLa	n.d. / 100	n.d. / 75	n.d. / 19	[108]
32f						n.d. / 73	n.d. / 35	
32g		32g				n.d. / 85	n.d. / 50	[108]
32h						n.d. / 57	n.d. / 10	
32i		32i				n.d. / 83	n.d. / 23	[70], [109]
32j						32j	n.d. / 75 n.d. / 30	
33		33-DOPE, 1:1 n = 10	pCMV	HeLa	40 / n.d.	30 / 21	n.d.	[110], [111]

Table 2. Continued

	CL structure	CL:helper lipid, molar ratio	Transferred NA	Cell type	IC ₅₀ ¹ , μM	TC ² , %	MFI ³ , rel. unit	Source		
					FBS (-) / FBS (+) ⁴					
34a		n = 10	34a-DOPE, 1:1	HeLa	40 / n.d.	48 / 24	n.d.	[110], [111]		
34b		n = 12				64 / 33				
34c		n = 14				48 / 26				
35a	n = 10	35a-DOPE, 1:1	pCMV			32 / 20				
35b	n = 12								98 / 50	
35c	n = 14								94 / 47	
36a	n = 10	36a-DOPE, 1:1							88 / 93	
36b	n = 12									16 / 25
36c	n = 14									8 / 13

¹IC₅₀ – liposome concentration at which cell growth is inhibited by 50%.²TC – transfected cells.³³MFI – mean fluorescence intensity.⁴FBS (-) / FBS (+) - absence / presence of fetal bovine serum (10%).⁵HeLa – cervical cancer cell line.⁶n.d. – no data.⁷EGFP – enhanced green fluorescent protein.

of the effectiveness of cationic liposomes remains one of the main factors limiting their use in gene or antisense therapy.

Synthetic and structural studies that aim to identify new CLs and the generation of liposomes on their basis open up new prospects in the development of nonviral systems for the delivery of NA in gene therapy. Among the most promising *in vitro* delivery systems are cholesterol- and spermine-based lipids with variations in composition, spacer length, and the type of linker used. However, in order to optimize the targeted delivery of NA, in addition to composition, it is also necessary to take into account

the physicochemical parameters of cationic liposomes and the complexes with NA formed by them. These parameters include the size and surface potential of the complexes, which depend on both the ratio of components and the composition of lipoplexes. Thus, in addition to the search for the optimal structures of CLs, it is necessary to determine the ratio of the component of lipoplexes providing the delivery of NA to target cells.

Acknowledgments

The study was supported by the Russian Foundation for Basic Research, project No. 18-33-00589.

The authors declare no conflicts of interest.

REFERENCES

- Ginn S.L., Alexander I.E., Edelstein M.L., Abedi M.R., Wixon J. Gene therapy clinical trials worldwide to 2012 – an update. *J. Gene Med.* 2013;15:65-77. <https://doi.org/10.1002/jgm.2698>
- Verma I.M., Weitzman M.D. Gene Therapy: Twenty-First Century Medicine. *Annu. Rev. Biochem.* 2005;74:711-738. <https://doi.org/10.1146/annurev.biochem.74.050304.091637>
- Zhang X.-X., McIntosh T.J., Grinstaff M.W. Functional lipids and lipoplexes for improved gene delivery. *Biochimie.* 2012;94:42-58. <https://doi.org/10.1016/j.biochi.2011.05.005>
- Elsabahy M., Nazarali A.M., Foldvari M. Non-viral nucleic acid delivery: key challenges and future directions. *Curr. Drug Deliv.* 2011;8:235-244. <https://doi.org/10.2174/156720111795256174>
- Gao Y., Liu X.L., Li X.R. Research progress on siRNA delivery with nonviral carriers. *Int. J. Nanomedicine.* 2011;6:1017-1025. <https://doi.org/10.2147/ij.n.s17040>
- Guo J., Fisher K.A., Darcy R., Cryan J.F., O'Driscoll C. Therapeutic targeting in the silent era: advances in non-viral siRNA delivery. *Mol. BioSyst.* 2010;6:1143-1161. <https://doi.org/10.1039/c001050m>
- Giacca M., Zacchigna S. Virus-mediated gene delivery for human gene therapy. *J. Controlled Release.* 2012;161(2):377-388. <https://doi.org/10.1016/j.jconrel.2012.04.008>
- Crespo-Barreda A., Encabo-Berzosa M.M., González-Pastor R., Ortiz-Teba P., Iglesias M., Serrano J.L., Martín-Duque P. Viral and nonviral vectors for *in vivo* and *ex vivo* gene therapies. *Translating Regenerative Medicine to the Clinic.* 2016; 155-177. <https://doi.org/10.1016/b978-0-12-800548-4.00011-5>
- Mertena O.-W., Gaillet B. Viral vectors for gene therapy and gene modification approaches. *Biochem. Eng. J.* 2016;108:98-115. <https://doi.org/10.1016/j.bej.2015.09.005>
- Baum C., Kustikova O., Modlich U., Li Z., Fehse B. Mutagenesis and oncogenesis by chromosomal insertion of gene transfer vectors. *Hum. Gene Ther.* 2006;17:253-263. <https://doi.org/10.1089/hum.2006.17.253>
- Bessis N., GarciaCozar F.J., Boissier M.-C. Immune responses to gene therapy vectors: influence on vector function and effector mechanisms. *Gene Therapy.* 2004;11:10-17. <https://doi.org/10.1038/sj.gt.3302364>
- Wachler R., Russell S.J., Curiel D.T. Engineering targeted viral vectors for gene therapy. *Nat. Rev. Genet.* 2007;8:573-587. <https://doi.org/10.1038/nrg2141>
- Thomas C.E., Ehrhardt A., Kay M.A. Progress and problems with the use of viral vectors for gene therapy. *Nat. Rev. Genet.* 2003;4:346-358. <https://doi.org/10.1038/nrg1066>
- Lollo C.P., Banaszczyk M.G., Chiou H.C. Obstacles and advances in non-viral gene delivery. *Curr. Opin. Mol. Ther.* 2000;2(2):136-142.
- Li S.O.-D., Huang L. Non-viral is superior to viral gene delivery. *J. Controlled Release.* 2007;123:181-183. <https://doi.org/10.1016/j.jconrel.2007.09.004>
- Mintzer M.A., Simanek E.E. Nonviral vectors for gene delivery. *Chem. Rev.* 2009;109:259-302. <https://doi.org/10.1021/cr800409e>
- Yin H., Kanasty R.L., Eltoukhy A.A., Vegas A.J., Dorkin J.R., Anderson D.J. Non-viral vectors for gene-based therapy. *Nat. Rev. Genet.* 2014;15(8):541-555. <https://doi.org/10.1038/nrg3763>
- Vlerken L.E., Vyas T.K., Amiji M.M. Poly(ethylene glycol)-modified nanocarriers for tumor-targeted and intracellular delivery. *Pharm. Res.* 2007;24(8):1405-1414. <https://doi.org/10.1007/s11095-007-9284-6>
- Balazs D.A., Godbey W.T. Liposomes for Use in Gene Delivery. *J. Drug Deliv.* 2011;2011:1-12. <https://doi.org/10.1155/2011/326497>
- Kang S.H., Cho H.J., Shim G., Lee S., Kim S.H., Choi H.G., Kim C.W., Oh Y.K. Cationic liposomal co-delivery of small interfering RNA and a MEK inhibitor for enhanced anticancer efficacy. *Pharm. Res.* 2011;28:3069-3078. <https://doi.org/10.1007/s11095-011-0569-4>
- Shim G., Han S.E., Yu Y.H., Lee S., Lee H.Y., Kim K., Kwon I.C., Park T.G., Kim Y.B., Choi Y.S., Kim C.-W., Oh Y.K. Trilysinoyleylamide-based cationic liposomes for systemic co-delivery of siRNA and an anticancer drug. *J. Controlled Release.* 2011;155:60-66. <https://doi.org/10.1016/j.jconrel.2010.10.017>

22. Zuhorn I.S., Engberts J.B.F.N., Hoekstra D. Gene delivery by cationic lipid vectors: overcoming cellular barriers. *Eur. Biophys. J.* 2017;36(4-5):349-362. <https://doi.org/10.1007/s00249-006-0092-4>
23. Movahedi F., MS., Hu R.G., PhD., Becker D.L., PhD., Xu C., PhD. Stimuli-responsive liposomes for the delivery of nucleic acid therapeutics. *Nanomedicine: Nanotechnology, Biology and Medicine.* 2015;11(6):1575-1584. <https://doi.org/10.1016/j.nano.2015.03.006>
24. Monopoli M.P., Bombelli F.B., Dawson K.A. Nanoparticle coronas take shape. *Nat. Nanotechnol.* 2011;6:11-12. <https://doi.org/10.1038/nnano.2011.267>
25. Walczyk D., Bombelli F.B., Monopoli M.P., Lynch I., Dawson K.A. What the cell "sees" in bionanoscience. *J. Am. Chem. Soc.* 2010;132:5761-5768. <https://doi.org/10.1021/ja910675v>
26. Allen L.T., Tosetto M., Miller I.S., O'Connor D.P., Penney S.C., Lynch I., Keenana A.K., Pennington S.R., Dawson K.A., Gallagher W.M. Surface-induced changes in protein adsorption and implications for cellular phenotypic responses to surface interaction. *Biomaterials.* 2006;27:3096-3108. <https://doi.org/10.1016/j.biomaterials.2006.01.019>
27. Senior J.H. Fate and behavior of liposomes *in vivo* — a review of controlling factors. *CRC Crit. Rev. Ther. Drug.* 1987;3:123-193.
28. Monopoli M.P., Walczyk D., Campbell A., Elia G., Lynch I., Bombelli F.B., Dawson K.A. Physical-chemical aspects of protein corona: relevance to *in vitro* and *in vivo* biological impacts of nanoparticles. *J. Am. Chem. Soc.* 2011;133:2525-2534. <https://doi.org/10.1021/ja107583h>
29. Aggarwal P., Hall J.B., McLeland C.B., Dobrovolskaia M.A., McNeil S.E. Nanoparticle interaction with plasma proteins as it relates to particle biodistribution, biocompatibility and therapeutic efficacy. *Adv. Drug Deliv. Rev.* 2009;61:428-437. <https://doi.org/10.1016/j.addr.2009.03.009>
30. Ishida T., Harashima H., Kiwada H. Liposome clearance. *Biosci. Rep.* 2002;22(2):197-224. <https://doi.org/10.1023/a:1020134521778>
31. Chonn A., Cullis P.R., Devine D.V. The role of surface-charge in the activation of the classical and alternative pathways of complement by liposomes. *J. Immunol.* 1991;146:4234-4241.
32. Senior J., Gregoriadis G. Is half-life of circulating liposomes determined by changes in their permeability? *FEBS Lett.* 1982;145(1):109-114. [https://doi.org/10.1016/0014-5793\(82\)81216-7](https://doi.org/10.1016/0014-5793(82)81216-7)
33. Judge A.D., Sood V., Shaw J.R., Fang D., McClintock K., MacLachlan I. Sequence-dependent stimulation of the mammalian innate immune response by synthetic siRNA. *Nat. Biotechnol.* 2005;23(4):457-462. <https://doi.org/10.1038/nbt1081>
34. Kleinman M.E., Yamada K., Takeda A., Chandrasekaran V., Nozaki M., Baffi J.Z., Albuquerque R.J.C., Yamasaki S., Itaya M., Pan Y.Z., Appukuttan B., Gibbs D., Yang Z.L., Kariko K., Ambati B.K., Wilgus T.A., DiPietro L.A., Sakurai E., Zhang K., Smith J.R., Taylor E.W., Ambati J. Sequence- and target-independent angiogenesis suppression by siRNA via TLR3. *Nature.* 2008;452:591-597. <https://doi.org/10.1038/nature06765>
35. Robbins M., Judge A., Ambegia E., Choi C., Yaworski E., Palmer L., McClintock K., MacLachlan I. Misinterpreting the therapeutic effects of small interfering RNA caused by immune stimulation. *Hum. Gene Ther.* 2008;19:991-999. <https://doi.org/10.1089/hum.2008.131>
36. Kedmi R., Ben-Arie N., Peer D. The systemic toxicity of positively charged lipid nanoparticles and the role of Toll-like receptor 4 in immune activation. *Biomaterials.* 2010;31:6867-6875. <https://doi.org/10.1016/j.biomaterials.2010.05.027>
37. Buyens K., Smedt S.C.D., Braeckmans K., Demeester J., Peeters L., Grunsvan L.A.V., Mollerat du Jeu X.D., Sawant R., Torchilin V., Farkasova K., Ogris M., Sanders N.N. Liposome based systems for systemic siRNA delivery: Stability in blood sets the requirements for optimal carrier design. *J. Controlled Release.* 2012;158:362-370. <https://doi.org/10.1016/j.jconrel.2011.10.009>
38. Conner S.D., Schmid S.L. Regulated portals of entry into the cell. *Nature.* 2003;422:37-44. <https://doi.org/10.1038/nature01451>
39. Jones C.H., Chen C.-K., Ravikrishnan A., Rane S., Pfeifer B.A. Overcoming nonviral gene delivery barriers: perspective and future. *Mol. Pharmaceutics.* 2013;10:4082-4098. <https://doi.org/10.1021/mp400467x>
40. Rehman Z.U., Hoekstra D., Zuhorn I.S. On the mechanism of polyplex- and lipoplex-mediated delivery of nucleic acids: real-time visualization of transient membrane destabilization without endosomal lysis. *ACS Nano.* 2013;7(5):3767-3777. <https://doi.org/10.1021/nn3049494>
41. Ward C.M., Read M.L., Seymour L.W. Systemic circulation of poly(L-lysine)/DNA vectors is influenced by polycation molecular weight and type of DNA: differential circulation in mice and rats and the implications for human gene therapy. *Blood.* 2001;97(8):2221-2229. <https://doi.org/10.1182/blood.v97.8.2221>
42. Van der Aa M.A., Mastrobattista E., Oosting R.S., Hennink W.E., Koning G.A., Crommelin D.J. The nuclear pore complex: the gateway to successful nonviral gene delivery. *Pharm. Res.* 2006;23(3):447-459. <https://doi.org/10.1007/s11095-005-9445-4>
43. Zhi D., Zhang S., Cui S., Zhao Y., Wang Y., Zhao D. The Headgroup evolution of cationic lipids for gene delivery. *Bioconjugate Chem.* 2013;24(4):487-519. <https://doi.org/10.1021/bc300381s>
44. Bottega R., Epand R.M. Inhibition of protein kinase C by cationic amphiphiles. *Biochemistry.* 1992;31:9025-9030. <https://doi.org/10.1021/bi00152a045>
45. Floch V., Loisel S., Guenin E., Herve A.C., Clement J.C., Yaouanc J.J., Abbayes H.D., Ferec C. Cation substitution in cationic phosphonolipids: a new concept to improve transfection activity and decrease cellular toxicity. *J. Med. Chem.* 2000;43:4617-4628. <https://doi.org/10.1021/jm000006z>
46. Ui-Teil K., Naito Y., Takahashi F., Haraguchi T., Ohki-Hamazaki H., Juni A., Ueda R., Saigo K. Guidelines for the selection of highly effective siRNA sequences for mammalian and chick RNA interference. *Nucleic Acids Research.* 2004;32(3):936-948. <https://doi.org/10.1093/nar/gkh247>
47. Rao G., Yadava P., Hughes J. Rationally designed synthetic vectors for gene delivery. *The Open Drug Deliv. J.* 2007;1:7-19. <https://doi.org/10.2174/1874126600701010007>
48. Choi J.S., Lee E.J., Jang H.S., Park J.S. New cationic liposomes for gene transfer into mammalian cells with high efficiency and low toxicity. *Bioconjugate Chem.* 2001;12:108-113. <https://doi.org/10.1021/bc000081o>
49. Liu D., Hu J., Qiao W., Li Z., Zhang S. Cheng L. Synthesis of carbamate-linked lipids for gene delivery. *Bioorg. Med. Chem. Lett.* 2005;15(12):3147-3150. <https://doi.org/10.1016/j.bmcl.2005.04.010>

50. Liu D., Qiao W., Li Z., Chen Y., Cui X., Li K., Yu L., Yan K., Zhu L., Guo Y. Cheng L. Structure–function relationship research of glycerol backbone-based cationic lipids for gene delivery. *Chem. Biol. Drug Des.* 2008;71:336-344. <https://doi.org/10.1111/j.1747-0285.2008.00644.x>
51. Tang F., Hughes J.A. Use of dithiodiglycolic acid as a tether for cationic lipids decreases the cytotoxicity and increases transgene expression of plasmid DNA *in vitro*. *Bioconjugate Chem.* 1999;10:791-796. <https://doi.org/10.1021/bc990016i>
52. Byk G., Wetzter B., Frederic M., Dubertret C., Pitard B., Jaslin G., Scherman D. Reduction-sensitive lipopolyamines as a novel nonviral gene delivery system for modulated release of DNA with improved transgene expression. *J. Med. Chem.* 2000;43:4377-4387. <https://doi.org/10.1021/jm000284y>
53. Reynier P., Briane D., Coudert R., Fadda G., Bouchemal N., Bissieres P., Taillandier, Cao A. Modifications in the head group and in the spacer of cholesterol-based cationic lipids promote transfection in melanoma B16-F10 cells and tumours. *J. Drug Target.* 2004;12(1):25-38. <https://doi.org/10.1080/10611860410001683040>
54. Muñoz-Úbeda M., Misra S. K., Barrán-Berdón A.L., Datta S., Aicart-Ramos C., Castro-Hartmann P., Kondaiah P., Junquera E., Bhattacharya S., Aicart E. How does the spacer length of cationic gemini lipids influence the lipoplex formation with plasmid DNA? Physicochemical and biochemical characterizations and their relevance in gene therapy. *Biomacromolecules.* 2012;13:3926-3937. <https://doi.org/10.1021/bm301066w>
55. Obata Y., Saito S., Takeda N., Takeoka S. Plasmid DNA-encapsulating liposomes: effect of a spacer between the cationic head group and hydrophobic moieties of the lipids on gene expression efficiency. *Biochim. Biophys. Acta.* 2009;1788:1148-1158. <https://doi.org/10.1016/j.bbamem.2009.02.014>
56. Du Z., Munye M.M., Tagalakakis A.D., Manunta M.D.I., Hart S.L. The role of the helper lipid on the DNA transfection efficiency of lipopolyplex formulations. *Scientific Rep.* 2015;4(7107):1-6. <https://doi.org/10.1038/srep07107>
57. Pisani M., Mobbili G. Bruni P. Neutral liposomes and DNA transfection. *Non-Viral Gene Ther.* 2011;319-348. <https://doi.org/10.5772/21283>
58. Zuhorn I.S., Bakowsky U., Polushkin E., Visser W.H., Stuur M. Engberts J., Hoekstra D. Nonbilayer phase of lipoplex–membrane mixture determines endosomal escape of genetic cargo and transfection efficiency. *Mol. Ther.* 2005;11(5):801-810. <https://doi.org/10.1016/j.ymthe.2004.12.018>
59. Maslov M.A., Kabilova T.O., Petukhov I.A., Morozova N.G., Serebrennikova G.A., Vlassov V.V., Zenkova M.A. Novel cholesterol spermine conjugates provide efficient cellular delivery of plasmid DNA and small interfering RNA. *J. Controlled Release.* 2012;160:182-193. <https://doi.org/10.1016/j.jconrel.2011.11.023>
60. Mochizuki S., Kanegae N., Nishina K., Kamikawa Y., Koiwai K., Masunaga H., Sakurai K. The role of the helper lipid dioleoylphosphatidylethanolamine (DOPE) for DNA transfection cooperating with a cationic lipid bearing ethylenediamine. *Biochim. Biophys. Acta.* 2013;1828:412-418. <https://doi.org/10.1016/j.bbamem.2012.10.017>
61. Chesnoy S., Huang L. Structure and function of lipid–DNA complexes for gene delivery. *Annu Rev. Biophys. Biomol. Struct.* 2000;29:27-47. <https://doi.org/10.1146/annurev.biophys.29.1.27>
62. Cho S.M., Lee H.Y., Kim J.C. pH-dependent release property of dioleoylphosphatidyl ethanolamine liposomes. *Korean J. Chem. Eng.* 2008;25(2):390-393. <https://doi.org/10.1007/s11814-008-0066-6>
63. Zuidam N.J., Barenholz Y. Electrostatic and structural properties of complexes involving plasmid DNA and cationic lipids commonly used for gene delivery. *Biochim. Biophys. Acta.* 1998;1368:115-128. [https://doi.org/10.1016/s0005-2736\(97\)00187-9](https://doi.org/10.1016/s0005-2736(97)00187-9)
64. Fletcher S., Ahmad A. Perouzel E., Jorgensen M.R., Miller A.D. A dialkynoyl analogue of DOPE improves gene transfer of lower-charged, cationic lipoplexes. *Org. Biomol. Chem.* 2006;4:196-199. <https://doi.org/10.1039/b514532e>
65. Dabkowska A.P., Barlow D.J., Hughes A.V., Campbell R.A., Quinn P.J., Lawrence M.J. The effect of neutral helper lipids on the structure of cationic lipid monolayers. *J. R. Soc. Interface.* 2012;9:548-561. <https://doi.org/10.1098/rsif.2011.0356>
66. Pozzi D., Marchini C., Cardarelli F., Amenitsch H., Chiara Garulli C., Bifone A., Caracciolo G. Transfection efficiency boost of cholesterol-containing lipoplexes. *Biochim. Biophys. Acta.* 2012;1818:2335-2343. <https://doi.org/10.1016/j.bbamem.2012.05.017>
67. Yang S., Zheng Y., Chen J., Zhang Q., Zhao D., Han D., Chen X. Comprehensive study of cationic liposomes composed of DC-Chol and cholesterol with different mole ratios for gene transfection. *Colloid. Surf., B: Biointerfaces.* 2013;101:6-13. <https://doi.org/10.1016/j.colsurfb.2012.05.032>
68. Bae Y.-U., Huh J.-W., Kim B.-K., Parka H.Y., Seu Y.-B., Doh K.-O. Enhancement of liposome mediated gene transfer by adding cholesterol and cholesterol modulating drugs. *Biochim. Biophys. Acta.* 2016;1858:3017-3023. <https://doi.org/10.1016/j.bbamem.2016.09.013>
69. Duarte S., Faneca H., Pedroso de Lima M.C. Non-covalent association of folate to lipoplexes: A promising strategy to improve gene delivery in the presence of serum. *J. Controlled Release.* 2011;149:264-272. <https://doi.org/10.1016/j.jconrel.2010.10.032>
70. Metwally A.A., Blagbrough I. S. Quantitative silencing of EGFP reporter gene by self-assembled siRNA lipoplexes of LinOS and cholesterol. *Mol. Pharmaceutics.* 2012;9:3384-3395. <https://doi.org/10.1021/mp300435x>
71. Tao J., Ding W.-F., Che X.-H., Chen Y.-C., Chen F., Chen, X.-D. Ye X.-L., Xiong S.-B. Optimization of a cationic liposome-based gene delivery system for the application of miR-145 in anticancer therapeutics. *Int. J. Mol. Med.* 2016;37:1345-1354. <https://doi.org/10.3892/ijmm.2016.2530>
72. Cui S., Zhi D., Zhao Y., Chen H., Meng Y., Zhang C., Zhang S. Cationic liposomes with folic acid as targeting ligand for gene delivery. *Bioorg. Med. Chem. Lett.* 2016;26(16):4025-4029. <https://doi.org/10.1016/j.bmcl.2016.06.085>
73. Rao N.M. Cationic lipid-mediated nucleic acid delivery: beyond being cationic. *Chem. Phys. Lipids.* 2010;163:245-252. <https://doi.org/10.1016/j.chemphyslip.2010.01.001>
74. Mevel M., Neveu C., Goncalves C., Yaouanc J.-J., Pichon C. Jaffres P.-A., Midoux P. Novel neutral imidazole-lipophosphoramides for transfection assays. *Chem. Commun.* 2008;(27):3124-3126. <https://doi.org/10.1039/b805226c>
75. Bogdanenko E.V., Sviridov Yu.V., Moskovtsev A.A., Zhdanov R.I. Non-viral gene transfer *in vivo* in gene therapy. *Voprosy meditsinskoi khimii = Issues of Medicinal Chemistry.* 2000;46(3):226-245 (in Russ.).

76. Kulkarni P.R., Yadav J.D., Vaidya K.A. Liposomes: a novel drug delivery system. *Int. J. Curr. Pharm. Res.* 2010;3(2):10-18.
77. Goyal P., Goyal K., Kumar S.G., Singh A., Katare O.P., Mishra D.N. Liposomal drug delivery systems – Clinical applications. *Acta Pharm.* 2005;55:1-25.
78. Byk T., Haddada H., Vainchenker W., Louache F. Lipofectamine and related cationic lipids strongly improve adenoviral infection efficiency of primitive human hematopoietic cells. *Hum. Gene Ther.* 1998;9:2493-2502. <https://doi.org/10.1089/hum.1998.9.17-2493>
79. Masotti A., Mossa G., Cametti C., Ortaggi G., Bianco A., Grosso N.D., Malizia D., Esposito C. Comparison of different commercially available cationic liposome–DNA lipoplexes: Parameters influencing toxicity and transfection efficiency. *Colloid. Surf., B: Biointerfaces.* 2009;68:136-144. <https://doi.org/10.1016/j.colsurfb.2008.09.017>
80. Cardarelli F., Digiacoio L., Marchini C., Amici A., Salomone F., Fiume G., Rossetta A., Gratton E., Pozzi D., Caracciolo G. The intracellular trafficking mechanism of lipofectaminebased transfection reagents and its implication for gene delivery. *Scientific Rep.* 2016;6(25879). <https://doi.org/10.1038/srep25879>
81. Zhao M., Yang H., Jiang X., Zhou W., Zhu B., Zeng Y., Yao K., Ren C. Lipofectamine RNAiMAX: an efficient siRNA transfection reagent in human embryonic stem cells. *Mol. Biotechnol.* 2008;40:19-26. <https://doi.org/10.1007/s12033-008-9043-x>
82. Zuris J.A., Thompson D.B., Shu Y., Guilinger J.P., Bessen J.L., Hu J.H., Maeder M.L., Joung J.K., Chen Z.Y., Liu D.R. Cationic lipid-mediated delivery of proteins enables efficient protein-based genome editing *in vitro* and *in vivo*. *Nat. Biotechnol.* 2015; 33:73-80. <https://doi.org/10.1038/nbt.3081>
83. Cui S., Zhang S., Chen H., Wang B., Zhao Y., Zhi D. The mechanism of lipofectamine 2000 mediated transmembrane gene delivery. *Engineering.* 2012;5:172-175. <https://doi.org/10.4236/eng.2012.410b045>
84. Dalby B., Cates S., Harris A., Ohki E.C., Tilkins M.L., Price P.J., Ciccione V.C. Advanced transfection with lipofectamine 2000 reagent: primary neurons, siRNA, and high-throughput applications. *Methods.* 2004;33:95-103. <https://doi.org/10.1016/j.ymeth.2003.11.023>
85. Mo R.H., Zaro J.L., Ou J., H.J., Shen W.-C. Effects of lipofectamine 2000/siRNA complexes on autophagy in hepatoma cells. *Mol. Biotechnol.* 2012;51:1-8. <https://doi.org/10.1007/s12033-011-9422-6>
86. Markowitz D., Liu C., Gurpreet M., Cunnig C., de Mollerat du Jeu X.J. Invivofectamine™-new non-viral delivery reagent for *in vivo* delivery of Stealth™ RNAi. *Mol. Ther.* 2009;17:391. [https://doi.org/10.1016/s1525-0016\(16\)39386-8](https://doi.org/10.1016/s1525-0016(16)39386-8)
87. Schlosser K., Taha M., Stewart D.J. Systematic assessment of strategies for lung-targeted delivery of microRNA mimics. *Theranostics.* 2018;8(5):1213-1226. <https://doi.org/10.7150/thno.22912>
88. Eadon M.T., Cheng Y.-H., Hato T., Benson E.A., Ipe J., Collins K.S., De Luca T., El-Achkar T.M., Bacallao R.L., Skaar T.D., Dagher P.C. *In vivo* siRNA delivery and rebound of renal LRP2 in mice. *J. Drug. Deliv.* 2017;2017:1-12. <https://doi.org/10.1155/2017/4070793>
89. Legendre J.Y., Szoka Jr F.C. Delivery of plasmid DNA into mammalian cell lines using pH-sensitive liposomes: comparison with cationic liposomes. *Pharm. Res.* 1992;9(10):1235-1242. <https://doi.org/10.1023/a:1015836829670>
90. Wang H., Wang B., Zhang Z. H. Inhibition of corneal neovascularization by vascular endothelia growth inhibitor gene. *Int. J. Ophthalmol.* 2010;3(3):196-199. <https://doi.org/10.3980/j.issn.2222-3959.2010.03.03>
91. Barthel F., Remy J.S., Loeffler J.P., Behr J.P. Laboratory methods: Gene transfer optimization with lipospermine-coated DNA. *DNA and Cell Biology.* 1993;12(6):553-560. <https://doi.org/10.1089/dna.1993.12.553>
92. Staedel C., Remy J.S., Hua Z., Broker T.R., Chow L.T., Behr J.P. High-efficiency transfection of primary human keratinocytes with positively charged lipopolyamine: DNA complexes. *J. Invest. Dermatol.* 1994;102(5):768-772. <https://doi.org/10.1111/1523-1747.ep12377673>
93. Mahato R.I., Kawabata K., Takakura Y., Hashida M. *In vivo* disposition characteristics of plasmid DNA complexed with cationic liposomes. *J. Drug Target.* 1995;3:149-157. <https://doi.org/10.3109/10611869509059214>
94. Mahato R.I., Kawabata K., Nomura T., Takakura Y., Hashida M. Physicochemical and pharmacokinetic characteristics of plasmid DNA/cationic liposome complexes. *J. Pharm. Sci.* 1995;84(11):1267-1271. <https://doi.org/10.1002/jps.2600841102>
95. Gebhart C.L., Kabanov A.V. Evaluation of polyplexes as gene transfer agents. *J. Controlled Release.* 2001;73:401-416. [https://doi.org/10.1016/s0168-3659\(01\)00357-1](https://doi.org/10.1016/s0168-3659(01)00357-1)
96. Ciccione V., Anderson D., Jianqing Lan J., Schifferli K., Joel Jessee J. DMRIE-C Reagent for transfection of suspension cells and for RNA transfection. *Focus.* 1995;17(3):84-87.
97. Groth-Pedersen L., Aits S., Corcelle-Termeau E., Petersen N.H.T, Nylandsted J., Jaattela M. Identification of cytoskeleton-associated proteins essential for lysosomal stability and survival of human cancer cells. *Plos One.* 2012;7(10):1-11. <https://doi.org/10.1371/journal.pone.0045381>
98. Alberts B., Bray D., Lewis J., Raff M., Roberts K., Watson J. *Molecular Biology of the Cell.* 3rd Edn. New York: Garland Publishing; 1994, 1361 p.
99. Cardarelli F., Pozzi D., Bifone A., Marchini C., Caracciolo G. Cholesterol-dependent macropinocytosis and endosomal escape control the transfection efficiency of lipoplexes in CHO living cells. *Mol. Pharmaceutics.* 2012;9:334-340. <https://doi.org/10.1021/mp200374e>
100. Pozzi D., Marchini C., Cardarelli F., Salomone F., Coppola S., Montani M., Zabaleta M.E., Digman M.A., Gratton E., Colapicchioni V., Caracciolo G. Mechanistic evaluation of the transfection barriers involved in lipid-mediated gene delivery: Interplay between nanostructure and composition. *Biochim. Biophys. Acta.* 2014;1838:957-967. <https://doi.org/10.1016/j.bbame.2013.11.014>
101. Biswas J., Mishra S.K., Kondaiah P., Bhattacharya S. Syntheses, transfection efficacy and cell toxicity properties of novel cholesterol-based gemini lipids having hydroxyethyl head group. *Org. Biomol. Chem.* 2011;9:4600-4613. <https://doi.org/10.1039/c0ob00940g>
102. Ma C.-C., He Z.-Y., Xia S., Ren K., Hui L.-W., Qin H.-X., Tang M.-H., Zeng J., Song X.-R. α , ω -Cholesterol-functionalized low molecular weight polyethylene glycol as a novel modifier of cationic liposomes for gene delivery. *Int. J. Mol. Sci.* 2014;15:20339-20354. <https://doi.org/10.3390/ijms151120339>
103. Ju J., Huan M.-L., Wan N., Hou Y.-L., Ma X.-X., Jia Y.-Y., Li C., Zhou S.-Y., Zhang B.-L. Cholesterol derived cationic lipids as potential non-viral gene delivery vectors and their serum compatibility. *Bioorg. Med. Chem. Lett.* 2016;26:2401-2407. <https://doi.org/10.1016/j.bmcl.2016.04.007>

104. Meers P., Hong K., Bentz J., Papahadjopoulos D. Spermine as a modulator of membrane fusion: interactions with acidic phospholipids. *Biochemistry*. 1986;25(11):3109-3118. <https://doi.org/10.1021/bi00359a007>
105. Patil S.P., Yi J.W., Bang E.-K., Jeon E.M. Kim B.H. Synthesis and efficient siRNA delivery of polyamine-conjugated cationic nucleoside lipids. *Med. Chem. Commun.* 2011;2(6):505-508. <https://doi.org/10.1039/c1md00014d>
106. Paecharoenchai O., Niyomtham N., Apirakaramwong A., Ngawhirunpat T., Rojanarata T., Yingyongnarongkul B.-E., Opanasopit P. Structure relationship of cationic lipids on gene transfection mediated by cationic liposomes. *AAPS PharmSciTech.* 2012;13(4):1302-1308. <https://doi.org/10.1208/s12249-012-9857-5>
107. Paecharoenchai O., Niyomtham N., Ngawhirunpat T., Rojanarata T., Yingyongnarongkul B.-E., Opanasopit P. Cationic niosomes composed of spermine-based cationic lipids mediate high gene transfection efficiency. *J. Drug Target.* 2012;20(9):783-792. <https://doi.org/10.3109/1061186x.2012.716846>
108. Metwally A.A., Reelfs O., Pourzand C., Blagbrough I.S. Efficient silencing of EGFP reporter gene with siRNA delivered by asymmetrical N^4,N^9 -diacyl spermines. *Mol. Pharmaceutics.* 2012;9(7):1862-1876. <https://doi.org/10.1021/mp200429n>
109. Metwally A.A., Pourzand C., Blagbrough I.S. Efficient gene silencing by self-assembled complexes of siRNA and symmetrical fatty acid amides of spermine. *Pharmaceutics.* 2011;3(2):125-140. <https://doi.org/10.3390/pharmaceutics3020125>
110. Niyomtham N., Apiratikul N., Suksen K., Opanasopit P., Yingyongnarongkul B.-E. Synthesis and *in vitro* transfection efficiency of spermine-based cationic lipids with different central core structures and lipophilic tails. *Bioorganic and Medicinal Chemistry Letters.* 2015;25:496-503. <https://doi.org/10.1016/j.bmcl.2014.12.043>
111. Niyomtham N., Apiratikul N., Chanchang K., Opanasopit P., Yingyongnarongkul B.-E. Synergistic effect of cationic lipids with different polarheads, central core structures and hydrophobic tails on gene transfection efficiency. *Biol. Pharm. Bull.* 2014;37(9):1534-1542. <https://doi.org/10.1248/bpb.b14-00349>

About the authors:

Aleksey A. Mikheev, Researcher, The 4th Research Department, Federal State Unitary Enterprise "Scientific Center "Signal" (8, Bolshaya Olenya ul., Moscow, 107014, Russia). E-mail: aa-mixeev@mail.ru. <https://orcid.org/0000-0001-9466-0824>

Elena V. Shmendel, Cand. of Sci. (Chemistry), Associate Professor, N.A. Preobrazhensky Department of Chemistry and Technology of Biologically Active Compounds, Medical and Organic Chemistry, M.V. Lomonosov Institute of Fine Chemical Technologies, "MIREA – Russian Technological University" (86, Vernadskogo pr., Moscow, 119571, Russia). E-mail: elena_shmendel@mail.ru. <https://orcid.org/0000-0003-3727-4905>

Elizaveta S. Zhestovskaya, Researcher, The 1th Research and Analytical Department, Federal State Unitary Enterprise "Scientific Center "Signal" (8, Bolshaya Olenya ul., Moscow, 107014, Russia). E-mail: zhestovskayae@gmail.com. <https://orcid.org/0000-0002-1297-8562>

Georgy V. Nazarov, Dr. of Sci. (Chemistry), Chief Researcher, Federal State Unitary Enterprise "Scientific Center "Signal" (8, Bolshaya Olenya ul., Moscow, 107014, Russia). E-mail: denis-1000@list.ru. <https://orcid.org/0000-0001-8805-6460>

Mikhail A. Maslov, Dr. of Sci. (Chemistry), Director of the Institute of Fine Chemical Technologies, Professor at the N.A. Preobrazhensky Department of Chemistry and Technology of Biologically Active Compounds, Medical and Organic Chemistry, M.V. Lomonosov Institute of Fine Chemical Technologies, "MIREA – Russian Technological University" (86, Vernadskogo pr., Moscow, 119571, Russia). E-mail: mamaslov@mail.ru. Scopus Author ID 7003427092, <https://orcid.org/0000-0002-5372-1325>

Об авторах:

Михеев Алексей Александрович, научный сотрудник 4-го научно-исследовательского отдела Федерального государственного унитарного предприятия «Научный Центр «Сигнал» (107014, Россия, Москва, ул. Большая Оленья, д. 8). E-mail: aa-mixeev@mail.ru. <https://orcid.org/0000-0001-9466-0824>

Шмендель Елена Васильевна, кандидат химических наук, доцент кафедры химии и технологии биологически активных соединений, медицинской и органической химии им. Н.А. Преображенского Института тонких химических технологий им. М.В. Ломоносова ФГБОУ ВО «МИРЭА – Российский технологический университет» (119571, Россия, Москва, пр-т Вернадского, д. 86). E-mail: elena_shmendel@mail.ru. <https://orcid.org/0000-0003-3727-4905>

Жестовская Елизавета Сергеевна, научный сотрудник 1-го научно-аналитического отдела Федерального государственного унитарного предприятия «Научный Центр «Сигнал» (107014, Россия, Москва, ул. Большая Оленья, д. 8). E-mail: zhestovskayae@gmail.com. <https://orcid.org/0000-0002-1297-8562>

Назаров Георгий Валерьевич, доктор химических наук, главный научный сотрудник Федерального государственного унитарного предприятия «Научный центр «Сигнал» (107014, Россия, Москва, ул. Большая Оленья, д. 8). E-mail: denis-1000@list.ru. <https://orcid.org/0000-0001-8805-6460>

Маслов Михаил Александрович, доктор химических наук, директор Института тонких химических технологий, профессор кафедры химии и технологии биологически активных соединений, медицинской и органической химии им. Н.А. Преображенского Института тонких химических технологий им. М.В. Ломоносова ФГБОУ ВО «МИРЭА – Российский технологический университет» (119571, Россия, Москва, пр-т Вернадского, д. 86). E-mail: mamaslov@mail.ru. Scopus Author ID 7003427092, <https://orcid.org/0000-0002-5372-1325>

Submitted: December 23, 2019; Reviewed: January 31, 2020; Accepted: February 10, 2020.

Translated from Russian into English by H. Moshkov

Edited for English language and spelling by Enago, an editing brand of Crimson Interactive Inc.

ISSN 2686-7575 (Online)

<https://doi.org/10.32362/2410-6593-2020-15-1-28-36>



UDC 544.31; 544.27; 544.22

Thermodynamic properties of L-menthol in crystalline and gaseous states

Andrey V. Blokhin[@], Yana N. Yurkshtovich

Belarusian State University, Minsk, 220006 Belarus

[@] Corresponding author, e-mail: blokhin@bsu.by

Objectives. Menthol causes a cooling sensation and reduces the nerve activity when it is applied locally, ingested, or inhaled. This feature explains its extensive use as both an aromatizer and a flavoring agent in food manufacturing, tobacco industry, cosmetics production, as well as a mild anesthetic and antiseptic in dentistry. This work aimed to perform a comprehensive thermodynamic study of L-menthol in both crystalline and gaseous states.

Methods. To determine the combustion energy of L-menthol in the crystalline state, combustion bomb calorimetry was used. The temperature dependence of L-menthol's heat capacity in the range of 5–370 K and the melting (fusion) parameters were determined using adiabatic calorimetry. Quantum chemical calculations were performed on a standalone virtual machine in the Google Cloud Platform using an eight-core Intel Xeon Scalable Processor (Skylake) with a 2.0 GHz (up to 2.7 GHz at peak load) clock frequency and 8 GB RAM.

Results. The energy and enthalpy of L-menthol combustion in the crystalline state were determined, and the standard enthalpy of L-menthol formation in the gaseous state was calculated using the standard enthalpy of sublimation. The standard thermodynamic functions (reduced enthalpy, entropy, and reduced Gibbs energy) of L-menthol in both crystalline and liquid states were obtained based on the smoothed values of heat capacity and melting parameters. The group of isodesmic reactions for the *ab initio* calculation of the enthalpy of formation for gaseous L-menthol was substantiated. Electronic energy and frequencies of normal modes of the molecules involved in these reactions were calculated using the Gaussian 4 composite quantum chemical method. Further, the sublimation enthalpy of L-menthol was calculated using the extended Politzer equation according to the electrostatic potential model.

Conclusions. The first comprehensive thermodynamic study of L-menthol in various states of aggregation was performed, and the values calculated using semiempirical methods were consistent with the experimental values within error limits, which confirms the reliability of the results.

Keywords: L-menthol, thermodynamic properties, calorimetry, heat capacity, enthalpy of formation, phase transition parameters, quantum chemical calculations.

For citation: Blokhin A.V., Yurkshtovich Ya.N. Thermodynamic properties of L-menthol in crystalline and gaseous states. *Tonk. Khim. Tekhnol. = Fine Chem. Technol.* 2020;15(1):28-36. <https://doi.org/10.32362/2410-6593-2020-15-1-28-36>

Термодинамические свойства L-ментола в кристаллическом и газообразном состояниях

А.В. Блохин[@], Я.Н. Юркштович

Белорусский государственный университет, Минск, 220006 Беларусь

[@] Автор для переписки, e-mail: blokhin@bsu.by

Цели. Ментол при местном воздействии, употреблении в пищу или вдыхании вызывает ощущение охлаждения и снижает нервную активность, что объясняет его широкое применение в качестве отдушки и вкусовой добавки в пищевой и табачной промышленности, косметике, а также в качестве мягкого анестетика и антисептика в стоматологии. Цель работы заключалась в комплексном термодинамическом исследовании L-ментола в кристаллическом и газообразном состояниях.

Методы. Методом бомбовой калориметрии сгорания была определена энергия сгорания L-ментола в кристаллическом состоянии. Методом адиабатической калориметрии была получена температурная зависимость теплоемкости L-ментола в интервале 5–370 К и найдены его параметры плавления. Квантово-химические вычисления производились на выделенной виртуальной машине в облачном сервисе Google Cloud Platform с использованием 8 вычислительных ядер Intel Xeon Scalable Processor (Skylake) с тактовой частотой 2.0 ГГц (до 2.7 ГГц при пиковой нагрузке) и 8 ГБ оперативной памяти.

Результаты. Были определены энергия и энтальпия сгорания L-ментола в кристаллическом состоянии. С использованием величины стандартной энтальпии сублимации был выполнен расчет стандартной энтальпии образования L-ментола в газообразном состоянии. На основании сглаженных значений теплоемкости и параметров плавления получены стандартные термодинамические функции (приведенная энтальпия, энтропия и приведенная энергия Гиббса) L-ментола в кристаллическом и жидком состояниях. Обоснована группа изодесмических реакций для *ab initio* расчета энтальпии образования газообразного L-ментола, и с использованием композитного квантово-химического метода Gaussian 4 вычислены электронная энергия и частоты нормальных колебаний молекул-участников этих реакций. В рамках модели электростатического потенциала по расширенному уравнению Политцера рассчитана энтальпия сублимации L-ментола.

Выводы. Впервые было проведено комплексное термодинамическое исследование L-ментола в различных агрегатных состояниях. Величины, рассчитанные с помощью полуэмпирических методов, согласуются в пределах погрешностей с опытными величинами, что подтверждает достоверность полученных результатов.

Ключевые слова: L-ментол, термодинамические свойства, калориметрия, теплоемкость, энтальпия образования, параметры фазовых переходов, квантово-химические расчеты.

Для цитирования: Блохин А.В., Юркштович Я.Н. Термодинамические свойства L-ментола в кристаллическом и газообразном состояниях. *Тонкие химические технологии*. 2020;15(1):28-36. <https://doi.org/10.32362/2410-6593-2020-15-1-28-36>

INTRODUCTION

At present, one of the most important tasks in physical chemistry is identification and development of methods that can predict the properties of substances based on molecular structure. The possibility of *ab initio* calculation of the properties allows us to move toward the streamlined synthesis of compounds, which significantly reduces both time and cost of research.

The values of the thermodynamic properties of substances are used to calculate the thermal characteristics of reactions and a number of technological parameters,

thus actualizing their determination for as many substances as possible.

Menthol causes a cooling sensation and reduces nerve activity when applied locally, ingested, or inhaled. This feature explains its extensive use as an aromatizer and a flavoring agent in food manufacturing, tobacco industry, cosmetics production, and in dentistry—as a mild anesthetic and antiseptic [1].

To determine the standard enthalpy of combustion of L-menthol in the crystalline state at $T = 298.15$ K, combustion bomb calorimetry was used, based on which the standard enthalpies of formation of crystalline

and gaseous substances at a certain temperature were determined. Moreover, the adiabatic calorimetry method was used to examine the temperature dependence of the heat capacity of L-menthol in both crystalline and liquid states, and the temperature and enthalpy of fusion were determined. Based on the smoothed heat capacities and melting parameters, the standard thermodynamic functions of L-menthol were calculated in the temperature range of 5–370 K.

The standard enthalpy of L-menthol formation in the gaseous state was calculated using the Gaussian 4 composite quantum chemical method [2], and the sublimation enthalpy was determined using the electrostatic potential model. Furthermore, the calculated values of the formation and sublimation enthalpies agreed with the experimental values within the combined error of their determination.

MATERIALS AND METHODS

The sample of L-menthol was provided by *Belpharmatsiya*, Belarus. Its purity (the content of L-menthol in the sample), which was determined using gas-liquid chromatography, was greater than or equal to 99.98 wt %. Fractional melting was used in two sets of experiments in an adiabatic calorimeter to determine the purity and the melting (fusion) temperature of L-menthol, and these parameters were found to be 99.73 ± 0.02 mol % and 315.60 ± 0.02 K, respectively. The experimental data were then approximated by a linear equation using the ordinary least squares method:

$$T = T_{\text{fus}} - \frac{RT_{\text{fus}}^2(1-x)}{\Delta_{\text{fus}}H_m} \frac{1}{f}, \quad (1)$$

where $(1-x)$ is the molar fraction of impurities in the initial sample; f is the equilibrium fraction of the

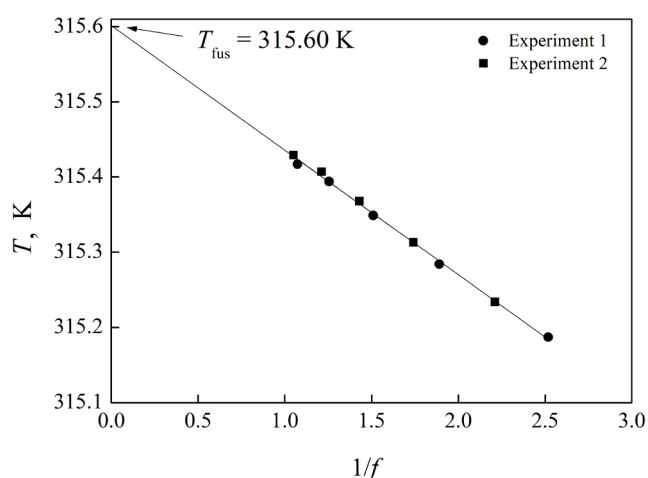


Fig. 1. Experimental results for the fractional melting of the L-menthol sample.

melt at a temperature T (equal to the ratio of the heat already used to melt the sample to the total fusion heat of the substance); and $\Delta_{\text{fus}}H_m^\circ$ ($\text{J} \times \text{mol}^{-1}$) is the fusion enthalpy of the substance at T_{fus} .

Figure 1 shows the dependence of the equilibrium temperature on the inverse melt fraction.

The enthalpy of L-menthol combustion was determined in an automatic isothermal-shell combustion calorimeter and a stationary self-sealing bomb (with a volume of 320 cm^3) [3, 4]. The temperature change during the experiment was recorded using a platinum resistance thermometer ($R = 500 \text{ } \Omega$). Furthermore, menthol was dried in a desiccator over phosphorus pentoxide before it was compressed into tablets, while the preparation of the substance for burning in the calorimeter was performed in the air. For the experiment, menthol was placed on a platinum wire ($d = 0.05 \text{ mm}$) in the form of compressed tablets. Before the start of the experiment, distilled water (1 ml) was added to the calorimetric bomb to saturate the system with water vapor. The reaction was initiated by electric current and was conducted in the oxygen atmosphere at a pressure of $\sim 30 \text{ atm}$.

The condensate formed in the bomb was quantitatively transferred to a beaker and titrated with 0.1 M NaOH solution to correct the results for the heat of nitrogen oxidation (this gas was an admixture in oxygen).

All data were read off the calorimeter using a computer. The initial and final periods contained 20 counts, and the main one contained 25 counts (interval between readouts 30 s). Table 1 shows the input parameters for calculating the combustion energy of menthol. The combustion energy was calculated considering the Washburn corrections [5].

Table 1. Input data for calculating the combustion energy of L-menthol

	Parameter	Value
1	Density, $\text{g} \times \text{cm}^{-3}$	0.946
2	Heat capacity, $\text{J} \times \text{g}^{-1} \times \text{K}^{-1}$	1.60045
3	$(\partial U / \partial P)_T$, $\text{J} \times \text{MPa}^{-1} \times \text{g}^{-1}$	−0.106
4	Heat of vaporization of platinum wire, $\text{J} \times \text{g}^{-1}$	−420

Heat capacities of crystalline and liquid L-menthol were in the range of 5–70 K and the parameters of melting were determined using a TAU-10 automatic vacuum adiabatic calorimeter (*Termis*, Moscow, Russia), according to a previously reported method [4, 6]. The temperature was measured with an iron–rhodium resistance thermometer ($R = 50 \text{ } \Omega$), placed on the inner surface of an adiabatic screen.

The adiabatic conditions in the calorimeter were maintained using a differential thermocouple (copper + 0.1% iron)/chromel and two heaters, i.e. the main one and the additional one, to eliminate temperature gradients over the length of the adiabatic shell. Heater control and visible energy detection, temperature measurements, and calculations of heat capacities in the calorimetric experiment were performed using the AK-6.25 automatic control unit.

A sample of the substance was placed in the air within a container (volume $\sim 1.0 \text{ cm}^3$) per 4/5 of its volume, and the container with the sample was degassed in vacuum for 30 min after sample loading. To ensure the rapid establishment of thermal equilibrium during calorimetric measurements, the container (after degassing) was filled with helium at 10 kPa, and then it was hermetically sealed with a bronze lid. An indium ring was used as a sealant. The container with the sample was weighed on a Mettler-Toledo AG245 balance (with a maximum error of $\pm 5 \times 10^{-5} \text{ g}$), and the hermiticity of the container was controlled by several curing cycles in the air and in vacuum to achieve a fixed mass. Liquid nitrogen was used as a refrigerant in the temperature range of 80–370 K, whereas liquid helium was used in the temperature range of 5–100 K. Error in measuring the heat capacity in the adiabatic calorimeter did not exceed $\pm 0.4\%$ in the range of 20–370 K, $\pm 1\%$ in the range of 10–20 K, and $\pm 2\%$ in the range of 5–10 K. The share of the sample's heat capacity in the total heat capacity of the filled calorimetric ampoule was greater than or equal to 45%.

The formation enthalpy of L-menthol in the gaseous state was calculated using the Gaussian 4 composite quantum chemical method. Total molecular energies and frequencies of normal modes were calculated using the GAUSSIAN 09 program. Calculations were performed on a standalone virtual machine in the Google Cloud Platform using an eight-core Intel Xeon Scalable Processor (Skylake) with a 2.0 GHz (up to 2.7 GHz at peak load) clock frequency and 8 GB RAM.

The sublimation enthalpy of L-menthol was determined using the extended Politzer equation, and the necessary molecular parameters of the substance were obtained using the Multiwfn 3.7 package.

RESULTS AND DISCUSSION

Based on a set of six experiments at $T = 298.15 \text{ K}$, the standard energy and enthalpy of combustion of L-menthol in the crystalline state were as follows:

$$\begin{aligned}\Delta_c U_{298}^\circ &= -(6304.4 \pm 1.3) \text{ kJ} \times \text{mol}^{-1}, \\ \Delta_c H_{298}^\circ &= -(3615.6 \pm 1.3) \text{ kJ} \times \text{mol}^{-1}.\end{aligned}$$

Moreover, the standard enthalpy of menthol formation in the crystalline state is

$$\Delta_f H_{298}^\circ(\text{cryst}) = -(477.8 \pm 1.9) \text{ kJ} \times \text{mol}^{-1}.$$

The standard enthalpy of menthol formation in the gaseous state at $T = 298.15 \text{ K}$, considering the recommended value of the sublimation enthalpy $\Delta_{\text{sub}} H^\circ = (84.4 \pm 1.7) \text{ kJ} \times \text{mol}^{-1}$ [7], is

$$\Delta_f H_{298}^\circ(\text{gas}) = -(393.4 \pm 2.5) \text{ kJ} \times \text{mol}^{-1}.$$

Figure 2 shows the dependence of the heat capacity of L-menthol in the condensed state on the temperature in the range of 5–370 K, under saturated vapor pressure. The values of relative atomic masses recommended by IUPAC [8] were used to calculate the molar heat capacities.

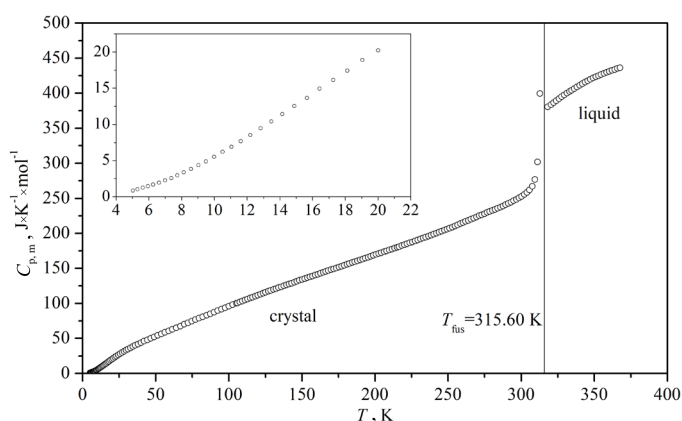


Fig. 2. Dependence of the heat capacity of L-menthol on temperature in the range of 5–370 K.

As determined in a set of four experiments at $T_{\text{fus}} = 315.60 \text{ K}$, the enthalpy and entropy of L-menthol fusion are

$$\begin{aligned}\Delta_{\text{fus}} H_m^\circ &= (13.47 \pm 0.06) \text{ J} \times \text{mol}^{-1} \times \text{K}^{-1} \text{ and} \\ \Delta_{\text{fus}} S_m^\circ &= (42.68 \pm 0.19) \text{ J} \times \text{mol}^{-1} \times \text{K}^{-1}.\end{aligned}$$

Table 2 lists the smoothed heat capacity values and standard thermodynamic functions of L-menthol in the condensed state in the range of 5–370 K. These values are also shown in Figs. 3–6.

The enthalpy of menthol formation in the gaseous state was calculated using the isodesmic reactions method (reactions in which the same number of same type bonds is preserved pre- and post-reaction). Menthol is a nonrigid molecule with a relatively large number of tops; therefore, the starting reagents have

Table 2. Standard thermodynamic functions of L-menthol in the temperature range of 5–370 K

T, K	$C_{p,\text{m}}^\circ$	$\Delta_0^T H_{\text{m}}^\circ / T$	$\Delta_0^T S_{\text{m}}^\circ$	$-\Delta_0^T G_{\text{m}}^\circ / T$
	$\text{J}\times\text{mol}^{-1}\times\text{K}^{-1}$			
Crystal				
5	0.858±0.017	0.2148±0.0043	0.2864±0.0057	0.0716±0.0014
25	27.36±0.30	10.49±0.15	15.64±0.23	5.151±0.073
50	53.14±0.21	25.84±0.19	43.18±0.40	17.34±0.14
100	95.95±0.38	50.28±0.24	93.27±0.60	42.98±0.24
150	134.0±0.5	72.00±0.32	139.5±0.8	67.55±0.34
200	169.3±0.7	91.90±0.39	182.9±1.0	91.02±0.43
250	206.5±0.8	111.0±0.5	224.6±1.1	113.6±0.5
298.15	250.1±1.0	129.8±0.5	264.6±1.3	134.7±0.6
300	252.3±1.0	130.6±0.5	266.1±1.3	135.5±0.6
315.60	272.3±1.1	137.1±0.6	279.4±1.3	142.3±0.6
Liquid				
315.60	376.1±1.5	179.8±0.7	322.1±1.5	142.3±0.6
350	422.3±1.7	201.5±0.8	363.5±1.7	162.0±0.7
370	437.0±1.7	213.9±0.9	387.5±1.8	173.6±0.8

a sufficient number of rotational degrees of freedom in the gas phase isodesmic reactions.

Table 3 lists the experimental values of the formation enthalpies of the participants of the isodesmic reactions, the electronic energy of molecules, the corrections for zero-point vibrations, and temperature correction.

Table 4 shows the values for the standard enthalpies of isodesmic reactions and the corresponding standard enthalpies of gaseous L-menthol formation.

The enthalpy of menthol formation calculated using the Gaussian 4 composite quantum chemical method agreed well with the experimental value. The good correlation between the calculated and experimental values was attributed to the proper selection of the group of isodesmic reactions, which consider the internal rotation energy of the menthol molecule owing to the inclusion of alkanes (general formula $\text{C}_n\text{H}_{2n+2}$; with a large number of spinning tops) in the isodesmic reactions. The calculations can be considered chemically accurate because the deviation from the experimental value does not exceed $4 \text{ kJ}\times\text{mol}^{-1}$.

The geometry optimization of the L-menthol molecule was performed as part of the calculations of its formation enthalpy in the gaseous state using the Gaussian 4 method. Figure 7 shows the optimized structure of the most stable L-menthol conformer.

The extended Politzer equation, which includes a measure of local polarity, has the following form [16]:

$$\Delta_{\text{sub}} H = a(SA)^2 + b\sqrt{\sigma_{\text{tot}}^2} \nu + c\Pi + d, \quad (2)$$

where SA is the molecular surface area; ν is the measure of the balance between positive and negative extremes on the surface of the molecule; σ_{tot}^2 is the measure of the potential variability on the molecular surface; and Π is the measure of local polarity.

The coefficients a , b , c , and d are selected by minimizing the deviations from the set of experimental values of sublimation enthalpies. The following coefficients were obtained previously [16]: $a = 0.0002606 \text{ kcal}\times\text{mol}^{-1}\times\text{\AA}^{-4}$; $b = 1.8247560$; $c = 0.3475950$; and $d = -0.8151050 \text{ kcal}\times\text{mol}^{-1}$.

The molecular parameters of L-menthol and its sublimation enthalpy, which was determined according to equation (2), are given in Table 5. The error in the calculated value of the sublimation enthalpy is taken as 3%. Moreover, the confidence intervals of the calculated and recommended [7] values of L-menthol sublimation enthalpy overlap with each other, which indicates the method's reliability.

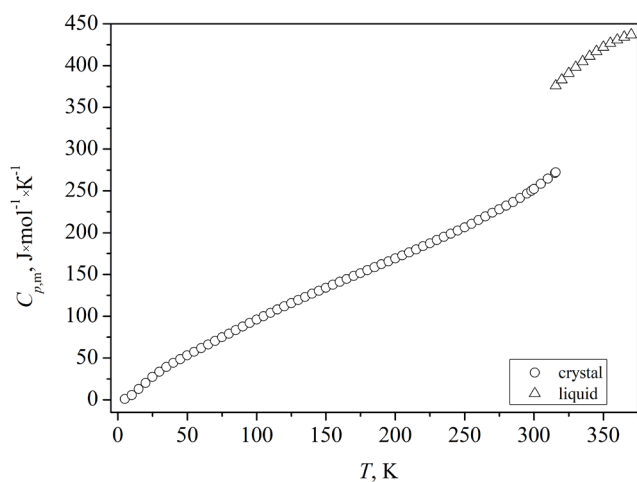


Fig. 3. Dependence of the smoothed heat capacity of L-menthol on temperature.

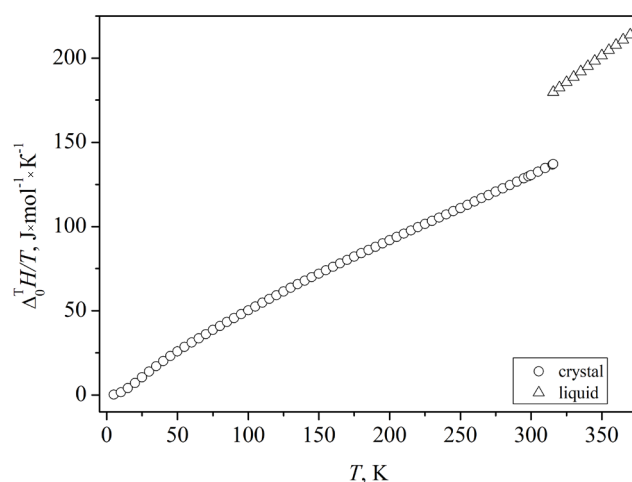


Fig. 4. Dependence of the specific enthalpy of L-menthol on temperature.

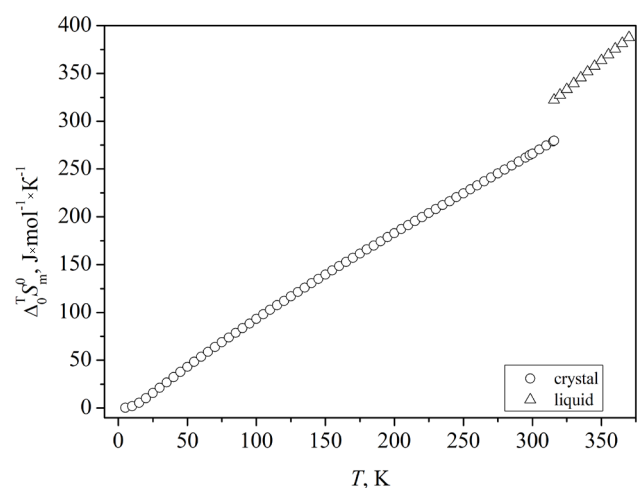


Fig. 5. Dependence of the entropy of L-menthol on temperature.

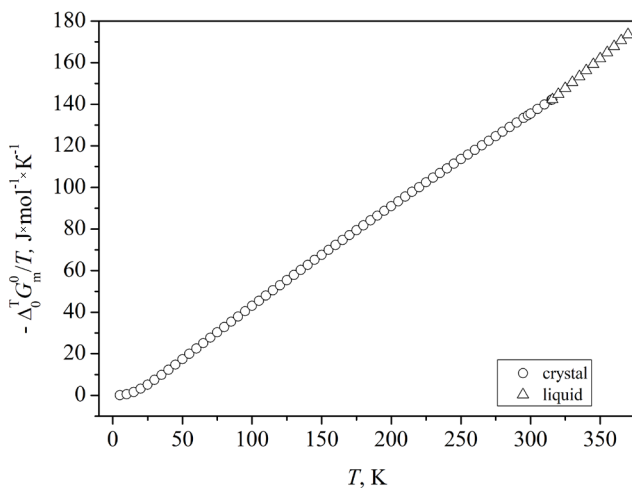


Fig. 6. Dependence of the specific Gibbs energy of L-menthol on temperature.

Table 3. Data for calculating the enthalpy of formation of L-menthol in a gaseous state using isodesmic reactions

	Compound	$\Delta_f H_{298,exp}^\circ$, kJ×mol ⁻¹	E_e , hartree	ZPVE*, hartree	ΔH_0^{298} , kJ×mol ⁻¹
a	Methane	-(74.6±0.3) [9]	-40.50941 [10]	0.044115	10.018
b	3-Methyl-1-butanol	-(301.3±1.5) [11]	-272.93124	0.162327	23.904
c	2-Butanol	-(293.0±1.5) [12]	-233.63117	0.134104	20.533
d	Ethane	-(84.0±0.4) [9]	-79.81155	0.073442	11.677
e	1-Propanol	-(257.3±0.4) [11]	-194.31848	0.106664	17.252
f	Isobutane	-(134.3±0.6) [13]	-158.42628 [10]	0.129264	11.672

Table 3. Continued

	Compound	$\Delta_f H_{298,exp}^\circ$, kJ×mol ⁻¹	E_e , hartree	ZPVE*, hartree	ΔH_0^{298} , kJ×mol ⁻¹
g	2,3-Dimethylbutane	-(177.8±1.0) [12]	-237.038739	0.184983	24.679
h	Cyclopentane	-(77.24±0.75) [15]	-196.51630 [10]	0.138268	16.273
i	2-Methylheptane	-(215.5±1.3) [14]	-315.65058	0.241232	31.942
j	2,3-Dimethylpentane	-(199.2±1.3) [14]	-276.34322	0.213000	28.451
k	Ethanol	-(234.7±0.3) [11]	-155.01281	0.078591	13.879
l	2-Methylbutane	-(154.5±0.84) [14]	-197.73172	0.157301	21.210
m	2-Methylhexane	-(195.0±1.3) [14]	-276.34430	0.213253	28.367
n	(-)-Menthol	-(393.4±2.5)	-468.26965	0.282084	35.712

* values are subject to scaling, $SF = 0.9854$.

Table 4. Standard enthalpies of isodesmic reactions and standard enthalpies of formation of L-menthol in a gaseous state

	Isodesmic reaction	$\Delta_r H_{298,exp}^\circ$, kJ×mol ⁻¹	$\Delta_f H_{298}^\circ$, kJ×mol ⁻¹
1	$h + f + e = n + 2a$	-71.6	-(391.2±1.2)
2	$b + g + d = n + 3a$	-54.0	-(393.3±2.1)
3	$h + b + d = n + 2a$	-83.0	-(396.4±1.8)
4	$b + j = n + 2a$	-46.5	-(397.8±2.1)
5	$c + j + d = n + 3a$	-42.3	-(394.7±2.2)
6	$b + i = n + d + a$	-31.8	-(390.0±2.0)
7	$l + g + k = n + 3a$	-49.3	-(392.5±1.6)
8	$m + b = n + 2a$	-44.3	-(391.4±2.1)

$$\langle \Delta_f H_{298}^\circ \rangle = -(393.4 \pm 1.9) \text{ kJ} \times \text{mol}^{-1}$$

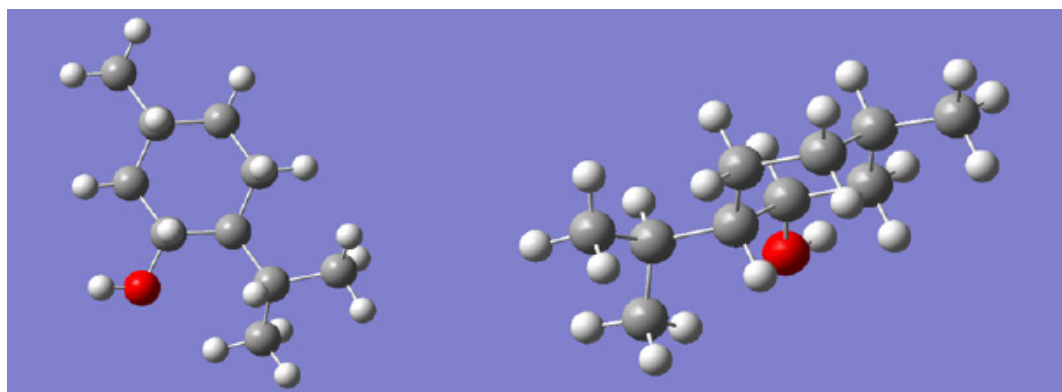


Fig. 7. Structure of the most stable conformer of L-menthol (DFT, B3LYP, 6-311G (2df, p)).

Table 5. Molecular parameters and enthalpy of sublimation of L-menthol calculated using the Politzer equation

$SA, \text{\AA}^2$	$\sigma_{tot}^2 \times \nu (\text{kcal} \times \text{mol}^{-1})^2$	$\Pi, \text{kcal} \times \text{mol}^{-1}$	$\Delta_{sub}H, \text{kcal} \times \text{mol}^{-1}$	$\Delta_{sub}H, \text{kJ} \times \text{mol}^{-1}$	$\Delta_{sub}H(\text{exp}), \text{kJ} \times \text{mol}^{-1}$
214.6	17.05	5.510	20.6±0.6	86.3±2.6	84.4±1.7

CONCLUSIONS

The standard combustion energy of crystalline L-menthol was determined using combustion bomb calorimetry, based on which the standard formation enthalpies in crystalline and gaseous states were calculated. L-menthol heat capacities in the temperature range of 5–370 K and the thermodynamic parameters of its melting were determined using the low-temperature adiabatic calorimetry method. The standard thermodynamic functions (reduced enthalpy, entropy, and reduced Gibbs energy) of L-menthol in the crystalline and liquid states were calculated. Moreover, geometry optimization and calculations of the frequencies of normal modes, electronic energy, and zero-point vibration correction

for the L-menthol molecule were performed using the Gaussian 4 composite quantum chemical method and GAUSSIAN 09 program. Moreover, the formation enthalpy in the gaseous state was obtained using isodesmic reactions. The sublimation enthalpy was calculated according to the electrostatic potential model using the Multiwfn 3.7 package. Finally, the calculated values of the formation enthalpy of the gaseous substance and the sublimation enthalpy of L-menthol were consistent with the experimental values (within error limits), thus confirming the reliability of the semiempirical methods that were used to determine the thermodynamic parameters of organic substances.

The authors declare no conflicts of interest.

REFERENCES

1. Eccles R. Menthol and Related Cooling Compounds. *J. Pharm. Pharmacol.* 1994;46(8):618-630. <https://doi.org/10.1111/j.2042-7158.1994.tb03871.x>
2. Curtiss L.A., Redfern P.C., Raghavachari K. Gaussian-4 theory. *J. Chem. Phys.* 2007;126(8):84108. <https://doi.org/10.1063/1.2436888>
3. Kabo G.J., Blokhin A.V., Kabo A.G. Investigation of thermodynamic properties of organic substances. In: Ivashkevich O.V. (Ed.) Chemical problems of the development of new materials and technologies. Iss.1. Minsk: BGU; 2003. P. 176–192.
4. Blokhin A.V., Kabo G.J., Paulechka Y.U. Thermodynamic Properties of $[\text{C}_{60}\text{mim}][\text{NTf}_2]$ in the Condensed State. *J. Chem. Eng. Data.* 2006;51(4):1377-1388. <https://doi.org/10.1021/je060094d>
5. Washburn E.W. Standard states for bomb calorimetry. *J. Res. Nat. Bur. Standards.* 1933;10:525-558.
6. Kabo G.J., Blokhin A.V., Paulechka E., Roganov G.N., Frenkel M., Yursha I.A., Diky V., Zaitsau D., Bazyleva A., Simirsky V.V., Karpushenkava L.S., Sevruck V.M. Thermodynamic properties of organic substances: Experiment, modeling, and technological applications. *J. Chem. Thermodynamics.* 2019;131:225-246. <https://doi.org/10.1016/j.jct.2018.10.025>
7. Štejfa V., Bazyleva A., Blokhin A.V. Polymorphism and thermophysical properties of L- and DL-menthol. *J. Chem. Thermodynamics.* 2019;131:524-543. <https://doi.org/10.1016/j.jct.2018.11.004>
8. IUPAC. Compendium of Chemical Terminology, 2nd ed. (the “Gold Book”). Compiled by A.D. McNaught and A. Wilkinson. Blackwell Scientific Publications, Oxford (1997). Online version (2019-) created by S.J. Chalk. ISBN 0-9678550-9-8. <https://doi.org/10.1351/goldbook>

СПИСОК ЛИТЕРАТУРЫ

1. Eccles R. Menthol and Related Cooling Compounds. *J. Pharm. Pharmacol.* 1994;46(8):618-630. <https://doi.org/10.1111/j.2042-7158.1994.tb03871.x>
2. Curtiss L.A., Redfern P.C., Raghavachari K. Gaussian-4 theory. *J. Chem. Phys.* 2007;126(8):84108. <https://doi.org/10.1063/1.2436888>
3. Kabo G.J., Blokhin A.V., Kabo A.G. Investigation of thermodynamic properties of organic substances. Chemical problems of the development of new materials and technologies: Сб. ст. Вып. 1, под. ред. О.А. Ивашкевича. Мн.: БГУ, 2003. С. 176–192.
4. Blokhin A.V., Kabo G.J., Paulechka Y.U. Thermodynamic properties of $[\text{C}_{60}\text{mim}][\text{NTf}_2]$ in the condensed state. *J. Chem. Eng. Data.* 2006;51(4):1377-1388. <https://doi.org/10.1021/je060094d>
5. Washburn E.W. Standard states for bomb calorimetry. *J. Res. Nat. Bur. Standards.* 1933;10:525-558.
6. Kabo G.J., Blokhin A.V., Paulechka E., Roganov G.N., Frenkel M., Yursha I.A., Diky V., Zaitsau D., Bazyleva A., Simirsky V.V., Karpushenkava L.S., Sevruck V.M. Thermodynamic properties of organic substances: Experiment, modeling, and technological applications. *J. Chem. Thermodynamics.* 2019;131:225-246. <https://doi.org/10.1016/j.jct.2018.10.025>
7. Štejfa V., Bazyleva A., Blokhin A.V. Polymorphism and thermophysical properties of L- and DL-menthol. *J. Chem. Thermodynamics.* 2019;131:524-543. <https://doi.org/10.1016/j.jct.2018.11.004>
8. IUPAC. Compendium of Chemical Terminology, 2nd ed. (the “Gold Book”). Compiled by A.D. McNaught and A. Wilkinson. Blackwell Scientific Publications, Oxford (1997). Online version (2019-) created by S.J. Chalk. ISBN 0-9678550-9-8. <https://doi.org/10.1351/goldbook>

9. Manion J.A. Evaluated Enthalpies of Formation of the Stable Closed-Shell C1 and C2 Chlorinated Hydrocarbons. *J. of Physical and Chemical Ref. Data*. 2002;31(1):123-127. <https://doi.org/10.1063/1.1420703>

10. EPAPS document no. E-JCPSA6-126-310707, Available from: http://ftp.aip.org/epaps/journ_chem_phys/E-JCPSA6-126-310707/ (Accessed March 15, 2019).

11. Chao J., Rossini F.D. Heats of Combustion, Formation, and Isomerization of Nineteen Alkanols. *J. Chem. Eng. Data*. 1965;10(4):374-379. <https://doi.org/10.1021/je60027a022>

12. Skinner H.A., Snelson A. The heats of combustion of the four isomeric butyl alcohols. *Transactions of the Faraday Society*. 1960;56:1776-1783. <https://doi.org/10.1039/TF9605601776>

13. Pittam D.A., Pilcher G. Measurements of heats of combustion by flame calorimetry. Part 8. Methane, ethane, propane, *n*-butane and 2-methylpropane. *J. Chem. Soc., Faraday Trans. 1*. 1972;68(0):2224-2229. <https://doi.org/10.1039/F19726802224>

14. Prosen E.J., Rossini F.D. Heats of combustion and formation of the paraffin hydrocarbons at 25°C. *J. Res. NBS*. 1945;34:263-269.

15. Prosen E.J., Johnson W.H., Rossini F.D. Heats of formation and combustion of the normal alkylcyclopentanes and cyclohexanes and the increment per CH₂ group for several homologous series of hydrocarbons. *J. Res. NBS*. 1946;37:51-56.

16. Suntsova M.A. *Prognozirovanie ental'pii obrazovaniya novykh azotsoderzhashchikh vysokoenergeticheskikh soedinenii na osnove kvantovo-khimicheskikh raschetov: dis ... kand. khim. nauk.* (Prediction of the enthalpies of formation of new nitrogen-containing high-energy compounds based on quantum chemical calculations: Cand. dissertation). Moscow: MGU, 2016. P. 101 (in Russ.).

9. Manion J.A. Evaluated Enthalpies of Formation of the Stable Closed-Shell C1 and C2 Chlorinated Hydrocarbons. *J. of Physical and Chemical Ref. Data*. 2002;31(1):123-127. <https://doi.org/10.1063/1.1420703>

10. EPAPS document no. E-JCPSA6-126-310707, URL: http://ftp.aip.org/epaps/journ_chem_phys/E-JCPSA6-126-310707/ (дата обращения: 15.03.19).

11. Chao J., Rossini F.D. Heats of Combustion, Formation, and Isomerization of Nineteen Alkanols. *J. Chem. Eng. Data*. 1965;10(4):374-379. <https://doi.org/10.1021/je60027a022>

12. Skinner H.A., Snelson A. The heats of combustion of the four isomeric butyl alcohols. *Transactions of the Faraday Society*. 1960;56:1776-1783. <https://doi.org/10.1039/TF9605601776>

13. Pittam D.A., Pilcher G. Measurements of heats of combustion by flame calorimetry. Part 8. Methane, ethane, propane, *n*-butane and 2-methylpropane. *J. Chem. Soc., Faraday Trans. 1*, 1972;68(0):2224-2229. <https://doi.org/10.1039/F19726802224>

14. Prosen E.J., Rossini F.D. Heats of combustion and formation of the paraffin hydrocarbons at 25°C. *J. Res. NBS*. 1945;34:263-269.

15. Prosen E.J., Johnson W.H., Rossini F.D. Heats of formation and combustion of the normal alkylcyclopentanes and cyclohexanes and the increment per CH₂ group for several homologous series of hydrocarbons. *J. Res. NBS*. 1946;37:51-56.

16. Сунцова М.А. Прогнозирование энтальпий образования новых азотсодержащих высокоэнергетических соединений на основе квантово-химических расчетов: дис ... канд. хим. наук. М.: МГУ, 2016. С. 101.

About the authors:

Andrey V. Blokhin, Dr. of Sci. (Chemistry), Professor, Head of the Department of Physical Chemistry, Belarusian State University (14, Leningradskaya ul., Minsk, 220006, Belarus). E-mail: blokhin@bsu.by. Scopus Author ID 7101971167, ResearcherID AAF-8122-2019, <https://orcid.org/0000-0003-4778-5872>

Yana N. Yurkshtovich, Student, Department of Physical Chemistry, Belarusian State University (14, Leningradskaya ul., Minsk, 220006, Belarus). E-mail: yanayursht@gmail.com. <https://orcid.org/0000-0002-8135-493X>

Об авторах:

Блохин Андрей Викторович, доктор химических наук, профессор, профессор кафедры физической химии Белорусского государственного университета (Беларусь, 220006, Минск, ул. Ленинградская, д. 14). E-mail: blokhin@bsu.by. Scopus Author ID 7101971167, ResearcherID AAF-8122-2019, <https://orcid.org/0000-0003-4778-5872>

Юрскиевич Яна Николаевна, студентка кафедры физической химии Белорусского государственного университета (Беларусь, 220006, Минск, ул. Ленинградская, д. 14). E-mail: yanayursht@gmail.com. <https://orcid.org/0000-0002-8135-493X>

Submitted: November 27, 2019; Reviewed: December 03, 2019; Accepted: February 04, 2020.

Translated from Russian into English by Crimson Interactive Inc. (Enago) Corporation

Improvement of high-viscosity oil production technology via the effective redistribution of energy resources

Sergey S. Rodin[@], Yuri L. Zotov, Vladimir Yu. Moroshkin, Evgeny A. Fedyanov, Evgeny V. Shishkin

Volgograd State Technical University, Volgograd, 400005 Russia

[@]Corresponding author, e-mail: rodin.s2012@yandex.ru

Objectives. The synthesis of high-viscosity oils is a fundamental aspect of oil refinement and contributes toward improvements in their production technologies. However, current methods of oil extraction are characterized by the inefficient use of energy resources. Therefore, refinement costs continue to increase. Furthermore, high production emissions affect the environment. For example, the Duosol-type process uses a large quantity of gas used in solvent recovery units in existing furnaces, and excess heat is wasted. Additionally, oil dewaxing plants use water steam, whose condensate can be contaminated with petroleum products or ketone-aromatic solvents. The purpose of this study was to identify ways of improving the efficiency of high-viscosity oil production technologies for energy efficiency and environmental safety as well as prove the feasibility of computational methods of oil production plants' improvement.

Methods. The heat quantity required for high-viscosity oil production is calculated using a thermal equation and data obtained from industrial equivalents, empirical dependencies, and reference data. The heat capacities and heat quantities of Duosol and dewaxing plants are calculated using conventional methods based on the heat recovery principle.

Results. At the solvent regeneration unit of a Duosol plant, excessive heating of the cube in one of the distillation columns was measured, leading to excessive heat consumption. This may result in contamination of the low boiling distillation component with water—one of the still bottom mixture components. Calculations show that the furnace should be divided into two chambers to lower the temperature of the column cube to help solve this problem. Water steam is currently used in the raw material preparation unit of the dewaxing plant. It has been found, however, that the quantity of heat carried away by the flue gases of the furnaces is sufficient to heat the raw material preparation unit of the oil dewaxing plant if water steam is completely excluded from this operation.

Conclusions. Technology improvement at Duosol and dewaxing plants, which are part of the process of obtaining high-viscosity oils at refineries, is possible through the effective redistribution of energy resources.

Keywords: Duosol, base oils, energy carriers, dewaxing, solvent regeneration, water steam, flue gases, production optimization.

For citation: Rodin S.S., Zotov Yu.L., Moroshkin V.Yu., Fedyanov E.A., Shishkin E.V. Improvement of high-viscosity oil production technology via the effective redistribution of energy resources. *Tonk. Khim. Tekhnol. = Fine Chem. Technol.* 2020;15(1):37-45. <https://doi.org/10.32362/2410-6593-2020-15-1-37-45>

Совершенствование технологии получения высоковязких масел с помощью эффективного перераспределения энергетических ресурсов

С.С. Родин[@], Ю.Л. Зотов, В.Ю. Морошкин, Е.А. Федянов, Е.В. Шишкин

Волгоградский государственный технический университет, Волгоград, 400005 Россия

[@] Автор для переписки, e-mail: rodin.s2012@yandex.ru

Цели. Производство высоковязких масел, как и совершенствование технологии их получения, является перспективным направлением нефтепереработки. Способы выделения масляных фракций из нефти экстракционными методами характеризуются малоэффективным использованием энергоресурсов и, как следствие, удорожанием процесса, а также относительно большим количеством выбросов, негативно влияющих на окружающую среду. Так, в процессе типа Дуосол используется большое количество природного газа, применяемого в печах на блоках регенерации селективных растворителей, избыточную теплоту которого возможно рекуперировать, а на установках депарафинизации масел используется водяной пар, конденсат которого может быть загрязнен нефтепродуктом или кетон-ароматическим растворителем. Цель данной работы заключалась в поиске путей повышения эффективности технологии получения высоковязких масел с точки зрения энергоэффективности и экологической безопасности, а также в доказательстве целесообразности вариантов улучшения установок масляного производства расчетными методами.

Методы. Количество тепла, необходимое для технологических операций, осуществляемых на установках получения высоковязких масел, определяли тепловым расчетом. Этот расчет был проведен на основании данных, полученных на промышленном аналоге; на основании эмпирических зависимостей, а также литературных справочных данных. Общепринятыми способами рассчитаны величины теплостойкости и тепловых потоков установок селективной очистки Дуосол и депарафинизации. В основу тепловых расчетов положен принцип рекуперации тепла.

Результаты. На блоке регенерации растворителя установки Дуосол выявлен избыточный нагрев куба одной из ректификационных колонн, приводящий к перерасходу тепла. Это может приводить к загрязнению низкокипящего компонента перегонки (пропана) водой, которая является одним из компонентов кубовой смеси. Расчет показал, что для решения этой проблемы целесообразно разделение печи на две камеры и понижение температуры в кубе колонны. На блоке подготовки сырья установки депарафинизации используется водяной пар. Установлено, что количество тепла, уносимого дымовыми газами печей установки Дуосол, достаточно для обеспечения теплом блока подготовки сырья установки депарафинизации масел при полном исключении водяного пара из данной операции.

Выводы. Совершенствование технологии на установках Дуосол и депарафинизации, являющихся частью процесса получения высоковязких масел на нефтеперерабатывающих заводах, возможно путем эффективного перераспределения энергоресурсов.

Ключевые слова: Дуосол, базовые масла, энергоносители, депарафинизация, регенерация растворителя, водяной пар, дымовые газы, оптимизация производства.

Для цитирования: Родин С.С., Зотов Ю.Л., Морошкин В.Ю., Федянов Е.А., Шишкин Е.В. Совершенствование технологии получения высоковязких масел с помощью эффективного перераспределения энергетических ресурсов. *Тонкие химические технологии*. 2020;15(1):37-45. <https://doi.org/10.32362/2410-6593-2020-15-1-37-45>

INTRODUCTION

Although refineries are key producers of energy, they themselves are large energy consumers. Therefore, it is no surprise that a key motivation of refineries is increasing the efficiency of oil processing,

in Russia as well as worldwide [1]. The current trend in oil refinement is the elimination of water steam as a heat and energy carrier [2]. This has been driven by tighter environmental standards controlling emissions and effluents—the inevitable waste products of oil refinement. Notably, high-viscosity oil production

is the largest consumer of energy resources among refinery types.

High-viscosity oil is a mixture of base oil obtained from oil distillation and the purification of the oil fraction with additives that create and improve certain properties of the final product. Despite the ever-expanding market of additives [3], there are negative aspects of using them with oil products [4]. Therefore, improving the technology for the production of base oils is an imperative task.

The technology used to produce motor, aviation, cylinder, compressor, transmission, and other oils combines sequential physical processes of isolating (via extraction) hydrocarbons having high-viscosity indices, improved low-temperature properties, and low-coking properties from oil fractions. Subsequent to the vacuum distillation of fuel oil, distillate fractions undergo selective purification and dewaxing, and residual fractions (i.e., tar) undergo deasphalting, selective purification, and dewaxing.

The Duosol process is a combined procedure of extracting oil fractions from tar. Subsequent to low-temperature solvent dewaxing, the fractions form the basis for highly viscous oils (e.g., MS-20) and insulating oils (e.g., KM-22). The Duosol process is based on the use of two mutually insoluble selective solvents. One of these selectively dissolves the desired

components of the feedstock, and the other dissolves the undesired ones. One of the solvents is propane, which exhibits deasphalting properties. The other is Selecto, a mixture of phenol and cresol. Thus, the Duosol process combines deasphalting and selective cleaning. As a result, a raffinate (target product) and a mixture of extract and asphalt (byproduct) are obtained [5].

MATERIALS AND METHODS

Solvents are sequentially regenerated from raffinates and extract solutions in distillation columns. The process of propane regeneration from the extract solution of a Duosol-type plant is conducted based on the technological scheme shown in Fig. 1.

The extract solution is mixed with the asphalt solution, and it sequentially passes H-5, H-18, and H-35 heat exchangers to enter the C-11 column. This column is designed to distil the main part of the propane contained in the extract solution. A vertical partition is installed at the bottom of the C-11 column. On one side of the partition, there is a suction pipe (cold part), and on the other side, there is an overflow to the C-17 column (hot part). The Selecto vapor from the C-17 column goes through the H-35 heat exchanger for dehydration, and the distillation

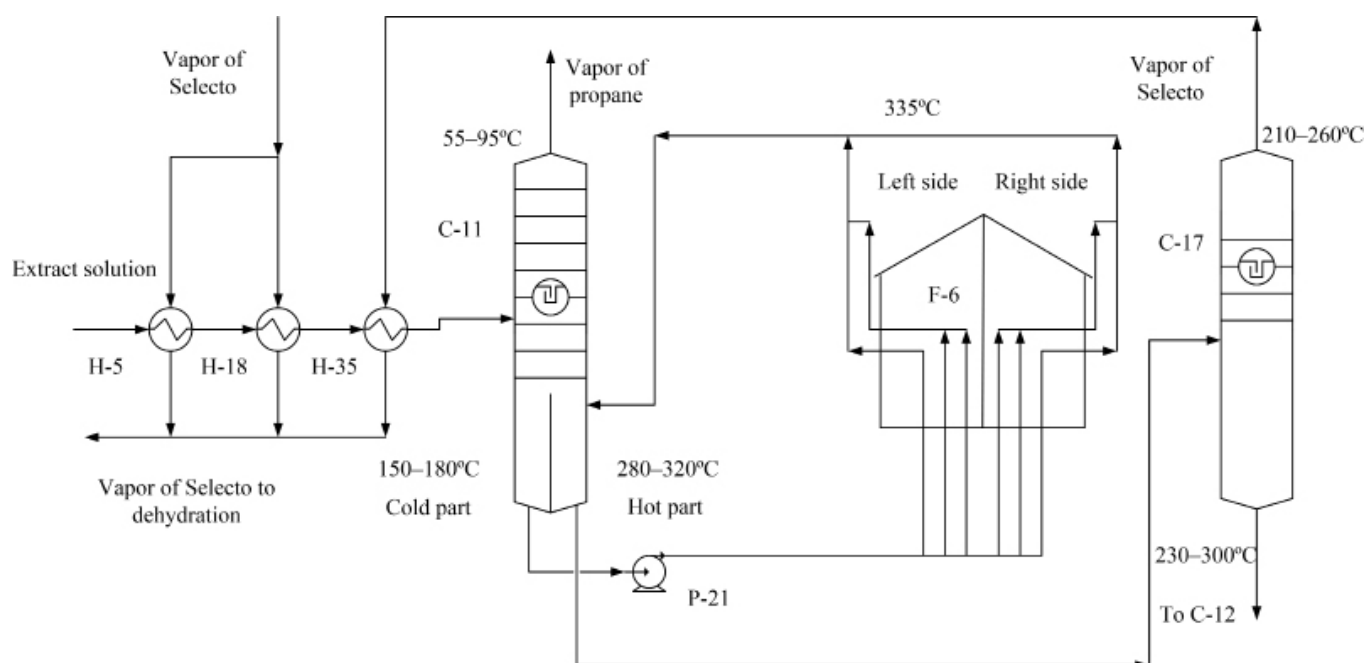


Fig. 1. Existing scheme of propane regeneration:
H-5, H-18, H-35—heat exchangers; C-11, C-17—packed columns;
F-6—furnace; P-21—pump.

residue goes to the C-12 column (not shown in the figure) and then further.

The heat required for propane evaporation is introduced by circulating the extract solution that enters the lower part of C-11 column through furnace F-6. The extract solution is obtained from the cold part of the bottom of the C-11 column using the P-21 pump and pumped in six flows through the F-6 furnace. The extract solution is heated up to 280–320°C.

The extract solution from the bottom of the C-11 column enters the C-17 column because of the pressure difference. Here, Selecto distillation takes place because of the excessive heat of the extract solution originating from the C-11 column. No additional heat supply is provided to the column.

A certain amount of dissolved water accumulated on the column plates enters the C-11 column along with the extract solution. As the temperature of the column top is lower than what is required for water removal as a vapor phase (55–95°C) and the still bottom temperature is higher than the temperature at which water removal in the liquid phase occurs, water discharge through the column top (along with the oil product) periodically occurs. This results in propane contamination with asphalt.

Analysis of the technological scheme of the solvent regeneration unit of the Duosol process, as well as the analysis of methods for increasing the distillation columns efficiency at oil refineries [6, 7], allows us to propose a decrease in the temperature of the C-11 column still bottom to the temperature required for propane separation and simultaneously organize the heating of the extract solution flow before the C-17 column to enable water removal along with the extract solution. For this, we propose to divide the F-6 furnace into two parts. One part should be used to heat the C-11 column and the other one—to heat the extract solution flow from C-11 to C-17.

Calculation of the temperature required for the regeneration of most propane from the extract solution comes down to the calculation of the heat required to convert propane to its gaseous state at a given pressure

(1.9 MPa). It is known [8] that propane saturation temperature at 1.9 MPa is 50°C, and its evaporation heat is 514.96 kJ/kg [9]. The composition of the extract solution (extract + solvent) per 100 mass parts (percent) of raw materials (tar) directed to the regeneration of solvents is known based on the data for an industrial equivalent [5]. The composition for 100 mass parts of the extract solution is provided in Table 1.

Based on the data of Table 1, one ton of the extract solution contains an average of 21% or 210 kg of propane and its conversion to gas (regeneration from solution) requires 108 141.6 kJ (the specific evaporation heat is 514.96 kJ/kg). Considering the heat capacities of the extract solution components [10] and their content in the mixture, the heat capacity of the extract solution is $c_p = 2.57 \text{ kJ}/(^{\circ}\text{C}\times\text{kg})$.

We calculate the temperature required for propane evaporation as follows:

$$T = \frac{Q}{c_p \times G}, \quad (1)$$

where Q is the amount of heat required for the evaporation of 210 kg of propane at 1.9 MPa; T is the temperature of propane evaporation from the extract solution, °C; c_p is the average heat capacity of the extract solution, kJ/(°C×kg); and G is the average propane content in the extract solution, $G = 210 \text{ kg}$.

The calculated minimal temperature for propane recovery from the extract solution is 201.16°C at 1.9 MPa. Thus, the C-11 column still bottom is heated to 280–320°C. This significantly exceeds the required temperature, and the main portion of propane can be distilled at a lower temperature. Reducing the temperature of the C-11 column still bottom would make it possible to remove water (along with the extract solution) and simultaneously organize the heating of the extract solution flow before the C-17 column. This can be done by dividing the flow from pump P-21 before furnace F-6 (the partition in the C-11

Table 1. Components of the extract solution

Component of the solution	Quantity per 100 mass parts of tar, mass %	Quantity per 100 mass parts of extract solution, mass %	Mass per 1 ton of raw materials, kg
Extract	41	10	100
Propane	86	21	210
Phenol : cresol = 1:1	277	69	690
Total	404	100	1000

still bottom should be removed) and dividing furnace F-6 into two parts. One part should be used to heat the C-11 column still bottom, and the other one—to heat the extract solution flow to C-17. One stream should be directed back to C-11, and the other one—to C-17. The suggested flow separation scheme is shown in Fig. 2.

The proposed scheme would eliminate water discharge at C-11, thus reducing the probability of propane vapor contamination with the extract, reducing the corrosion of C-11 and its service lines, and reducing the probability of asphaltene cracking by shortening its residence time in the high-temperature zone. Moreover, the temperature decrease allows reducing the consumption of fuel (natural gas) upon combustion in furnaces, which could also result in reduced energy costs.

While analyzing the production of high-viscosity oils, we noticed that the regeneration of solvent pairs (i.e., propane and phenol-cresol mixture) at Duosol plants was performed in distillation columns using the heat of the flue gases from fuel combustion in furnaces. In typical plants for solvent dewaxing, we found that water steam was used for raw material preheating (80°C).

The flue gases of the Duosol furnaces are directed into the chimneys with the outlet temperature of up to 350°C. On average, the temperature is in the range of 250–260°C. If we consider that 60–100 m³/h of natural

gas is burned (on average) every hour per one ton of the raw materials, it is clear that the recovery of this amount of heat is possible.

Water steam is used in dewaxing plants as a working fluid in ejectors of columns used for solvent regeneration from final products and for raw materials' preheating. This is required to obtain a true oil solution, from which pure paraffin crystals are separated at a later stage.

In recent years, there has been a trend of not using water steam as a working fluid in vacuum devices or as a heat transfer agent in oil refineries owing to the possibility of contaminated effluents' formation. Moreover, there is an efficient method [11] of solvent regeneration in nitrogen. Therefore, the complete repudiation of using water steam at the stage of raw material preheating is of practical interest, if water steam could be replaced by an efficient and economical energy carrier.

RESULTS AND DISCUSSION

We have proposed the redistribution of energy resources for the production of oil products at Duosol and dewaxing plants, which are often located near oil refineries. Furthermore, we have shown that it is possible to rationally design process pipelines from furnaces to heat exchangers. Using the heat of the flue gases of Duosol furnaces will allow the reduction of water vapor, and fuel gases with lower temperatures will have less impact on the environment.

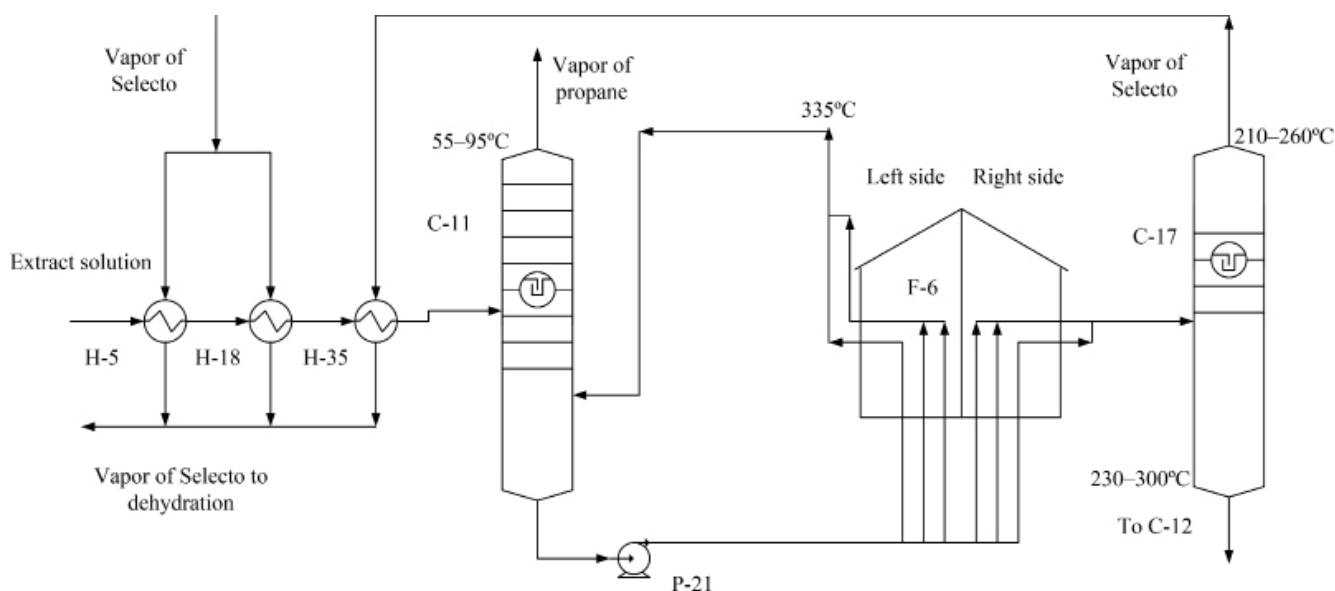


Fig. 2. Proposed scheme of propane regeneration:
H-5, H-18, H-35—heat exchangers; C-11, C-17—packed columns;
F-6—furnace; P-21—pump.

During the Duosol process, solvent pairs are used to extract the raffinate. The latter is subsequently subjected to low-temperature dewaxing using a ketone-aromatic solvent, and the extract serves as a raw material for producing oxidized bitumen. It is known that prior to leaving the unit, the main product (raffinate) and the byproduct (extract) of the Duosol process undergo solvent regeneration because of the heat of the flue gases produced by the combustion of gaseous fuels in furnaces [12].

To support the feasibility of using the heat of flue gases, a thermal calculation was presented. The amount of heat required to heat the dewaxed raw material was determined. The calculation used the initial data of the material balance of the Duosol plant. In accordance with it, 3.36 parts of propane and 3.52 parts of Selecto solvent corresponded to 1 part of tar (i.e., the raw material of the Duosol plant). The phenol-cresol ratio was 1:1.04, or 49 and 51%, respectively.

The evaporation heat of propane, phenol, and tricresol (components of Selecto) are 431 800, 446 200, and 438 800 kJ/t, respectively [13]. Therefore, we calculated the amount of heat required for the regeneration of solvent pairs with a specific productivity of one ton of raw material per hour (100 mass %) (Table 2). Hereinafter, calculations are performed for this specific productivity.

Typically, the furnaces of refinery plants use gas of their own production or natural gas from nearby pipelines. In addition to methane, fuel gases contain a certain amount of ethane (up to 0.7%), propane (up to 0.1%), butane (up to 0.1%), nitrogen (up to 2.8%), acidic CO₂ gases (up to 0.2%), and traces of sulfur compounds. Therefore, the calculation considers the composition of the energy carrier, which affects the specific heat of combustion (35.13 MJ/m³) [14]. Moreover, fuel gases contain compounds that can cause corrosion of the heat exchange equipment. When using conventional natural gas for the calculation, its specific consumption was 84.56 m³/(t_{raw mat.} × h), which is typical at Duosol refineries.

The volume V_{cp} of the combustion products of 1 m³ of natural gas (with a given composition) and

the volumetric heat capacity of these products were calculated using conventional methods [15]. In typical Duosol furnaces, 10.85 m³ of combustion products are obtained from 1 m³ of natural gas. The heat capacity of the flue gases at the outlet of a Duosol furnace pipe and accordingly, at the heat exchanger inlet is 1.4191 kJ/(m³ × K) at $t_{in} = 260^\circ\text{C}$.

The heat capacity of the flue gases at the heat exchanger outlet (at a permissible temperature of 170°C) is $c'_p = 1.4037$ kJ/(m³ × K). The permissible temperature is chosen such as to prevent the condensation of water vapor and avoid the formation of corrosive compounds that results in equipment wear.

The heat Q_{cp} that can be obtained from the flue gases of the Duosol plant in the heat exchanger of the dewaxing unit is determined by the difference in the enthalpies at the heat exchanger inlet and outlet:

$$Q_{cp} = H_{in} - H_{out} \quad (2)$$

The enthalpy of the flue gases at the heat exchanger inlet at 260°C per one ton of raw material is

$$H_{out} = c'_p \times t_{out} \times V_{cp} \times V_{gas} = 1.419 \times 260 \times 10.85 \times 84.56 = 351690 \text{ kJ/t}_{\text{raw mat.}}$$

At the heat exchanger outlet at 170°C:

$$H_{out} = c'_p \times t_{out} \times V_{cp} \times V_{gas} = 1.4037 \times 170 \times 10.85 \times 84.56 = 224320 \text{ kJ/t}_{\text{raw mat.}}$$

Then the heat Q_{cp} obtained from the flue gases in the heat exchanger (calculated per one ton of raw material) is 127 369 kJ/t_{raw mat.}

Exhaust steam (130°C, 0.3 MPa) is typically used for the preparation of raw material at dewaxing plants [14]. The amount of heat required to heat the oil (the

Table 2. Amount of heat required for solvent regeneration in the Duosol process

Solvent		mass %, (ton/ton _{raw materials})		Amount of heat, kJ/ton _{raw materials}	
Propane		336 (3.36)		1 450 848	
Selecto, of them:	Phenol	352 (3.52)	172 (1.72)	1 519 936	742 696
	Cresol		180 (1.80)		777 240
Total		788 (7.88)		2 970 784	

raffinate of the Duosol process and the raw material of the dewaxing unit) can be calculated by the following formula:

$$H_{\text{lig}} = \frac{1}{\sqrt{d_{15}^{15}}} \times (0.0015 \times T^2 + 0.726 \times T - 334.25), \quad (3)$$

where H_{lig} is the enthalpy of the liquid oil product, kJ/kg; d_{15}^{15} is the relative density of the oil product to be dewaxed; and T is temperature, K.

In this case, the relative density of the oil product to be dewaxed is 0.840, and the heating temperature is 80°C (or 353 K). On this basis, the amount of heat Q_{heat} required to heat the raw material to be dewaxed from 20 to 80°C is 122 650 kJ/t_{raw mat.}

As seen from the calculation, the heat that can be obtained from the flue gases of the Duosol furnace at 260°C meets the demand for heating at the dewaxing units for raw material preparation: $Q_{\text{cp}} > Q_{\text{heat}}$.

Considering the heat-carrier properties of the flue gases of the Duosol process, we suggest that a one-way counter-flow shell-and-tube heat exchanger be used. In this heat exchanger, the intertubular space should be used to heat the selective purification raffinates or Duosol raffinates.

Heat transfer surface F required for heating the raw material to be dewaxed can be calculated using the following formula:

$$F = \frac{Q_{\text{heat}}}{\Delta t_m \times K_T}, \quad (4)$$

where Δt_m is the average temperature difference in the heat exchanger, and K_T is the average heat transfer coefficient over the heat exchange surface.

The required heat transfer surface F at $\Delta t_m = 220^\circ\text{C}$ and $K_T = 70 \text{ W}/(\text{m}^2 \times \text{K})$ (from the gas to the organic liquid), calculated for a specific productivity of one ton raw material per hour, is 8.27 m².

CONCLUSIONS

1. To avoid propane contamination with water steam and reduce the probability of propane vapor contamination with the extract solution, we have suggested dividing the furnace of the propane regeneration unit at the Duosol plant into two chambers.

2. The heat of the flue gases leaving the Duosol furnaces, with a temperature of 260°C and above, is sufficient to preheat the raw material of the dewaxing unit.

3. For Duosol plants, we have shown the possibility of efficient redistribution of energy resources from oil production plants. For this purpose, it is necessary to partially (or completely, in the case of solvent regeneration in nitrogen) eliminate water steam. As a result, contaminated effluents at oil dewaxing plants could be avoided.

The authors declare no conflicts of interest.

REFERENCES

1. Dobrova A.A., Ilchibaeva A.K., Hidiyatullin A.S., Haritsky D.K., Antipin O.S., Khafizova S.R., Rudnev N.A. Analysis and optimization of heat transfer equipment of atmospheric and vacuum distillation of oil refining. *Neftegazokhimiya*. 2017;1:40-46 (in Russ.). <https://doi.org/10.24411/2310-8266-2017-00006>
2. Shcherbakov A.A., Dyusembaeva A.A. Modernization of regeneration solution of solvent of deparafinization plant of oils. *Herald of Omsk University*. 2018;23(4):98-102 (in Russ.). [https://doi.org/10.25513/1812-3996.2018.23\(4\).98-102](https://doi.org/10.25513/1812-3996.2018.23(4).98-102)
3. Kolchina G.Yu., Tuxvatullin R.F., Babaev E.R., Movsumzade E.M. Sterically hindered phenols as antioxidant, anticorrosion and antimicrobial additives to mineral lubricating oils. *Neftegazokhimiya*. 2017;1:10-13 (in Russ.). <https://doi.org/10.24411/2310-8266-2017-00001>
4. Vafayev O.Sh., Sottikulov E.S., Tajihodzhayev Z.A., Yuldashev N.H., Jalilov A.T. Influence of a pour-point depressant additive on qualitative indicators of diesel fuel. *Universum: Technical Sciences*. 2018;9(54) (in Russ.). Available from: <http://7universum.com/ru/tech/archive/item/6357>
5. Kapustin V.M., Tonkonogov B.P., Fuks I.T. *Tekhnologiya pererabotki nefti. Chast' 3. Proizvodstvo neftyanykh smazochnykh materialov. Uchebnoe posobie* (Oil refining technology. Part 3. Production of petroleum lubricants. Textbook). Moscow: Khimiya; 2014. 328 p. (in Russ.).

СПИСОК ЛИТЕРАТУРЫ

1. Доброва А.А., Ильчибаева А.К., Хидиятуллин А.С., Харицкий Д.К., Антипин О.С., Хафизова С.Р., Руднев Н.А. Анализ и оптимизация работы теплообменного оборудования установок атмосферно-вакуумной перегонки нефти. *НефтеГазоХимия*. 2017;1:40-46. <https://doi.org/10.24411/2310-8266-2017-00006>
2. Щербакова А.А., Дюсембаева А.А. Модернизация блока регенерации растворителя установки депарафинизации масел. *Вестник ОмГУ*. 2018;23(4):98-102. [https://doi.org/10.25513/1812-3996.2018.23\(4\).98-102](https://doi.org/10.25513/1812-3996.2018.23(4).98-102)
3. Колчина Г.Ю., Тухватуллин Р.Ф., Бабаев Э.Р., Мовсумзаде Э.М. Пространственно-затрудненные фенолы как антиокислительные, антикоррозионные и антимикробные присадки к минеральным смазочным маслам. *НефтеГазоХимия*. 2017;1:10-13. <https://doi.org/10.24411/2310-8266-2017-00001>
4. Вафаев О.Ш., Соттикулов Э.С., Таджиходжаев З.А., Юлдашев Н.Х., Джалилов А.Т. Влияния депрессорной присадки на качественные показатели дизельного топлива. *Universum: технические науки*. 2018;9(54). URL: <http://7universum.com/ru/tech/archive/item/6357>
5. Капустин В.М., Тонконогов Б.П., Фукс И.Т. *Технология переработки нефти. Часть 3. Производство нефтяных смазочных материалов. Учебное пособие*. М.: Химия; 2014. 328 с.

6. Polyakov K.M., Nosenko V.N. Influence of various feeds of distillation columns to energy consumption of the crude oil distillation unit. *Herald of Omsk University*. 2018;23(1):53-59 (in Russ.).
[https://doi.org/10.25513/1812-3996.2018.23\(1\).53-59](https://doi.org/10.25513/1812-3996.2018.23(1).53-59)
7. Ermolaeva V.A., Nikolaeva D.M., Stoletov N.G. Mathematical modeling of rectification of multicomponent mix. *International Journal of Humanities and Natural Sciences*. 2019;2-2:35-39 (in Russ.).
<https://doi.org/10.24411/2500-1000-2019-10567>
8. Sokolov B.A. *Neft'* (Oil). Sokolov V.A. (Ed.). Moscow: Nedra; 1970. 384 p. (in Russ.).
9. Tilicheev M.D. (Ed.). *Fiziko-khimicheskie svoistva individual'nykh uglevodorodov. Vypusk 4.* (Physical and chemical properties of individual hydrocarbons. Issue 4). Moscow-Leningrad: Gosudarstvennoe nauchno-tekhnicheskoe izdatel'stvo neftyanoi i gorno-toplivnoi literatury; 1953. 438 p. (in Russ.).
10. Mishchenko K.P., Ravdel' A.A. (eds.). *Kratkii spravochnik fiziko-khimicheskikh velichin* (Quick reference of physical and chemical quantities). Leningrad: Khimiya; 1974. 200 p. (in Russ.).
11. Yakovlev S.I., Kerm L.J. *Sposob regeneratsii rastvoritelya v protsessakh deparafinizatsii i obezmaslivaniya* (Method of solvent regeneration in dewaxing and deoiling processes). Pat. 2 532 808. Russian Federation: IPC C10G 21/06 C10G 21/28 C10G 73/06; applicant and patentee of the "VOKSTEK" LLC; Appl. 20.08.2013; publ. 10.11.2014 (in Russ.). Available from:
<https://patents.google.com/patent/RU2700701C1/ru>
12. Lide D.R. (Ed.). *CRC Handbook of Chemistry and Physics*. 90th edition. CRC Press; Taylor and Francis, 2009. 2828 p.
13. Golomshtok L.I., Haldej K.Z. *Snizhenie potrebleniya energii v protsessakh pererabotki nefti* (Reduction of energy consumption in oil refining processes). Moscow: Khimiya; 1990. 144 p. ISBN: 5-7245-0532-0 (Fuel and energy savings) (in Russ.).
14. Aznabaev Sh.T., Nigmatullin V.R., Nigmatullin I.R. *Izbratel'nye rastvoriteli i khladagenty v pererabotke nefiti. Spravochnoe posobie* (Selective solvents and refrigerants in oil refining: a reference guide). Olkov P.L. (Ed.). Ufa: UGNTU; 2000. 85 p. (in Russ.).
15. Kulchitskii A.R. *Topliva dlya energoustanovok. Raschet termokhimicheskikh pokazatelei: ucheb. posobie* (Fuel for power plants. Calculation of thermochemical parameters: Textbook). Kulchitskii A.R. (Ed.). Vladimir: Izdatel'stvo Vladimirskego gosudarstvennogo universiteta; 2009. 100 p. (in Russ.).
6. Поляков К.М., Носенко В.Н. Влияние различных видов питания ректификационных колонн на энергопотребление установки первичной переработки нефти. *Вестник ОмГУ*. 2018;23(1):53-59.
[https://doi.org/10.25513/1812-3996.2018.23\(1\).53-59](https://doi.org/10.25513/1812-3996.2018.23(1).53-59)
7. Ермолаева В.А., Николаева Д.М., Столетовых Н.Г. Математическое моделирование ректификации многокомпонентной смеси. *Международный журнал гуманитарных и естественных наук*. 2019;2-2:35-39.
<https://doi.org/10.24411/2500-1000-2019-10567>
8. Соколов. Б.А. *Нефть*. Соколов В.А. (ред.). М.: Недра; 1970. 384 с.
9. Тиличеев М.Д. (ред.). *Физико-химические свойства индивидуальных углеводородов*. Выпуск 4. М.: Москва - Ленинград: Государственное научно-техническое издательство нефтяной и топливной аппаратуры, 1953. 438 с.
10. Мищенко К.П., Равдель А.А. (ред.). *Краткий справочник физико-химических величин*. Л.: Химия; 1974 г. 200 с.
11. Яковлев С.И., Керм Л.Я. *Способ регенерации растворителя в процессах депарафинизации и обезмасливания*. Патент 2532 808. Российская Федерация: МПК C10G 21/06 C10G 21/28 C10G 73/06; заявитель и патентообладатель ООО «ВОКСТЭК»; заявл. 20.08.2013; опубл. 10.11.2014. URL:
<https://patents.google.com/patent/RU2700701C1/ru>
12. Lide D.R. (Ed.). *CRC Handbook of Chemistry and Physics*. 90th edition. CRC Press; Taylor and Francis, 2009. 2828 p.
13. Голомшток Л.И., Халдей К.З. *Снижение потребления энергии в процессах переработки нефти*. М.: Химия; 1990. 144 с. ISBN: 5-7245-0532-0 (Экономия топлива и электроэнергии).
14. Азнабаев Ш.Т., Нигматуллин В.Р., Нигматуллин И.Р. *Избирательные растворители и хладагенты в переработке нефти: Справочное пособие*. Ольков П.Л. (ред.). Уфа: Изд-во УГНТУ; 2000. 85 с.
15. Кульчицкий А.Р. *Топлива для энергоустановок. Расчет термодинамических показателей: учеб. пособие*. Кульчицкий А.Р. (ред.). Владимир: Изд-во Владимирского государственного университета, 2009. 100 с.

About the authors:

Sergey S. Rodin, Master Student, Chemical Technology of Natural and Carbon Materials Program, Department of Technology of Organic and Petrochemical Synthesis, Volgograd State Technical University (28, Lenina pr., Volgograd, 400005 Russia). E-mail: rodin.s2012@yandex.ru. <http://orcid.org/0000-0001-8683-6519>

Yuri L. Zotov, Dr. of Sci. (Chemistry), Professor, Department of Technology of Organic and Petrochemical Synthesis, Volgograd State Technical University (28, Lenina pr., Volgograd, 400005 Russia). E-mail: ylzotov@mail.ru. Scopus Author ID 7003371961, <http://orcid.org/0000-0001-6301-0570>

Vladimir Yu. Moroshkin, Leading Specialist, Technical Supervision Department, LUKOIL-Volgogradneftepererabotka LLC (55, 40 let Komsomola ul., Volgograd, 400029 Russia). E-mail: vmoros@yandex.ru. <http://orcid.org/0000-0002-7206-2580>

Evgeny A. Fedyanov, Dr. of Sci. (Engineering), Professor, Head of the Department of Heat Engineering and Hydraulics, Volgograd State Technical University (28, Lenina pr., Volgograd, 400005 Russia). E-mail: fedyanov@vstu.ru. Scopus Author ID 6507068214, Researcher ID Q-7217-2017, <http://orcid.org/0000-0001-8718-8808>

Eugeny V. Shishkin, Dr. of Sci. (Chemistry), Professor, Department of Technology of Organic and Petrochemical Synthesis, Dean of the Department of Chemistry and Technology, Volgograd State Technical University (28, Lenina pr., Volgograd, 400005 Russia). E-mail: shishkin@vstu.ru. Scopus Author ID 7004314557, <http://orcid.org/0000-0002-2994-422X>

Об авторах:

Родин Сергей Сергеевич, магистрант программы подготовки «Химическая технология природных энергоносителей и углеродных материалов» кафедры «Технология органического и нефтехимического синтеза» Волгоградского государственного технического университета (Россия, 400005, г. Волгоград, проспект им. В.И. Ленина, д. 28). E-mail: rodin.s2012@yandex.ru. <http://orcid.org/0000-0001-8683-6519>

Зотов Юрий Львович, доктор химических наук, профессор кафедры «Технология органического и нефтехимического синтеза» Волгоградского государственного технического университета (Россия, 400005, г. Волгоград, проспект им. В.И. Ленина, д. 28). E-mail: ylzotov@mail.ru. Scopus Author ID 7003371961, <http://orcid.org/0000-0001-6301-0570>

Морошкин Владимир Юрьевич, ведущий специалист отдела технического надзора ООО «ЛУКОЙЛ-Волгограднефтепереработка» (Россия, 400029, г. Волгоград, ул. 40 лет ВЛКСМ, 55). E-mail: vmoros@yandex.ru. <http://orcid.org/0000-0002-7206-2580>

Федянов Евгений Алексеевич, доктор технических наук, профессор, заведующий кафедрой «Теплотехника и гидравлика» Волгоградского государственного технического университета (Россия, 400005, г. Волгоград, проспект им. В.И. Ленина, д. 28). E-mail: fedyanov@vstu.ru. Scopus Author ID 6507068214, Researcher ID Q-7217-2017, <http://orcid.org/0000-0001-8718-8808>

Шишкин Евгений Вениаминович, доктор химических наук, профессор кафедры «Технология органического и нефтехимического синтеза», декан химико-технологического факультета Волгоградского государственного технического университета (Россия, 400005, г. Волгоград, проспект им. В.И. Ленина, д. 28). E-mail: shishkin@vstu.ru. Scopus Author ID 7004314557, <http://orcid.org/0000-0002-2994-422X>

Submitted: October 08, 2019; Reviewed: October 29, 2019; Accepted: February 03, 2020.

Translated from Russian into English by M. Povorin

Edited for English language and spelling by Enago, an editing brand of Crimson Interactive Inc.

ISSN 2686-7575 (Online)

<https://doi.org/10.32362/2410-6593-2019-15-1-46-54>



UDC 66.0:519.6

Drawing PT-phase envelopes and calculating critical points for multicomponent systems using flash calculations

Luis A. Toro^{1,2,@}

¹Departamento de Matemáticas y Estadística, Universidad Nacional de Colombia sede Manizales, Cra. 27 No. 64-60, Manizales, Colombia

²Departamento de Física y Matemáticas, Universidad Autónoma de Manizales, Antigua Estación del Ferrocarril, Manizales, Colombia

@Corresponding author, e-mail: latoroc@unal.edu.co

Objectives. This study aims to draw PT-phase envelopes and calculate the critical points for multicomponent systems using flash calculations.

Methods. Flash calculations with an equation of state and a mixing rule were used to construct phase envelopes for multicomponent systems. In general, the methodology uses the Soave-Redlich-Kwong equation of state and Van der Waals mixing rules; and the Peng-Robinson equation of state with Wong-Sandler mixing rules and the non-random two-liquid activity coefficient model.

Results. The method was applied to the following mixtures: ethane (1)-butane (2) (four different compositions); ethane (1)-propane (2) (four different compositions); butane (1)-carbon dioxide (2) (three different compositions); C2C3C4C5C6 (one composition); isobutane-methanol-methyl tert-butyl ether-1-butene (one composition); and propylene-water-isopropyl alcohol-diisopropyl ether (one composition).

Conclusions. Our results agreed to a large extent with the experimental data available in the literature. For mixtures that contained CO₂, the best results were obtained using the Peng-Robinson equation of state and the Wong-Sandler mixing rules. Our methodology, based on flash calculations, equations of state, and mixing rules, may be viewed as a shortcut procedure for drawing phase envelopes and estimating critical points of multicomponent systems.

Keywords: flash calculations, critical points, phase envelopes.

For citation: Toro L.A. Drawing PT-phase envelopes and calculating critical points for multicomponent systems using flash calculations. *Tonk. Khim. Tekhnol. = Fine Chem. Technol.* 2020;15(1):46-54. <https://doi.org/10.32362/2410-6593-2020-15-1-46-54>

Построение РТ-фазовых диаграмм и расчет критических точек для многокомпонентных систем с использованием флэш-вычислений

Л.А. Торо^{1,2,@}

¹Факультет математики и статистики, Национальный университет Колумбии, Штаб-квартира Манизалес, Манизалес, Колумбия

²Факультет физики и математики, Автономный университет Манизалеса, Манизалес, Колумбия

@ Автор для переписки, e-mail: latoroc@unal.edu.co

Цели. Построение РТ-фазовых диаграмм и расчет критических точек для многокомпонентных систем с использованием флэш-вычислений.

Методы. Для построения фазовых диаграмм многокомпонентных систем использовали флэш-вычисления на основе уравнения состояния и правила смешения. В общем случае методология использует уравнение состояния Соаве–Редлиха–Квонга и правило смешения Ван дер Ваальса; уравнение состояния Пенга–Робинсона и правило смешения Вонга–Сэндлера, а также неслучайная двухжидкостная модель активных коэффициентов.

Результаты. Метод был применен к следующим смесям: этан (1)–бутан (2) (четыре разных состава); этан (1)–пропан (2) (четыре разных состава); бутан (1)–диоксид углерода (2) (три разных состава); C2C3C4C5C6 (один состав); изобутан–метанол–метил-трет-бутиловый эфир–1-бутен (один состав); и пропилен–вода–изопропиловый спирт–диизопропиловый эфир (ДИПЭ) (один состав).

Выводы. Согласно нашим результатам, метод флэш-вычислений, базирующийся на уравнении состояния и правилах смешения, используемый для построения фазовых диаграмм, на основе которых проводится оценка критических точек для многокомпонентных смесей, хорошо согласуется с экспериментальными данными, имеющимися в литературе. Для смесей, содержащих CO₂, лучшие результаты получены с использованием уравнения состояния Пенга–Робинсона и правила смешения Вонга–Сэндлера.

Ключевые слова: флэш-вычисления, критические точки, фазовые диаграммы.

Для цитирования: Toro L.A. Drawing PT-phase envelopes and calculating critical points for multicomponent systems using flash calculations. *Tonk. Khim. Tekhnol. = Fine Chem. Technol.* 2020;15(1):46-54. <https://doi.org/10.32362/2410-6593-2020-15-1-46-54>

INTRODUCTION

The knowledge of phase envelopes and critical points is valuable for the calculation of phase equilibria and solving various problems in chemical engineering. Also, from a modeling point of view, knowledge of critical data is of paramount importance, as it provides information about real fluids, as well as characterizes phase change boundaries in mixtures with the help of phase diagrams. Through the combination of excess properties, phase equilibrium data, and critical data, it is possible to encompass the major thermodynamic aspects of multicomponent mixtures. In this paper, we present a methodology of constructing phase envelopes of multicomponent mixtures, from which the critical points follow. In the available literature, there is a variety of methods (both theoretical and experimental) to construct and estimate critical points.

A methodology has been proposed [1] to calculate critical points of multicomponent mixtures using a modification of the Gibbs plane tangent. A group of researchers [2] solved the Heidemann and Khalil formulation [3] using a Newton method with defined intervals to calculate critical points of binary and ternary mixtures.

Calculations of the critical points of multicomponent mixtures have been reported [4–6], where the optimization problem was solved in such a way that the function to minimize is the Gibbs plane tangent criterion. Other researchers [7] have also solved the Heidemann and Khalil formulation with a simulated annealing algorithm [8, 9] and determined the critical properties of some multicomponent mixtures. Besides, predictive equations of state have been used [10] to construct natural gas phase envelopes and to calculate its critical points.

A general algorithm has been suggested [11] for the calculation of dew and bubble points for multicomponent mixtures, representing a continuation method that can be used to draw phase envelopes and estimate critical points. The Soave–Redlich–Kwong equation of state (SRK EoS) and its derivatives have been used [12] to construct the phase envelope of binary mixtures, with dew and bubble point calculations.

Another study [13] reports the use of the perturbed-chain statistical associating fluid theory (PC-SAFT) equation of state to calculate critical points of multicomponent mixtures containing hydrocarbons and non-hydrocarbon components. Furthermore, the simplified critical-point criteria [14] have been presented for some multicomponent systems, based on a thermodynamic model where the Helmholtz energy depends on the composition average model parameters. There is also a report [15] on a method for calculation of critical points for refrigerant mixtures, using mixture models based on Helmholtz energy equations of state. The Peng–Robinson (PR), SAFT, and PC-SAFT equations of state have been used [16] for calculating critical points of hydrocarbon mixtures. The development of a new flow apparatus is reported [17] for the experimental determination of critical points of pure components and binary mixtures. Moreover, a dynamic-synthetic apparatus [18] can be used to determine the critical properties of pure and multicomponent mixtures.

From a theoretical point of view, the aforementioned methods for drawing phase envelopes and calculating critical points of multicomponent mixtures require sophisticated mathematical procedures and complex algorithms. It is possible to do the same task for some mixtures, using the flash evaporation that is a well-known operation of separation in chemical engineering [19, 20]. The simple mathematical model of this operation permits several calculations, such as bubble and dew points, molar fractions in the phases (vapor and liquid) for constructing vapor–liquid equilibrium diagrams for mixtures, evaporated fraction, isotherms and vapor pressures versus temperature for pure substances.

In this report, we used flash calculations with an equation of state and a mixing rule to construct phase envelopes for multicomponent systems, from which the critical points of mixtures are estimated. This methodology was applied to some binary and multicomponent mixtures reported in the literature, and our results are in good agreement with the reported data. In general, the methodology uses the SRK EoS and Van der Waals (VdW) mixing rules; but for mixtures that contain CO₂, the best results were obtained with the PR EoS and Wong–Sandler mixing rules (WS MR). The presented methodology might be seen as a shortcut procedure when an easy method for drawing phase envelopes and estimating critical points of a multicomponent system is needed.

MATERIALS AND METHODS

Suppose that a stream F is fed to a flash evaporator with a global composition $z = [z_1, z_2, \dots, z_n]$ (molar fraction) of n components. The pressure P and temperature T are constant in the evaporator. Depending on the nature of the components and the feed composition, there is a vapor phase and one or two liquid phases. The first situation is shown in Fig. 1. The outlet streams, V and L , are in equilibrium at P and T .

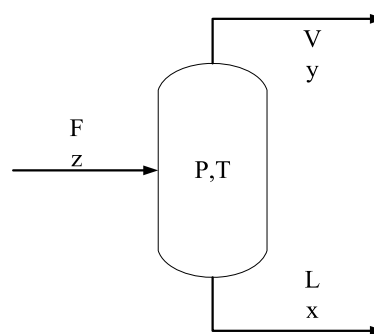


Fig. 1. Flash evaporator scheme.

Applying the material balance for the i -component, it follows that

$$Fz_i = Lx_i + Vy_i, i = 1, 2, \dots, n. \quad (1)$$

Since the outlet streams are in equilibrium, then

$$y_i = K_i x_i, i = 1, 2, \dots, n. \quad (2)$$

A total material balance gives

$$F = L + V. \quad (3)$$

Let α be

$$\alpha = \frac{V}{F}. \quad (4)$$

From equations (3) and (4) we obtain

$$z_i = (1 - \alpha)x_i + \alpha K_i x_i, i = 1, 2, \dots, n. \quad (5)$$

Plugging (5) into (1) gives

$$z_i = (1 - \alpha)x_i + \alpha y_i, i = 1, 2, \dots, n. \quad (6)$$

Using (2), an equivalent equation is

$$z_i = (1 - \alpha)x_i + \alpha K_i x_i, i = 1, 2, \dots, n. \quad (7)$$

The molar fraction condition gives the following equations in both phases:

$$\sum_{i=1}^n x_i = 1, \sum_{i=1}^n y_i = 1. \quad (8)$$

From (8)

$$\sum_{i=1}^n x_i - \sum_{i=1}^n y_i = 0. \quad (9)$$

To draw the phase envelope for a multicomponent mixture, the following procedure is implemented. From equation (4), if $\alpha = 0$, there is no vapor phase as $V = 0$ and only the liquid phase exists. Thus, bubble point calculation is made and a bubble point curve is obtained. If $\alpha = 1$, there is no liquid phase as $L = 0$ and only the vapor phase exists. Then, a dew point calculation is made and a dew point curve is obtained. By drawing the two curves in the same coordinates (PT-system), we observe their intersection in the critical point of the mixture and the PT-phase envelope is obtained.

Next, the construction of a bubble point curve is explained. In this case, $\alpha = 0$ and the only known data is $z = [z_1, z_2, \dots, z_n]$ that is held constant. It is necessary to calculate the equilibrium compositions from equation (2), that depends on K_i and this is unknown, but it is also possible to use an EoS such as SRK or PR (with the appropriate mixing rules), that involves the equilibrium compositions that is the $\phi - \phi$ method [21]:

$$K_i = \phi_{\text{liq}} / \phi_{\text{vap}}. \quad (10)$$

When the WS MR are used in PR EoS [22], the excess Helmholtz free energy, at infinite pressure, is equal to the excess Gibbs free energy, and the non-random two-liquid (NRTL) activity coefficient model is adopted for the calculation of required parameters for WS MR [23].

Combining equations (6), (7), (9), (10) (from EoS), a set of nonlinear equations containing temperature, pressure, equilibrium compositions, and constants as unknowns is obtained and needs to be solved. For the solution of the final nonlinear equation system, a *Matlab* code that incorporates its built-in function *fsolve* was written, and it was used for drawing the dew point curve for which $\alpha = 1$. For obtaining the points in both curves, α is varied and P is calculated along with the equilibrium compositions and corresponding constants. The initial equilibrium compositions and temperature must be guesstimated for testing convergence. This is necessary to avoid unreal results.

RESULTS AND DISCUSSION

In this section, the results obtained by applying the exposed methodology to several mixtures are shown. The relative error ε_r is calculated as follows:

$$\varepsilon_r = \left| \frac{\text{Exp. value} - \text{Calc. value}}{\text{Exp. value}} \right| \times 100. \quad (11)$$

Ethane (1)–n-butane (2) system

This system was studied in four different compositions. For drawing the phase envelopes for this system, SRK EoS with VdW mixing rule and a binary interaction parameter $k_{ij} = 0.0$ were used. Figure 2 shows the graphical results for this system.

Table 1 summarizes the results for critical points of the studied system and from this, we conclude that the calculated data are in good agreement with the experimental data.

Ethane (1)–propane (2) system

This system was studied in four different compositions. For drawing the phase envelopes for this system, SRK EoS with VdW mixing rule and a binary interaction parameter $k_{ij} = 0.0$ were used. Figure 3 shows the graphical results for this system.

Table 2 summarizes the results for critical points of the studied system, and from this we conclude that the calculated data are in good agreement with the experimental ones.

Multicomponent systems

Three multicomponent systems were studied. For drawing the phase envelopes of such systems, SRK EoS with VdW mixing rule and a binary interaction parameter $k_{ij} = 0.0$ were employed. Figure 4 shows the graphical results of the studied systems. The results reported in [11] are in a graphical form, too. The critical points of the mixtures were read from such graphics. The comparison between both results is shown in Table 3. Despite 10.63% in critical pressure, the results obtained by the presented methodology are in good agreement with the literature.

n-Butane (1)–carbon dioxide (2) system

This system was studied in three different compositions. The binary interaction parameter used in all mixing rules for PR and SRK was 0.133. The following mixing rules (MR) were used: a) VdW; b) WS; c) VdW; d) WS; e) VdW; and f) WS. Figure 5 shows the graphical results for this system. As follows from Fig. 5, the best results were obtained with PR EoS and the NRTL activity model.

Table 4 shows the results for critical points of the studied system, and from this, we conclude that the calculated data are in good agreement with the experimental data, when using PR EoS and the NRTL activity model.

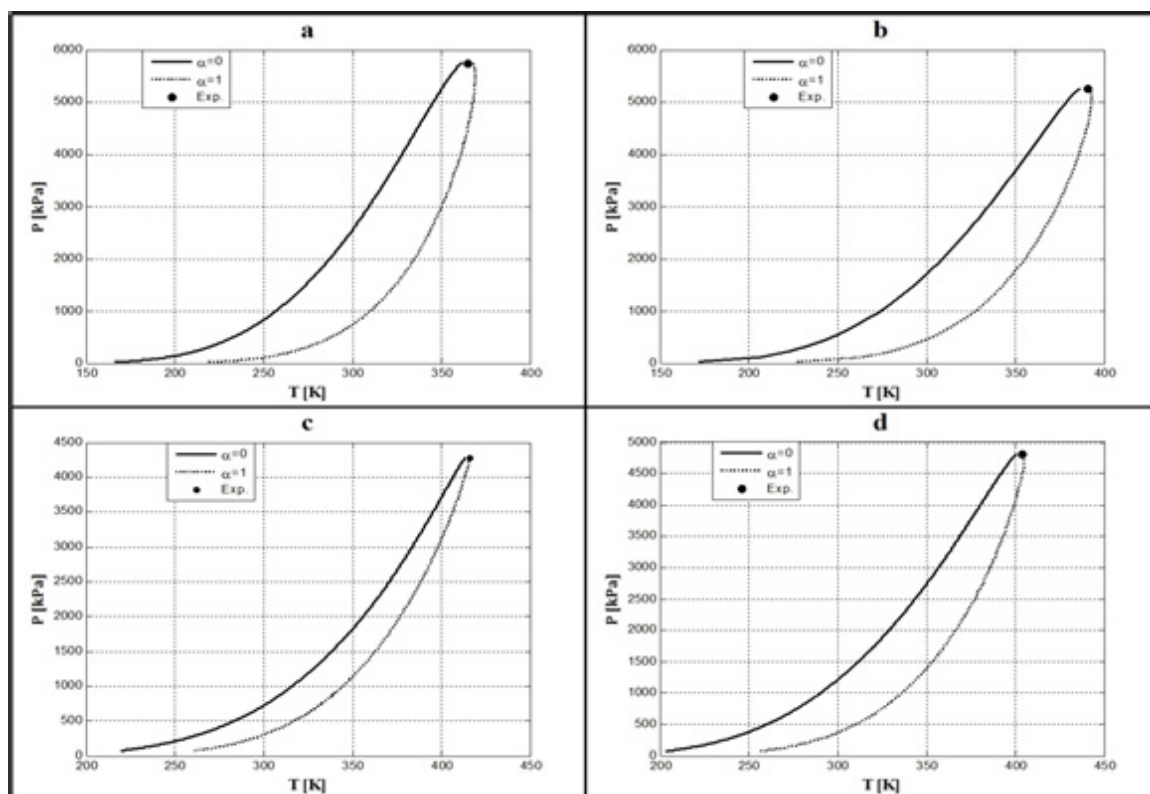


Fig. 2. Ethane (1)–n-butane (2) mixtures. Phase envelope using SRK EoS and VdW MR.
a) $z = [0.5605 \ 0.4395]$; **b)** $z = [0.4402 \ 0.5598]$; **c)** $z = [0.1496 \ 0.8504]$; **d)** $z = [0.2990 \ 0.7010]$.

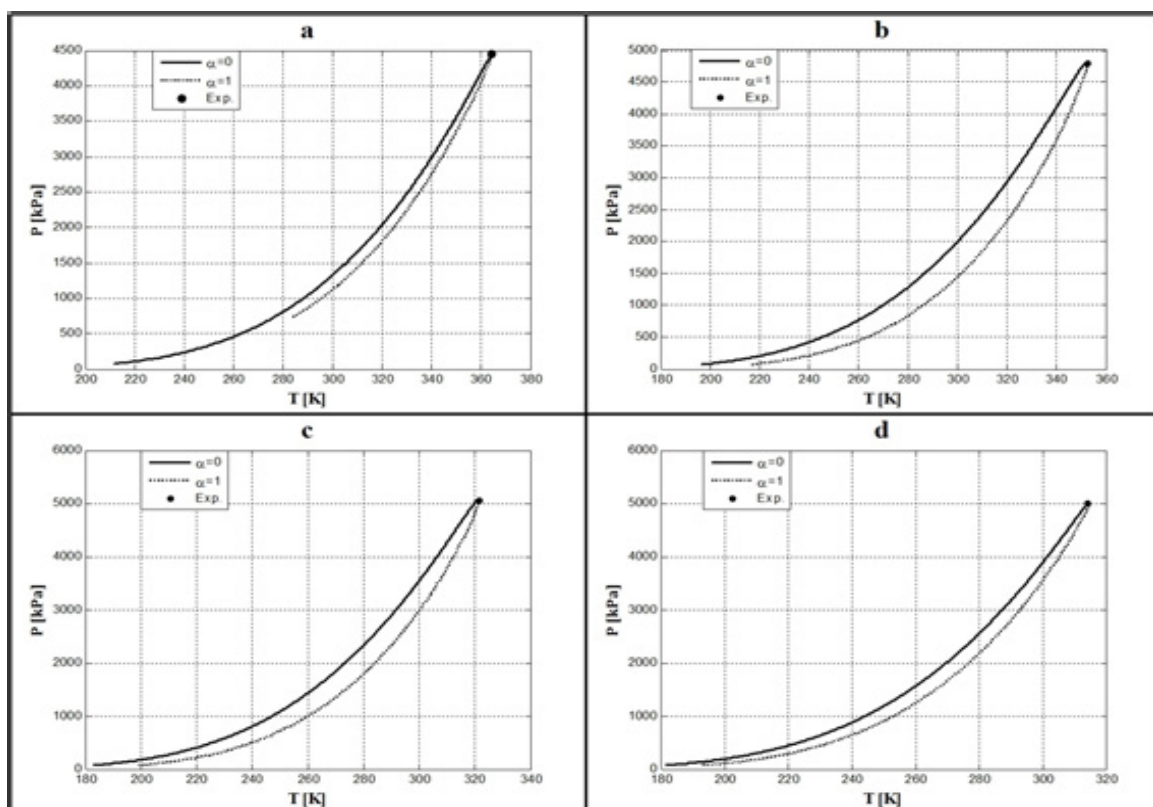


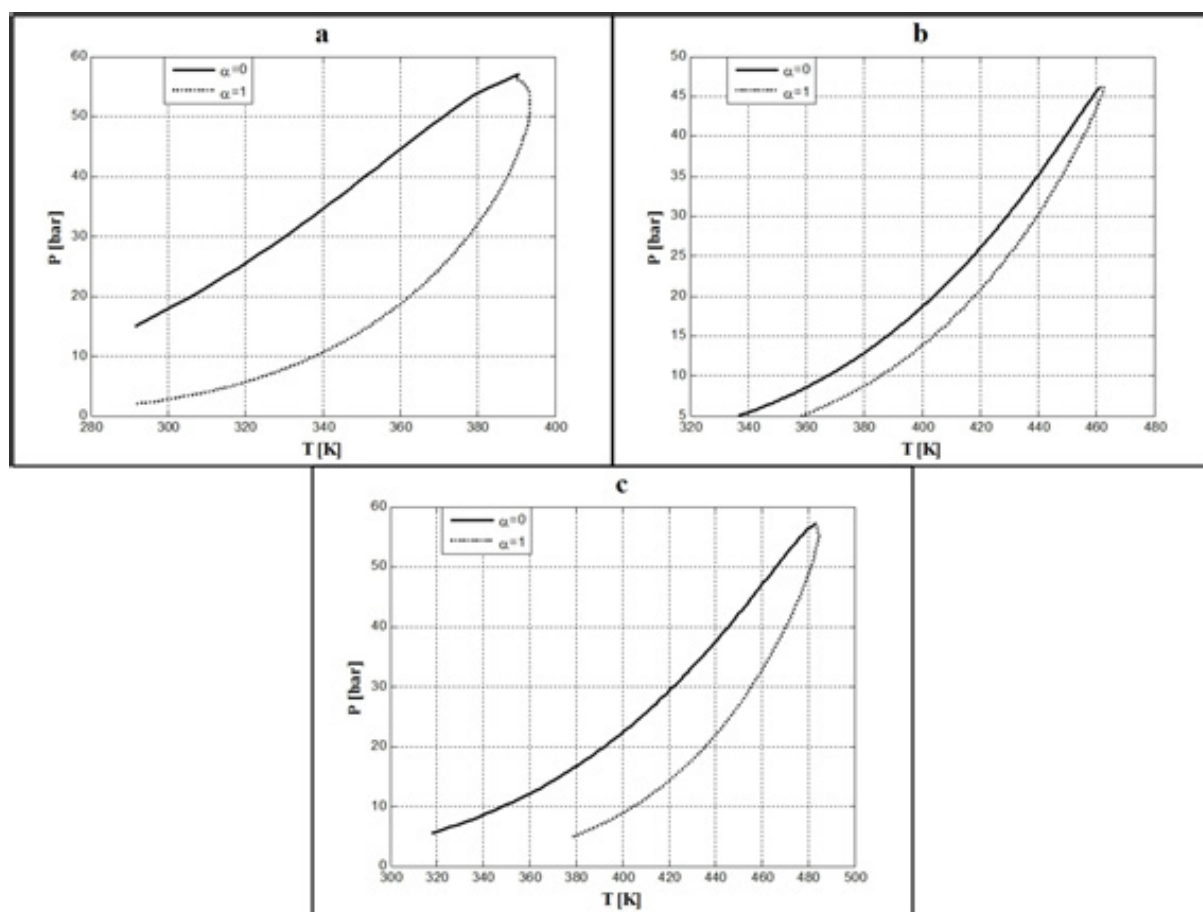
Fig. 3. Ethane (1)–propane (2) mixtures. Phase envelope using SRK EoS and VdW MR.
a) $z = [0.1202 \ 0.8798]$; **b)** $z = [0.3598 \ 0.6402]$; **c)** $z = [0.8205 \ 0.1795]$; **d)** $z = [0.8997 \ 0.1003]$.

Table 1. Ethane (1)–*n*-butane (2) mixtures; comparison with experimental results [5]

z_1	T_c (K) (calc.)	P_c (kPa) (calc.)	T_c (K) (exp.)	P_c (kPa) (exp.)	$\varepsilon_r T_c$	$\varepsilon_r P_c$
0.5605	379.5	5597	377.54	5598	0.52	0.02
0.4402	392.2	5266	390.67	5266	0.39	0.00
0.1496	415.8	4285	415.72	4285	0.02	0.00
0.2990	404.8	4810	403.82	4810	0.24	0.00

Table 2. Ethane (1)–propane (2) mixtures; comparison with experimental results [5]

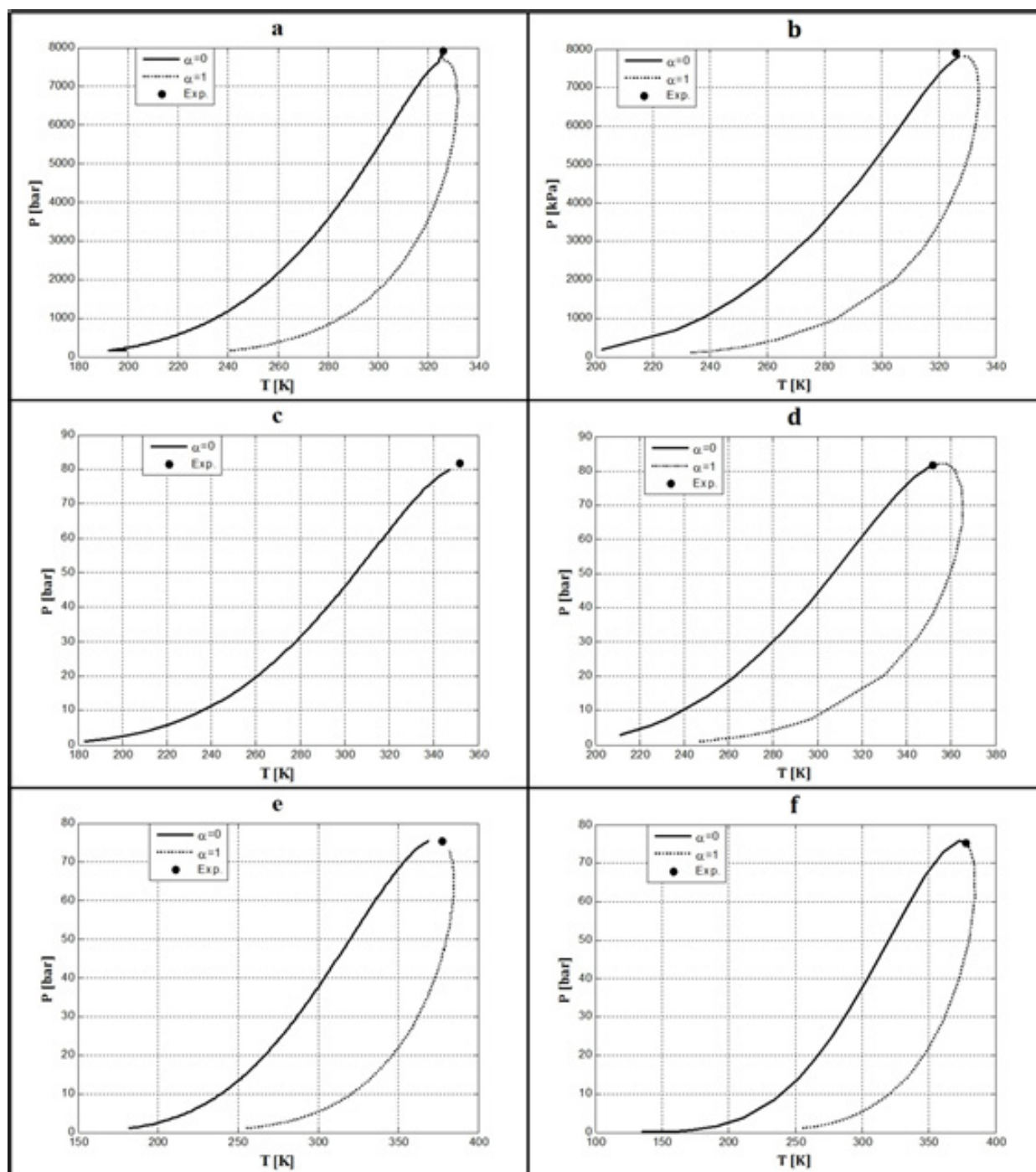
z_1	T_c (K) (calc.)	P_c (kPa) (calc.)	T_c (K) (exp.)	P_c (kPa) (exp.)	$\varepsilon_r T_c$	$\varepsilon_r P_c$
0.1202	364.6	4447	363.96	4447	0.180	0.000
0.3598	352.4	4798	352.45	4798	0.014	0.000
0.8205	321.4	5065	321.38	5065	0.060	0.000
0.8997	314.7	5017	314.10	5017	0.190	0.000

**Fig. 4.** Multicomponent mixtures. Phase envelopes using SRK EoS and VdW MR.

- a) C2C3C4C5C6 mixture, $z = [0.39842 \ 0.29313 \ 0.20006 \ 0.07143 \ 0.03696]$;
 b) isobutane–methanol–MTBE–1-butene mixture, $z = [0.25 \ 0.25 \ 0.25 \ 0.25]$;
 c) propylene–water–isopropyl alcohol (IPA)–diisopropyl ether (DIPE) mixture,
 $z = [0.25 \ 0.25 \ 0.25 \ 0.25]$.

Table 3. Multicomponent mixtures; comparison with reported data [11]

System	T_c (K) (calc.)	P_c (bar) (calc.)	T_c (K) (from graphics)	P_c (kPa) (from graphics)	$\varepsilon_r T_c$	$\varepsilon_r P_c$
a)	390.71	57	390	56	0.18	1.79
b)	462.52	46.45	459	46	0.77	0.98
c)	483.07	57.2	64	493	2.01	10.63


Fig. 5. *n*-Butane (1)–carbon dioxide (2) mixtures. Phase envelope using PR EoS.

a) VdW MR, $z = [0.1694 \ 0.8306]$; b) WS MR, $z = [0.1694 \ 0.8306]$;
c) VdW MR, $z = [0.3334 \ 0.6666]$; d) WS MR, $z = [0.3334 \ 0.6666]$;
e) VdW MR, $z = [0.4984 \ 0.5016]$; f) WS MR, $z = [0.4984 \ 0.5016]$.

Table 4. *n*-Butane (1)–carbon dioxide (2) mixtures; comparison with experimental results [5]

z_i	$T_c(\text{K})$ (calc.)	$P_c(\text{kPa})$ (calc.)	$T_c(\text{K})$ (exp.)	$P_c(\text{kPa})$ (exp.)	$\varepsilon_r T_c$	$\varepsilon_r P_c$
0.1694	327.94	7815.99	325.9	7908	0.6300	1.1600
0.3334	351.67	8169.68	351.7	8170	0.0085	0.0039
0.4984	377.27	7535.68	377.2	7536	0.0190	0.0042

Table 4 shows the results for critical points of the studied system, and from this, we conclude that the calculated data are in good agreement with the experimental data, when using PR EoS and the NRTL activity model.

CONCLUSIONS

This work presents a methodology (based on flash evaporation) for drawing phase envelopes, from which critical points of multicomponent mixtures can be estimated. The SRK EoS with VdW MR, SRK EoS with WS MR, and NRTL activity coefficient model were used. For the studied mixtures whose experimental critical data are available in the literature, our results were in good agreement with the experimental data. The methodology was capable of reproducing phase

envelopes for multicomponent mixtures reported in [11], where a method which included the solution of a set of ordinary differential equations was used for drawing the phase envelopes. For the *n*-butane (1)–carbon dioxide (2) mixtures, both SRK and PR EoS were used, and the best results were obtained with PR EoS (WS MR and NRTL activity coefficient model). It is important to note that when the presented methodology was applied to the systems ethane (1)–*n*-butane (2), ethane (1)–propane (2), and *n*-butane (1)–carbon dioxide (2), the results were basically the same as when global optimization for obtaining critical points was applied to these systems, as reported in [5]. The presented methodology may be viewed as a shortcut procedure when an easy method for drawing the phase envelopes and estimating critical points of a multicomponent system is needed.

REFERENCES

- Michelsen M.L. Calculation of Phase Envelopes and Critical Points for Multicomponent Mixtures. *Fluid Phase Equilibria*. 1980;4(1-2):1-10.
[https://doi.org/10.1016/0378-3812\(80\)80001-X](https://doi.org/10.1016/0378-3812(80)80001-X)
- Stradi A.B., Brennecke F.J., Khon P.J., Stadtherr A.M. Reliable Computation of Mixture Critical Points. *A.I.Ch.E. Journal*. 2001;47(1):212-221.
<https://doi.org/10.1002/aic.690470121>
- Heidemann R.A., Khalil A.M. The Calculation of Critical Points. *A.I.Ch.E. Journal*. 1980;26(5):769-779.
<https://doi.org/10.1002/aic.690260510>
- Henderson N., Freitas L., Platt M.G. Prediction of Critical Points: a new methodology using global optimization. *A.I.Ch.E. Journal*. 2004;50(6):1300-1314.
<https://doi.org/10.1002/aic.10119>
- Freitas L., Platt G., Henderson N. Novel approach for the calculation of critical points in binary mixtures using global optimization. *Fluid Phase Equilibria*. 2004;225:29-37.
<https://doi.org/10.1016/j.fluid.2004.06.063>
- Justo-García D.N., García-Sánchez F. Cálculo de Puntos Críticos de sistemas multicomponentes utilizando optimización global. XX Congreso Nacional de Termodinámica. Apizaco, Tlaxcala, 5-9 de Septiembre de 2005. P. 342-366 (in Spanish).
- Sánchez-Mares F., Bonilla-Petriciolet A. Cálculo de Puntos Críticos empleando una estrategia de optimización global estocástica. *Afinidad*. 2005;63(525):396-403 (in Spanish).
- Goffe W.L., Ferrier G.D., Rogers J. Global Optimization of statistical functions with simulated annealing. *J. Econometrics*. 1994;60(1-2):65-99.
[https://doi.org/10.1016/0304-4076\(94\)90038-8](https://doi.org/10.1016/0304-4076(94)90038-8)
- Corana A., Marchesi M., Martini C., Ridella S. Minimizing multimodal functions of continuous variables with simulated annealing algorithm. *ACM Trans. Math. Software*. 1987;13(3):262-280.
<http://dx.doi.org/10.1145/29380.29864>
- Tabrizi F.F., Nasrifar Kh. Application of predictive equations of state in calculating natural gas phase envelopes and critical points. *Journal of Natural Gas Science and Engineering*. 2010;2(1):21-28.
<https://doi.org/10.1016/j.jngse.2009.12.005>
- Cardona C.A., Sánchez C.A., Gutiérrez L.F. *Destilación Reactiva: Análisis y Diseño Básico*. Manizales, Colombia: Universidad Nacional de Colombia; 2007 (in Spanish).
- Reid R.C., Prausnitz J.M., Poling B.E. *The Properties of Gases and Liquids*. 4th Edition. New York: McGraw-Hill; 1987. 741 p.
- Justo-García D.N., García-Sánchez F., Díaz-Ramírez N.L., Romero-Martínez A. Calculation of critical points for multicomponent mixtures containing hydrocarbon and nonhydrocarbon components with the PC-SAFT equation of state. *Phase Fluid Equilibria*. 2008;265:192-194.
<https://doi.org/10.1016/j.fluid.2007.12.006>
- Jun Cai, Ying Hu, Prausnitz J.M. Simplified critical-point criteria for some multicomponent systems. *Chemical Engineering Science*. 2010;65(8):2443-2453.
<https://doi.org/10.1016/j.ces.2009.11.024>
- Akasaka R. Calculation of the critical point for mixtures using mixture models based on Helmholtz energy equations of state. *Fluid Phase Equilibria*. 2008;263(1):102-108.
<https://doi.org/10.1016/j.fluid.2007.10.007>

16. Alfradique M.F., Castier M. Critical points of hydrocarbon mixtures with the Peng-Robinson, SAFT, and PC-SAFT equations of state. *Fluid Phase Equilibria*. 2007;257(1):78-101.
<https://doi.org/10.1016/j.fluid.2007.05.012>
17. Horstman S., Fisher K., Gahmeling J. Experimental determination of critical points of pure components and binary mixtures using a flow apparatus. *Chemical Engineering & Technology*. 1999;22(10):839-842.
[https://doi.org/10.1002/\(SICI\)1521-4125\(199910\)22:10%3C839::AID-CEAT839%3E3.0.CO;2-L](https://doi.org/10.1002/(SICI)1521-4125(199910)22:10%3C839::AID-CEAT839%3E3.0.CO;2-L)
18. Chien-Bin Soo, Thévenau P., Coqulet C., Ramjugemath D., Richon D. Determination of critical points of pure and multi-component mixtures using a “dynamic-synthetic” apparatus. *J. of Supercritical Fluids*. 2010;55(2):545-553.
<https://doi.org/10.1016/j.supflu.2010.10.022>
19. Holland Ch.D. *Fundamentos de destilación de mezclas multicomponentes*. Limusa, Noriega Editores; 1992. 200 p. (in Spanish).
20. Seader J.D., Henley E.J. *Separation Process Principles*. 2nd Edition. John Wiley and Sons, Inc. 2006. 800 p.
21. Smith J.M., Van Ness H.C., Abbott M.M. *Introducción a la Termodinámica en Ingeniería Química*. McGraw-Hill; 2007. 836 p. (in Spanish).
22. Peng D., Robinson D.D. A New Two-Constant Equation of State. *Ind. Eng. Chem. Fund.* 1976;15(1):59-64.
<https://doi.org/10.1021/i160057a011>
23. Tester J.W., Modell M. *Thermodynamics and Its Applications*, 3rd Edition. Prentice Hall. 1996. 960 p.

About the author:

Luis A. Toro, Associate Professor, Ph.D. (Eng.), Doctor of Philosophy, Mathematics, Department of Mathematics and Statistics, National University of Colombia (headquarters Manizales, Manizales-Caldas, Colombia); Autonomous University of Manizales, Manizales-Caldas, Colombia (Autónoma University of Manizales). E-mail: latoroc@unal.edu.co.
<https://orcid.org/0000-0002-6706-8179>

Об авторе:

Торо Луис Альберто, доктор философии, доцент, Национальный университет Колумбии (штаб-квартира Манизалес, Манизалес-Кальдас, Колумбия); Автономный университет Манизалеса (Колумбия). E-mail: latoroc@unal.edu.co.
<https://orcid.org/0000-0002-6706-8179>

Submitted: December 18, 2019; Reviewed: January 16, 2020; Accepted: February 10, 2020.

The text was submitted by the author in English.

Edited for English language and spelling by Enago, an editing brand of Crimson Interactive Inc.

ISSN 2686-7575 (Online)

<https://doi.org/10.32362/2410-6593-2019-15-1-55-61>

UDC 547.729

Investigation of propylene carbonate synthesis regularities by the interaction of propylene glycol with carbamide

Aleksandr V. Sulimov[@], Anna V. Ovcharova, Grigory M. Kravchenko, Yulia K. Sulimova

Nizhny Novgorod State Technical University n.a. R.E. Alekseev, Nizhny Novgorod, 603950 Russia

[@]Corresponding author, e-mail: epoxide@mail.ru

Objectives. Cyclic carbonates are important products of organic synthesis, which are widely used as solvents, catalysts, and reagents for the production of various compounds (in particular, urethane-containing polymers) by the non-isocyanate method. The process of carbamide alcoholysis with polybasic alcohols is a promising method for the synthesis of cyclic carbonates. The purpose of this study is to determine the reaction conditions for the interaction of propylene glycol with carbamide in the presence of zinc acetate as a catalyst.

Methods. We conducted experiments to study the synthesis of propylene carbonate in a batch laboratory apparatus. Moreover, we analyzed the starting reagents and final products using gas-liquid chromatography.

Results. We studied the synthesis of propylene carbonate by carbamide alcoholysis with propylene glycol in the presence of a catalyst (zinc acetate) by varying the following parameters: initial molar ratio of propylene glycol/carbamide = (0.5–5):1, synthesis temperature 130–190°C, reagent residence time in the reactor 0.5–4 h, and the catalyst amount in the reaction mixture 0–1.5 wt %.

Conclusions. We determined the technological parameters of propylene carbonate synthesis in a batch reactor. Moreover, we showed that the process allowed the production of propylene carbonate with a sufficiently high yield of 80%—at the initial molar ratio of propylene glycol/carbamide = 3:1, temperature 170°C, and residence time 2 h.

Keywords: cyclocarbonates, propylene carbonate, propylene glycol, carbamide, catalysis.

For citation: Sulimov A.V., Ovcharova A.V., Kravchenko G.M., Sulimova Yu.K. Investigation of propylene carbonate synthesis regularities by the interaction of propylene glycol with carbamide. *Tonk. Khim. Tekhnol. = Fine Chem. Technol.* 2020;15(1):55-61. <https://doi.org/10.32362/2410-6593-2020-15-1-55-61>

Изучение закономерностей синтеза пропиленкарбоната взаимодействием пропиленгликоля с карбамидом

А.В. Сулимов[@], А.В. Овчарова, Г.М. Кравченко, Ю.К. Сулимова

Нижегородский государственный технический университет им. Р.Е. Алексеева, Нижний Новгород, 603950 Россия

[@]Автор для переписки, e-mail: epoxide@mail.ru

Цели. Циклические карбонаты являются важными продуктами органического синтеза, которые находят широкое применение в качестве растворителей, катализаторов и реагентов для получения ряда соединений, в частности, уретансодержащих полимеров неизоцианатным методом. Одним из перспективных методов их синтеза является процесс алкоголиза карбамида многоосновными спиртами. Цель данной работы – определение условий реакции взаимодействия пропиленгликоля с карбамидом в присутствии ацетата цинка в качестве катализатора.

Методы. Экспериментальное исследование процесса синтеза пропиленкарбоната на лабораторной установке периодического действия. Анализ исходных реагентов и полученных продуктов с использованием газожидкостной хроматографии.

Результаты. Изучены закономерности получения пропиленкарбоната алкоголизом карбамида пропиленгликолем в присутствии катализатора (ацетата цинка) при варьировании основных параметров процесса в следующих диапазонах: начальное молярное соотношение реагентов пропиленгликоль/карбамид составляло (0.5–5):1, температура синтеза 130–190 °С, время пребывания реагентов в реакторе 0.5–4 ч, содержание катализатора в реакционной смеси 0–1.5 масс. %.

Выводы. Рекомендованы технологические параметры синтеза пропиленкарбоната, протекающего в реакторе периодического действия. Показано, что осуществление процесса при начальном молярном соотношении пропиленгликоля и карбамида 3:1, при температуре 170 °С и времени пребывания 2 ч позволяет получать пропиленкарбонат с достаточно высоким выходом – 80%.

Ключевые слова: циклокарбонаты, пропиленкарбонат, пропиленгликоль, карбамид, катализ.

Для цитирования: Сулимов А.В., Овчарова А.В., Кравченко Г.М., Сулимова Ю.К. Изучение закономерностей синтеза пропиленкарбоната взаимодействием пропиленгликоля с карбамидом. *Тонкие химические технологии*. 2020;15(1):55-61. <https://doi.org/10.32362/2410-6593-2020-15-1-55-61>

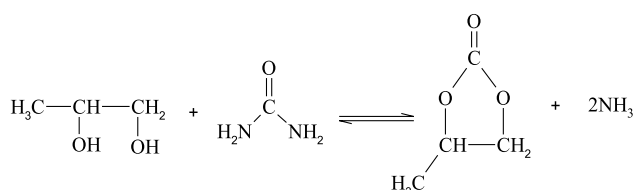
INTRODUCTION

Propylene carbonate is an important product of organic synthesis. Because it possesses a number of valuable properties, it is widely used as a solvent and intermediate product in various syntheses. Its use as a solvent is attributed to the good dissolving ability, low toxicity, biodegradability, and high boiling point. Propylene carbonate is used in the production of polyacrylonitrile fibers, in the separation of CO₂ and H₂S, as a component of lubricating oils, hydraulic fluids, and electrolytes in lithium-ion batteries [1]. In addition, propylene carbonate is used as a starting component to obtain polymer compositions in pharmaceuticals [2] and in the synthesis of dimethyl carbonate [3].

Currently, propylene carbonate is commercially produced by the direct cyclocarboxylation of propylene oxide with carbon dioxide under catalysis by alkali metal

salts, ammonium, phosphines, and metal complexes [4]. However, in addition to the traditional disadvantages inherent to homogeneous catalytic processes, this method is characterized by the rather stringent conditions of implementation (200°C and 5–10 MPa) [5]. Economic and environmental requirements dictate the need to develop new catalytic systems and technological processes for the synthesis of propylene carbonate.

A promising method for producing propylene carbonate is the interaction of propylene glycol and carbamide [6]:



The undoubted advantage of this process is that it is based on available raw materials, which can be obtained from renewable sources. Specifically, carbamide under industrial conditions is obtained by the interaction of ammonia and carbon dioxide; the reserves of the latter in the environment are practically inexhaustible [7, 8]. Propylene glycol is commercially produced from propylene oxide. However, even today, when the chemical market is oversaturated with bio-glycerin, many studies are published on its transformation to propylene glycol [9, 10]; in the future, the proportion of propylene glycol will only increase [11]. In general, possible options for raw materials for obtaining propylene carbonate can be represented as a diagram (Fig. 1).

The direct cyclocarboxylation of propylene oxide or propylene glycol is of considerable interest. However, this process, even when implemented on an industrial scale, is characterized by certain disadvantages (e.g., the need to use very high pressures) [5]. It is worth noting the studies regarding the catalytic systems based on

ionic liquids and various metal complexes [12–14]. The use of these catalysts allows the cyclocarboxylation of propylene oxide to be carried out with carbon dioxide at low temperatures and pressures. Despite the rather high yield of propylene carbonate (greater than 90–95%), the process of obtaining such catalytic systems is complex and expensive, which casts doubt on the possibility of their industrial use, at least in the near future.

The use of propylene glycol and carbamide to produce propylene carbonate allows the process to be carried out under milder conditions at lower temperatures (130–180°C) and pressures (0.05–0.1 MPa) [15]. The possibility of its implementation is determined by the presence of effective catalytic systems. Previous studies [15, 16] have shown that metal acetates can catalyze the reaction of propylene glycol with carbamide to form propylene carbonate. Moreover, zinc acetate is most active in this process [16]. Therefore, we have investigated the synthesis of propylene carbonate by the interaction of propylene glycol with carbamide in the presence of zinc acetate as a catalyst.

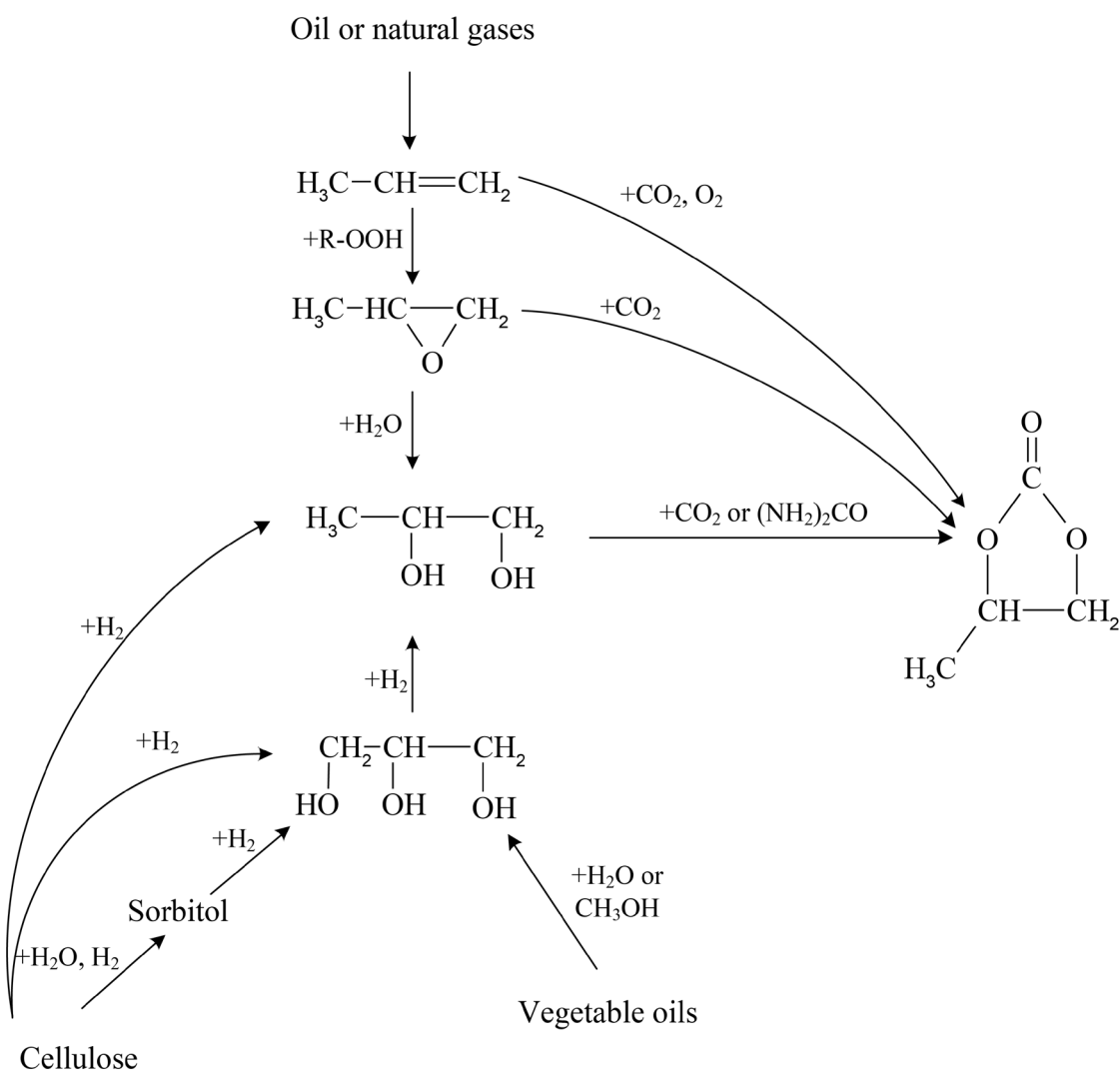


Fig. 1. Possible routes for the synthesis of propylene carbonate.

MATERIALS AND METHODS

The following reagents were used in this study (the purity grade is indicated in brackets): propylene glycol (puriss.), carbamide (p.a.), zinc acetate (p.a.).

The synthesis of propylene carbonate was carried out in a batch laboratory apparatus consisting of a glass reactor with electric heating, a reflux condenser, a temperature measurement and control system, and a magnetic mixing device. The calculated amounts of propylene glycol, carbamide, and zinc acetate were loaded into the reactor, and the heating and stirring of the reaction mixture were started. Upon reaching the set temperature, the start time of the synthesis was recorded. The reaction mass was kept for a certain time (0.5–4 h) at a constant temperature (130–190°C). At the end of the synthesis, samples (0.5 g) were taken from the reaction mass and quantitatively dissolved in the excess amount of absolute isopropyl alcohol.

The analysis of the reaction mixtures to determine the content of propylene glycol and propylene carbonate was carried out by gas chromatography on a Chromos GC-1000 instrument equipped with a flame ionization detector on a VB-1701 capillary column (30 m × 0.25 mm × 0.25 μm). Helium was used as the carrier gas; its flow rate through the column was 60 mL × min⁻¹. The temperatures of the evaporator and column thermostat were maintained at 200°C and 150°C, respectively. The technique was evaluated based on 5–7 parallel experiments, and their mean square error did not exceed 5%. The yield of propylene carbonate was determined relative to carbamide.

RESULTS AND DISCUSSION

On the basis of the reference data [17], the thermodynamic calculations of the reaction under standard conditions ($p = 0.1013$ MPa and $T = 298.15$ K) show that the change in enthalpy (ΔH) and the change in the Gibbs free energy (ΔG) of the reaction are 51.60 kJ/mol and 13.99 kJ/mol, respectively. A positive change in enthalpy means that the reaction between propylene glycol and carbamide proceeds with heat absorption. Thus, an increase in the temperature of the process will contribute to a shift in equilibrium toward the reaction products. However, a positive change in the Gibbs free energy indicates that the reaction cannot proceed at the temperature of 298.15 K. The dependence of ΔG on the reaction temperature is shown in Fig. 2.

The isobaric–isothermal potential decreases with an increase in the reaction temperature and becomes equal to zero at 62°C (335 K). This suggests that at

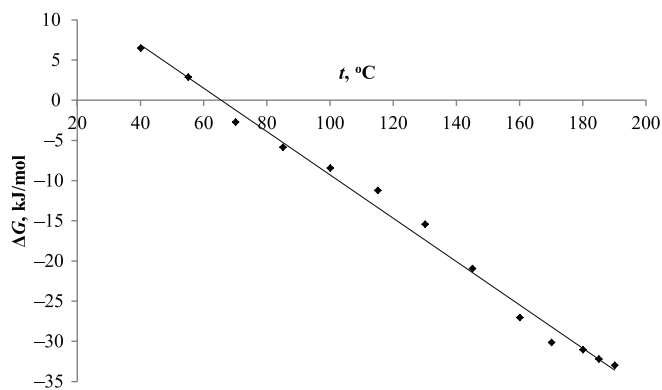


Fig. 2. Dependence of ΔG of the reaction on temperature.

temperatures higher than the abovementioned value, the reaction can proceed in the forward direction.

The equilibrium constant of the reaction at 130°C is 99.8; at 190°C, the equilibrium constant reaches 5271.3, which indicates a considerable shift in the equilibrium toward the reaction products with an increase in the temperature to 190°C.

Thus, calculations show that the synthesis of propylene carbonate from propylene glycol and carbamide is thermodynamically possible. However, to increase the speed of the process and reduce the time required to achieve equilibrium, kinetic factors should also be considered.

On the basis of the results obtained by calculation, the effect of temperature on the yield of propylene carbonate was studied in the temperature range of 130–190°C (Fig. 3).

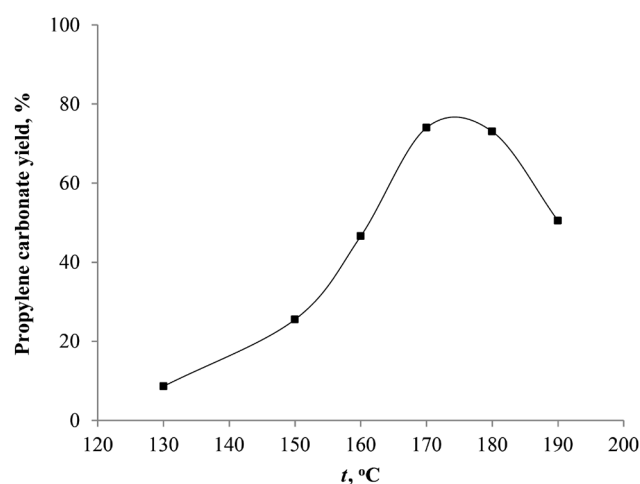


Fig. 3. Dependence of the propylene carbonate yield on the synthesis temperature (initial molar ratio propylene glycol/carbamide = 1:1, catalyst content 1 wt %, synthesis time 2 h).

The analysis of the results shows that with an increase in the temperature to 170–180°C, an increase in the yield of propylene carbonate is observed. A further increase in the temperature leads to a decrease in the yield of the target product, which is clearly associated with the occurrence of side processes (e.g., oligomerization of propylene carbonate). Thus, to implement the process, it is advisable to maintain the temperature in the range of 170–180°C. Under these conditions, the propylene carbonate yield of 74–75% is achieved.

To evaluate the effect of the initial molar ratio of propylene glycol/carbamide on the yield of propylene carbonate, a series of experiments was carried out with this indicator varying in the range of (0.5–5):1. The results are shown in Fig. 4.

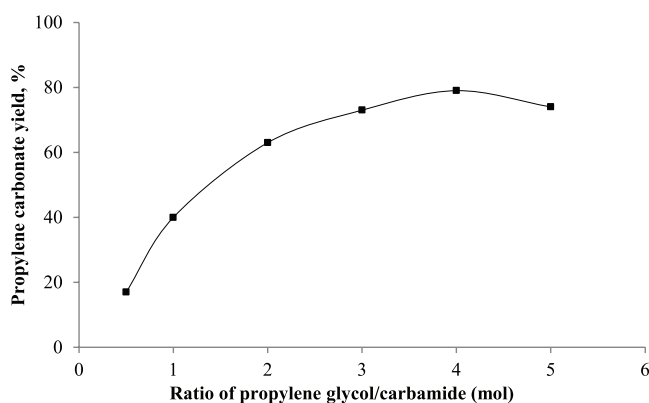


Fig. 4. Dependence of the propylene carbonate yield on the initial propylene glycol/carbamide ratio (synthesis temperature 170°C, catalyst content 1 wt %, synthesis time 2 h).

Figure 4 shows that a noticeable increase in the yield of propylene carbonate is observed with an increase in the ratio of reagents to 4:1. It is recommended to perform the synthesis of propylene carbonate in the presence of a 3–4-fold molar excess of propylene glycol. Unreacted propylene glycol is supposed to be isolated from the reaction using mass transfer processes and recycled to the chemical conversion step.

Based on the propylene carbonate yield–synthesis time dependence (Fig. 5), the optimal time was selected from 2 to 2.5 h. An increase in the reaction time beyond this value is undesirable because it leads to a certain decrease in the yield of propylene carbonate, which is most likely owing to the participation of the target product in further transformations.

Finally, we have investigated the dependence of propylene carbonate yield on the catalyst content in the reaction mixture (Fig. 6).

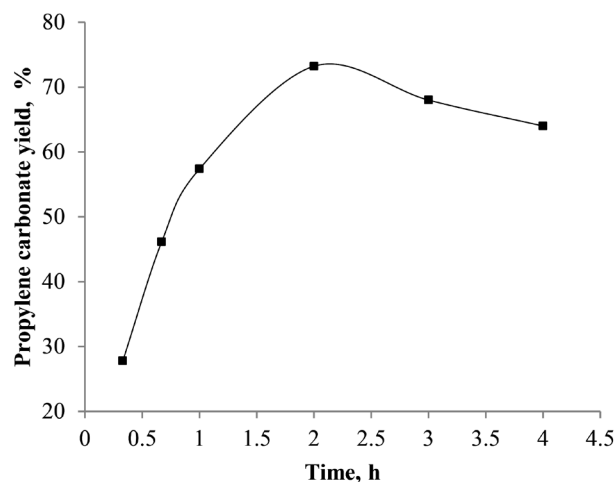


Fig. 5. Dependence of the propylene carbonate yield on the duration of the synthesis (synthesis temperature 170°C, initial molar ratio of propylene glycol/carbamide = 3:1, catalyst content 1 wt %).

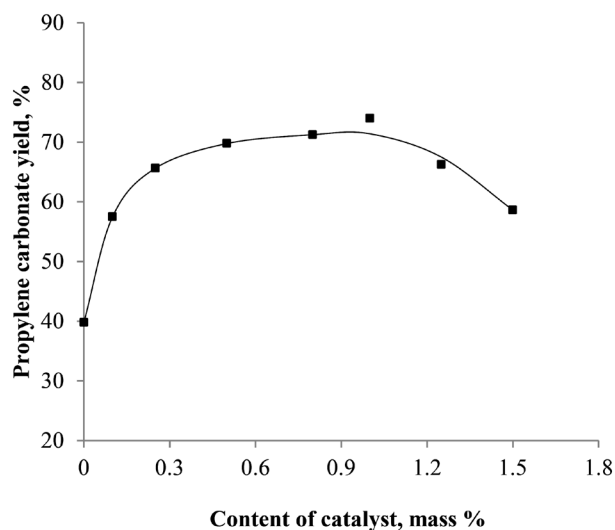


Fig. 6. Dependence of the propylene carbonate yield on the catalyst content (synthesis temperature 170°C, initial molar ratio of propylene glycol/carbamide = 3:1, synthesis time 2 h).

As expected, an increase in the catalyst amount in the reaction mixture promotes an increase in the yield of propylene carbonate. This dependence can be explained by an increase in the process rate; during the same time (2 h) a larger amount of propylene carbonate is formed with a higher catalyst content. This trend continues until the catalyst content is 1 wt %. With a further increase in

the concentration of the catalyst, propylene carbonate in the reaction mixture can participate in side reactions, and its yield decreases, which is confirmed by the observed regularities.

In addition, the reaction can occur in the absence of a catalyst. At fixed parameters (temperature 170°C, propylene glycol/carbamide ratio = 3:1, contact duration 2 h), the yield of propylene carbonate does not exceed 40%. This value is relatively small, and it is unlikely that the non-catalytic process can be considered as an alternative. However, this fact is important and should be considered in further studies on the kinetics of propylene carbonate synthesis.

REFERENCES

1. Shaikh A.G., Sivaram S. Organic Carbonates. *Chem. Rev.* 1996;96(3):951-976.
<https://doi.org/10.1021/cr950067i>
2. Debotton N., Dahan A. Applications of Polymers as Pharmaceutical Excipients in Solid Oral Dosage Forms. *Med. Res. Rev.* 2017;37(1):52-97.
<https://doi.org/10.1002/med.21403>
3. Zhou J., Dongfang W., Zhang B., Guo Y. Synthesis of propylene carbonate from urea and 1,2-propylene glycol over metal carbonates. *Chem. Ind. Chem. Eng. Q.* 2011;17(3):323-331.
<https://doi.org/10.2298/CICEQ101123018Z>
4. Suib S.L. (Ed.) *New and Future Developments in Catalysis*. Elsevier: Amsterdam; 2013. 478 p. ISBN 978-0-444-53882-6
5. Darensbourg D.J., Holtcamp M.W. Catalysts for the reactions of epoxides and carbon dioxide. *Coord. Chem. Rev.* 1996;153:155-174.
[https://doi.org/10.1016/0010-8545\(95\)01232-X](https://doi.org/10.1016/0010-8545(95)01232-X)
6. Shukla K., Srivastava V.C. Synthesis of organic carbonates from alcoholysis of urea: A review. *Catal. Rev.* 2017;59(1):1-43.
<https://doi.org/10.1080/01614940.2016.1263088>
7. Aresta M., Dibenedetto A. Utilisation of CO₂ as a chemical feedstock: opportunities and challenges. *Dalton Transactions*. 2007;28:2975-2992.
<https://doi.org/10.1039/B700658F>
8. Mikkelsen M., Jorgensen M., Krebs F.C. The teraton challenge. A review of fixation and transformation of carbon dioxide. *Energ. Environ. Sci.* 2010;3(1):43-81.
<https://doi.org/10.1039/B912904A>
9. Dasari M.A., Kiatsimku P.-P., Sutterlin W.R., Suppes G.J. Low-pressure hydrogenolysis of glycerol to propylene glycol. *Appl. Catal. A-G.* 2005;281(1):225-231.
<https://doi.org/10.1016/j.apcata.2004.11.033>
10. Maris E.P., Davis R.J. Hydrogenolysis of glycerol over carbon-supported Ru and Pt catalysts. *J. Catal.* 2007;249(2):328-337.
<https://doi.org/10.1016/j.jcat.2007.05.008>

About the authors:

Aleksandr V. Sulimov, Dr. of Sci. (Engineering), Professor, Department of Chemical and Food Technologies, Nizhny Novgorod State Technical University n.a. R.E. Alekseev (49, Gaidara ul., Dzerzhinsk, Nizhny Novgorod oblast, 606000, Russia). Scopus Author ID 56497239500, ResearcherID K-5437-2015, <https://orcid.org/0000-0002-8399-6231>

Anna V. Ovcharova, Cand. of Sci. (Chemistry), Associate Professor, Department of Chemical and Food Technologies, Nizhny Novgorod State Technical University n.a. R.E. Alekseev (49, Gaidara ul., Dzerzhinsk, Nizhny Novgorod oblast, 606000, Russia). Scopus Author ID 55263080200

CONCLUSIONS

Thermodynamic calculations and kinetic studies of the reaction between propylene glycol and carbamide in the presence of zinc acetate as a catalyst allowed us to identify the range of parameters, ensuring high yields of the target product (75–80%). Based on our analysis, we recommend the following parameter values: temperature 170–180°C, initial ratio propylene glycol/carbamide (2–3):1, synthesis time between 1.5 and 2 h, and catalyst content 1 wt %.

The authors declare no conflicts of interest.

11. Xiu Z.-L., Zeng A.-P. Present state and perspective of downstream processing of biologically produced 1,3-propanediol and 2,3-butanediol. *Appl. Microbiol. Biotechnol.* 2008;78(6):917-926.
<https://doi.org/10.1007/s00253-008-1387-4>
12. Sulimov A.V., Ovcharova A.V., Ovcharov A.A., Ryabova T.A., Kravchenko G.M., Lysanov S.A. Synthesizing cyclic carbonates from olefin oxides and carbon dioxide. I: Catalysis with ionic liquids. *Catalysis in Industry*. 2016;8(4):300-309.
<https://doi.org/10.1134/s2070050416040103>
13. Decortes A., Castilla A.M., Kleij A.W. Salen-Complex-Mediated Formation of Cyclic Carbonates by Cycloaddition of CO₂ to Epoxides. *Angew. Chem. Int. Ed.* 2010;49(51):9822-9837.
<https://doi.org/10.1002/anie.201002087>
14. Sheng, X., Guo H., Qin Y., Wang X., Wang F. A novel metalloporphyrin-based conjugated microporous polymer for capture and conversion of CO₂. *RSC Advances*. 2015;5(40):31664-31669.
<https://doi.org/10.1039/C4RA16675B>
15. Li Q., Zhao N., Wei W., Sun Y. Catalytic performance of metal oxides for the synthesis of propylene carbonate from urea and 1,2-propanediol. *J. Mol. Catal. A-Chem.* 2007;270(1):44-49.
<https://doi.org/10.1016/j.molcata.2007.01.018>
16. Zhao X., Sun N., Wang S., Li F. Synthesis of Propylene Carbonate from Carbon Dioxide and 1,2-Propylene Glycol over Zinc Acetate Catalyst. *Ind. Eng. Chem. Res.* 2008;47(5):1365-1369.
<https://doi.org/10.1021/ie070789n>
17. Gurvich L.V., Veyts I.V., Medvedev V.A. Thermodynamic properties of individual substances. Vol. 1, part 1. New York, United States: 1989. 551 p.

Grigory M. Kravchenko, Master Student, Department of Chemical and Food Technologies, Nizhny Novgorod State Technical University n.a. R.E. Alekseev (49, Gaidara ul., Dzerzhinsk, Nizhny Novgorod oblast, 606000, Russia).

Yulia K. Sulimova, Master Student, Department of Chemical and Food Technologies, Nizhny Novgorod State Technical University n.a. R.E. Alekseev (49, Gaidara ul., Dzerzhinsk, Nizhny Novgorod oblast, 606000, Russia). <https://orcid.org/0000-0003-4417-884X>

Об авторах:

Сулимов Александр Владимирович, доктор технических наук, профессор кафедры «Химические и пищевые технологии», Нижегородский государственный технический университет им. Р.Е. Алексеева (606000, Россия, Нижегородская обл., г. Дзержинск, ул. Гайдара, д. 49). Scopus Author ID 56497239500, ResearcherID K-5437-2015, <https://orcid.org/0000-0002-8399-6231>

Овчарова Анна Владимировна, кандидат химических наук, доцент кафедры «Химические и пищевые технологии», Нижегородский государственный технический университет им. Р.Е. Алексеева (606000, Россия, Нижегородская обл., г. Дзержинск, ул. Гайдара, д. 49). Scopus Author ID 55263080200

Кравченко Григорий Михайлович, магистрант кафедры «Химические и пищевые технологии», Нижегородский государственный технический университет им. Р.Е. Алексеева (606000, Россия, Нижегородская обл., г. Дзержинск, ул. Гайдара, д. 49).

Сулимова Юлия Константиновна, магистрант кафедры «Химические и пищевые технологии», Нижегородский государственный технический университет им. Р.Е. Алексеева (606000, Россия, Нижегородская обл., г. Дзержинск, ул. Гайдара, д. 49). <https://orcid.org/0000-0003-4417-884X>

Submitted: December 23, 2019; Reviewed: February 07, 2020; Accepted: February 17, 2020.

Translated from Russian into English by S. Durakov

Edited for English language and spelling by Enago, an editing brand of Crimson Interactive Inc.

Calculating the composition of dispersion-filled polymer composite materials of various structures

Chong N. Nguyen, Minzalya V. Sanyarova[@], Igor D. Simonov-Emel'yanov

MIREA – Russian Technological University (M.V. Lomonosov Institute of Fine Chemical Technologies),
Moscow 119571, Russia

[@]Corresponding author, e-mail: sanyarova.minzalya@mail.ru

Objectives. The aim is to calculate the composition of dispersion-filled polymer composite materials with different fillers and structures and to highlight differences in the expression of said composition in mass and volume units.

Methods. The paper presents the calculation of compositions in mass and volume units for various types of structures comprising dispersion-filled polymer composite materials according to their classification: diluted, low-filled, medium-filled, and highly-filled systems.

Results. For calculations, we used fillers with densities ranging from 0.00129 g/cm³ (air) to 22.0 g/cm³ (osmium) and polymer matrices with densities between 0.8 g/cm³ and 1.5 g/cm³, which represent almost all known fillers and polymer matrices used to create dispersion-filled polymer composite materials. The general dependences of the filler content on the ratio of the filler density to the density of the polymer matrix for dispersion-filled polymer composite materials with different types of dispersed structures are presented. It is shown that to describe structures comprising different types of dispersion-filled polymer composite materials (diluted, low-filled, medium-filled, and highly-filled) it is necessary to use only the volume ratios of components in the calculations. Compositions presented in mass units do not describe the construction of dispersion-filled polymer composite material structures because using the same composition in volume units, different ratios of components can be obtained for different fillers.

Conclusions. The dependences of the properties of dispersion-filled polymer composite materials should be represented in the coordinates of the property–content of the dispersed phase only in volume units (vol % or vol. fract.) because the structure determines the properties. Compositions presented in mass units are necessary for receiving batches upon receipt of dispersion-filled polymer composite materials. Formulas are given for calculating and converting dispersion-filled polymer composite material compositions from bulk to mass units, and vice versa.

Keywords: polymers, fillers, dispersion-filled polymer composite materials, structure, properties.

For citation: Nguyen Ch.N., Sanyarova M.V., Simonov-Emel'yanov I.D. Calculating the composition of dispersion-filled polymer composite materials of various structures. *Tonk. Khim. Tekhnol. = Fine Chem. Technol.* 2020;15(1):62-66. <https://doi.org/10.32362/2410-6593-2020-15-1-62-66>

Расчет составов дисперсных наполненных полимерных композиционных материалов с разной структурой

Ч.Н. Нгуен, М.В. Саньярова[@], И.Д. Симонов-Емельянов

МИРЭА – Российский технологический университет (Институт тонких химических технологий имени М.В. Ломоносова), Москва 119571, Россия

[@]Автор для переписки, e-mail: sanyarova.minzalya@mail.ru

Цели. Цель работы – предоставить расчеты по составам дисперсно-наполненных полимерных композиционных материалов (ДНПКМ) с разными наполнителями и структурами, а также показать существенные различия при выражении состава в массовых и объемных единицах.

Методы. В работе приведены расчеты составов в массовых и объемных единицах для различных видов структур дисперсно-наполненных полимерных композиционных материалов согласно их классификации: разбавленные, низконаполненные, средненаполненные и высоконаполненные системы.

Результаты. Для расчетов использованы наполнители с плотностью от 0.00129 (воздух) до 22.0 г/см³ (осмий) и полимерные матрицы с плотностью от 0.8 до 1.5 г/см³, которые охватывают практически все известные наполнители и полимерные матрицы, используемые для создания ДНПКМ. Представлены обобщенные зависимости содержания наполнителей от отношения плотности наполнителя к плотности полимерной матрицы для ДНПКМ с разными видами дисперсной структуры. Показано, что для описания разных видов структур ДНПКМ – разбавленные, низконаполненные, средненаполненные и высоконаполненные – необходимо в расчетах использовать только объемные соотношения компонентов. Составы, представленные в массовых единицах, не описывают построение структур ДНПКМ, так как при одном составе в объемных единицах можно получить для разных наполнителей разное соотношение компонентов.

Выводы. Зависимости свойств ДНПКМ следует представлять в координатах свойство–содержание дисперсной фазы только в объемных единицах (об. % или об. д.), так как структура определяет свойства. Составы, представленные в массовых единицах, необходимы для получения навесок при получении ДНПКМ. Приведены формулы для расчета и перевода составов ДНПКМ из объемных в массовые единицы и наоборот.

Ключевые слова: полимеры, наполнители, дисперсно-наполненные полимерные композиционные материалы, структура, свойства.

Для цитирования: Нгуен Ч.Н., Саньярова М.В., Симонов-Емельянов И.Д. Расчет составов дисперсных наполненных полимерных композиционных материалов с разной структурой. *Тонкие химические технологии*. 2020;15(1):62-66. <https://doi.org/10.32362/2410-6593-2020-15-1-62-66>

Determining the content of initial components in dispersion-filled polymer composite materials (DFPCM) with different structures and the design and calculation of such compositions is generally performed in mass units (mass fract. or mass %) [1–5]. Mass units indicate the presence of initial components in DFPCM (alongside weighed portions) but do not reflect the construction of various types of dispersed structures. These structures are divided into diluted (DS), low-filled (LFS), medium-filled (MFS), and highly-filled (HFS) systems [6]. Analysis of scientific and technical literature showed that when discussing the structure and properties of DFPCM, data and the dependence of properties based on the content of the dispersed phase were provided primarily in units of mass.

Research on polymer materials highlights that material structure determines their properties. However, the structure of DFPCM and their parameters can be described only in volume units (vol. fract. or vol %) because when using mass units, the density ratio of the initial components in the dispersed system must be taken into account. Therefore, in the case of DFPCM, at a constant volume fraction (φ_v , vol. fract.), e.g., 0.16 vol. fract. of the dispersed phase of the filler with different particle densities (from 0.00129 to 22.0 g/cm³), the mass fraction will vary from 0.0007 to 0.96 at the constant density of the polymer matrix [7].

Calculation of fillers in this work was performed using density ranging from 0.00129 (air) to 22.0 g/cm³ (osmium); this included the range for all known fillers for polymer

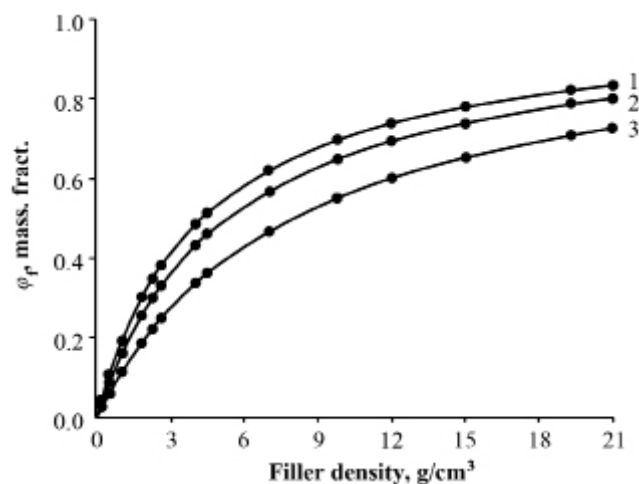


Fig. 1. Dependence of filler content φ_f in mass fractions (mass fract.) in DFPCM with a polymer matrix density $\rho_p = 0.8 \text{ g/cm}^3$ (1), $\rho_p = 1.0 \text{ g/cm}^3$ (2), $\rho_p = 1.5 \text{ g/cm}^3$ (3) at constant volumetric content $\varphi_f = 0.16 \text{ vol. fract.}$ on the density of filler.

composite materials. Figure 1 shows the dependences of the content of the dispersed phase in DFPCM expressed in mass fractions, at different densities of the polymer matrix (0.8–1.5 g/cm³), as well as a constant filler content at 0.16 vol. fract. of filler density.

The presented data show that at constant structural parameters ($\varphi_f = 0.16 \text{ vol. fract.}$), the composition of DFPCM expressed in mass units (mass fract.) was determined by the true density of the filler and the matrix and varied from 0.0007 to 0.96 mass fract.

In a generalized form, the graphs in Fig. 1 can be shown in different coordinates where the X-axis displays the ratio of densities (filler to polymer matrix). When doing so, the curve does not change according to the density of the polymer matrix. To determine the content of the dispersed phase in mass units at a constant volume fraction (0.16 vol. fract.), density ratio ρ_f / ρ_p should be calculated first for a specific DFPCM (Fig. 2).

This example convincingly shows that the structural parameters of DFPCM can be correctly expressed only in volume units (vol. fract. or vol %). In this case, they were not dependent on the density of the dispersed filler or the polymer matrix, which allowed us to compare the results for filled systems with different fillers and matrices. Thus, when designing DFPCM compositions with a set of specified properties and when representing dependences, data should only be provided in volume units (vol. fract. or vol %) as shown in [7].

Recalculation of DFPCM composition from mass unit ($\varphi_{\text{mass},f}$) to volume unit ($\varphi_{v,f}$), and vice versa, can be done for a two-phase system (filler + polymer matrix) by employing the following equations [6]:

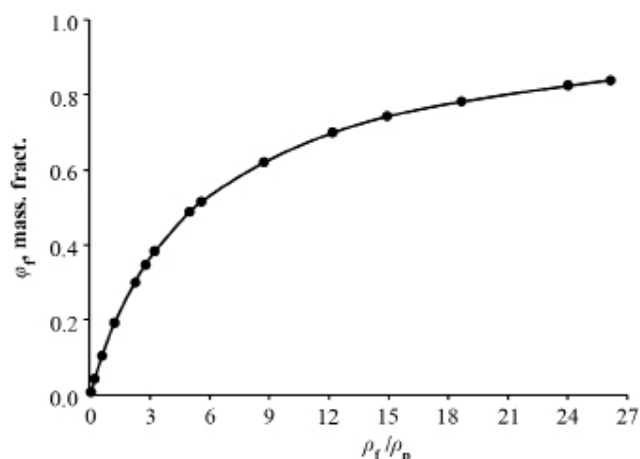


Fig. 2. Dependence of filler content φ_f in mass fractions (mass fract.) in a DFPCM on the density ratio of the filler to the polymer matrix at constant volumetric content $\varphi_f = 0.16 \text{ vol. fract.}$

$$\varphi_{v,f} = \frac{\left(\frac{\rho_p}{\rho_f}\right)}{\left(\frac{1}{\varphi_{\text{mass},f}}\right) + \left(\frac{\rho_p}{\rho_f}\right) - 1}, \text{ vol. fract.} \quad (1)$$

$$\varphi_{\text{mass},f} = \frac{\varphi_{v,f}}{\varphi_{v,f} \left(1 - \frac{\rho_p}{\rho_f}\right) + \frac{\rho_p}{\rho_f}}, \text{ mass fract.} \quad (2)$$

The content of the dispersed filler is selected according to the classification of dispersed systems, based on the structural principle [6], lattice parameters (coordination number Z and packing density coefficient k_p), and the generalized structural parameter θ —the proportion of the polymer matrix for the formation of interlayers between dispersed particles.

The structural classification of DFPCM allows them to be divided into DS, LFS, MFS, and HFS types. Generalized parameter θ serves as the basis for the classification of all DFPCM based on the structural principle: DS: *diluted systems* – $1.0 \geq \theta \geq 0.90 \text{ vol. fract.}$; LFS: *low-filled systems* – $0.90 \geq \theta \geq 0.75 \text{ vol. fract.}$; MFS: *medium-filled systems* – $0.75 \geq \theta \geq 0.20 \text{ vol. fract.}$; MFS-1 – $0.75 \geq \theta \geq 0.45 \text{ vol. fract.}$ (up to yield stress); MFS-2 – $0.45 \geq \theta \geq 0.20 \text{ vol. fract.}$ (after yield stress); HFS: *highly-filled systems* – $0.20 \geq \theta \geq 0.0 \text{ vol. fract.}$

When the maximum dispersed filler packing (φ_m) is known and filler content varies, the generalized structural parameter θ can be found using the following formula [6]:

$$\theta = \frac{(\varphi_m - f^3 \varphi_{v,f})}{\varphi_m}, \quad (3)$$

где $\varphi_{v,f}$ is the volumetric content of dispersed filler and $f^3 = \left(1 + \frac{2\delta}{d}\right)$ is the coefficient that takes into account the ratio of the thickness of the boundary layer (δ) to diameter (d) of the dispersed particle.

When the boundary layer thickness δ in a DFPCM ranges from 50 to 500 nm and for dispersed particles with a diameter of more than 10 μm , a simplified formula can be used to calculate filler content [6]:

$$\theta = \frac{(\varphi_m - \varphi_{v,f})}{\varphi_m}. \quad (4)$$

When the generalized structural parameter θ is found, the dispersed filler content and the composition of the polymer can be determined for each type of DFPCM—DS, LFS, MFS, or HFS. The calculations below serve as an example for the content of dispersed filler in volume units at a value of $\varphi_m = 0.64$ for various dispersed systems according to their classification: DS: 0.076 vol. fract.; LFS: 0.16 vol. fract.; MFS-1: 0.255 vol. fract.; MFS-2: 0.34 vol. fract.; HFS: 0.52 and 0.64 vol. fract.

For DFPCM of different structures, it is possible to construct generalized dependences for the dispersed filler content in mass units at different constant values of the filler content in volume units. This will help to determine the construction of dispersions of various types of structures—DS, LFS, MFS, and HFS. Figure 3 shows the dependences of $\varphi_{\text{mass},f}$ in DFPCM at constant values of $\varphi_{v,f}$ which are characteristic of different types of structures, on the density ratio of the filler to the polymer matrix.

For dispersed fillers with different φ_m values, the content of the filler in volume units ($\varphi_{v,f}$) was determined by formulas (1) and (2) for different types of DFPCM structures (DS, LFS, MFS, and HFS); then, $\varphi_{\text{mass},f}$ was found at a constant $\varphi_{v,f}$ (Fig. 3). The data noted in Fig. 3—based on calculations of the DFPCM compositions in mass and volume units—include almost all known polymer matrices and fillers.

Data on DFPCM properties presented in mass units are true only for a specific polymer matrix and dispersed filler. They are not related to the structure of the composite material and do not allow for comparing dispersed systems with one another. Thus, to design the structure—DS, LFS, MFS, and HFS—the composition of DFPCM should be calculated, and the

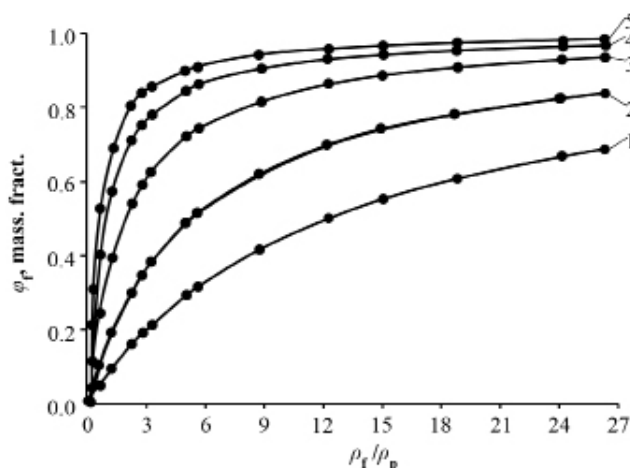


Fig. 3. Dependence of filler content $\varphi_{\text{mass},f}$ in mass fractions (mass fract.) in DFPCM on density ratio

ρ_f / ρ_p at constant volumetric content $\varphi_{v,f}$:

- 1 – DS, 0.076 vol. fract. ($\theta = 0.90$ vol. fract.);
- 2 – LFS, 0.16 vol. fract. ($\theta = 0.75$ vol. fract.);
- 3 – MFS, 0.255 vol. fract. ($\theta = 0.60$ vol. fract.);
- 4 – HFS, 0.52 vol. fract. ($\theta = 0.20$ vol. fract.);
- 5 – HFS, 0.64 vol. fract. ($\theta = 0.0$ vol. fract.).

feature–filler content functions should be considered using only volume units.

The results presented herein enable a purposeful calculation of the DFPCM composition of different types of structures, determining the content of dispersed filler in both volume and mass units for almost all polymer matrices and fillers and correctly describing the composition–property dependences in the volume ratios of components.

CONCLUSIONS

This paper presented calculations for the composition of various types of DFPCM structures according to their classification in mass and volume units. Additionally, the necessity for using only volumetric ratios of components in calculations to describe different types of DFPCM structures was underscored because in doing so, different compositions can be compared, since the obtained structural parameters will not depend on the densities of components. Rather, the specific structure will determine the properties. Accordingly, the dependences of DFPCM properties must be represented in the property–dispersed phase content coordinates only in volume units (vol % or vol. fract.).

The authors declare no conflicts of interest.

REFERENCES

1. Katz G.S., Milevski D.V. *Napolniteli dlya polimernykh kompozitsionnykh materialov* (Fillers for polymer composites). Moscow: Chemistry; 1981. 736 p. (in Russ.).
2. Lipatov Yu. S. *Fizicheskaya khimiya napolnennykh polimerov* (Physical chemistry of filled polymers). Moscow: Chemistry; 1977. 204 p. (in Russ.).
3. Shklovsky B.I. Percolation Theory and Conductivity of Highly Inhomogeneous Media. *Advances in the physical sciences*. 1975;117(3):401 (in Russ.).
4. Gennes, P. G. de. *Scaling concepts in polymer physics*. Ithaca, N.Y.: Cornell University Press; 1979. 324 p.
5. Bobryshev A.N., Kozomazov A.N., Babin L.O., Solomatov V.I. *Sinergetika kompozitsionnykh materialov* (Synergetics of composite materials). Lipetsk: SPA «ORIUS»; 1994. 154 p. (in Russ.).
6. Simonov-Emel'yanov I.D. Construction of structures in dispersion-filled polymers and properties of composite materials. *Plastics masses*. 2015;9-10:29-36 (in Russ.).
7. Simonov-Emel'yanov I.D. Structure and calculation of the compositions of dispersed-filled elastomeric materials in mass and volume units. *Rubber and Rubber*. 2019;78(1):42-43 (in Russ.).

СПИСОК ЛИТЕРАТУРЫ

1. Кац Г.С., Милевски Д.В. (ред.). *Наполнители для полимерных композиционных материалов*. М.: Химия; 1981. 736 с.
2. Липатов Ю.С. *Физическая химия наполненных полимеров*. М.: Химия; 1977. 204 с.
3. Шкловский Б.И. Теория протекания и проводимость сильно неоднородных сред. *Успехи физических наук*. 1975;117(3):401.
4. Жен П. де. *Идеи скейлинга в физике полимеров*. М.: Мир; 1982. 368 с.
5. Бобрышев А.Н., Козомазов А.Н., Бабин Л.О., Соломатов В.И. *Синергетика композиционных материалов*. Л.: НПО «ОРИУС»; 1994. 153 с.
6. Симонов-Емельянов И.Д. Построение структур в дисперсно-наполненных полимерах и свойства композиционных материалов. *Пластические массы*. 2015;9-10:29-36.
7. Симонов-Емельянов И.Д. Структура и расчет составов дисперсно-наполненных эластомерных материалов в массовых и объемных единицах. *Каучук и резина*. 2019;78(1):42-43.

About the authors:

Chong N. Nguyen, Graduate Student, Department of Chemistry and Technology of Plastic Processing and Polymer Composites, M.V. Lomonosov Institute of Fine Chemical Technologies, MIREA – Russian Technological University (86, Vernadskogo pr., Moscow 119571, Russia). E-mail: nguyen.chong@mail.ru. <https://orcid.org/0000-0002-1540-2649>

Minzalya V. Sanyarova, Master Student, Department of Chemistry and Technology of Plastic Processing and Polymer Composites, M.V. Lomonosov Institute of Fine Chemical Technologies, MIREA – Russian Technological University (86, Vernadskogo pr., Moscow 119571, Russia). E-mail: sanyarova.minzalya@mail.ru. <https://orcid.org/0000-0001-5926-4973>

Igor D. Simonov-Emel'yanov, Dr. of Sci. (Engineering), Professor, Head of the Department of Chemistry and Technology of Plastic Processing and Polymer Composites, M.V. Lomonosov Institute of Fine Chemical Technologies, MIREA – Russian Technological University (86, Vernadskogo pr., Moscow 119571, Russia). E-mail: simonov@mitht.ru. Scopus Author ID 6603181099

Об авторах:

Нгуен Чонг Нгуа, аспирант кафедры «Химия и технология переработки пластмасс и полимерных композитов» Института тонких химических технологий им. М.В. Ломоносова ФГБОУ ВО «МИРЭА – Российский технологический университет» (119571, Россия, Москва, пр-т Вернадского, д. 86). E-mail: nguyen.chong@mail.ru. <https://orcid.org/0000-0002-1540-2649>

Саньярова Минзала Венеровна, магистрант кафедры «Химия и технология переработки пластмасс и полимерных композитов» Института тонких химических технологий им. М.В. Ломоносова ФГБОУ ВО «МИРЭА – Российский технологический университет» (119571, Россия, Москва, пр-т Вернадского, д. 86). E-mail: sanyarova.minzalya@mail.ru. <https://orcid.org/0000-0001-5926-4973>

Симонов-Емельянов Игорь Дмитриевич, профессор, доктор технических наук, заведующий кафедрой «Химия и технология переработки пластмасс и полимерных композитов» Института тонких химических технологий им. М.В. Ломоносова ФГБОУ ВО «МИРЭА – Российский технологический университет» (119571, Россия, Москва, пр-т Вернадского, д. 86). E-mail: simonov@mitht.ru. Scopus Author ID 6603181099

Submitted: August 26, 2019; Reviewed: October 10, 2019; Accepted: January 31, 2020.

Translated from Russian into English by H. Moshkov

Edited for English language and spelling by Enago, an editing brand of Crimson Interactive Inc.

Development of a nasal spray containing aminocaproic acid and a copolymer of *N*-vinylpyrrolidone and 2-methyl-5-vinylpyridine for use in the prevention of influenza and other viral respiratory infections

Anastasiya S. Karpova

Institute of Pharmaceutical Technology, Moscow, 121353 Russia

@Corresponding author, e-mail: karpova@ipt.ru.com

Objectives. Prevention of influenza and viral respiratory infections is one of the major public health problems today. The aim of the study was to develop the formulation and production conditions for a nasal spray that can be used in the prevention of influenza and other viral respiratory infections, based on aminocaproic acid and a copolymer of *N*-vinylpyrrolidone and 2-methyl-5-vinylpyridine.

Methods. The influence of pH and temperature on the transparency of the copolymer solution was investigated using a turbidimeter to determine the optimal pH for the dosage form. The pH value was determined using a pH meter equipped with a combined glass electrode. The presence or absence of opalescence in the solution was determined visually, whereas the dynamic viscosity of the solution was determined at $25.0 \pm 0.5^\circ\text{C}$ using a rotational viscometer. The optimal temperature and mixing speeds were selected as part of the technological development process. Quantitation of the active substances in the resulting drug was conducted using a previously reported high performance liquid chromatography method. A preliminary evaluation of the drug's shelf life was performed via stability studies using the accelerated aging method.

Results. Drug stability was ensured when the pH range of the dosage form was between 5.5 and 6.2. The addition of a thickening agent is not advisable due to undesired interactions between the excipients and the active substances during storage. Ideally, the drug composition for nasal use was aminocaproic acid (1 wt %) and the copolymer (0.5 wt %) in aqueous solution. A phosphate buffer solution with pH 5.5 was selected as the solvent for the dosage form to ensure the stability of the drug solution and ease-of-use without any disruptions in the normal functioning of the cilia in the nasal cavity. The optimal technology for drug production was determined, and the control parameters for this process were highlighted. Drug stability studies conducted via the accelerated aging method revealed that the estimated shelf life of the dosage form was 2 years.

Conclusions. A new formulation and optimized production conditions were developed for a drug based on aminocaproic acid and a copolymer of *N*-vinylpyrrolidone and 2-methyl-5-vinylpyridine, in the form of a nasal spray, for the prevention of influenza and other viral respiratory infections.

Keywords: aminocaproic acid, copolymer of *N*-vinylpyrrolidone and 2-methyl-5-vinylpyridine, nasal spray, prevention of influenza, viral respiratory infections.

For citation: Karpova A.S. Development of a nasal spray containing aminocaproic acid and a copolymer of *N*-vinylpyrrolidone and 2-methyl-5-vinylpyridine in the prevention of influenza and other viral respiratory infections. *Tonk. Khim. Tekhnol. = Fine Chem. Technol.* 2020;15(1):67-75. <https://doi.org/10.32362/2410-6593-2020-15-1-67-75>

Создание назального спрея на основе аминокaproновой кислоты и сополимера *N*-винилпирролидона и 2-метил-5-винилпиридина для профилактики гриппа и ОРВИ

А.С. Карпова

Институт фармацевтических технологий, Москва, 121353 Россия

@Автор для переписки, e-mail: karpova@ipt.ru.com

Цели. В настоящее время одной из первоочередных задач здравоохранения в мире является профилактика гриппа и острых респираторных вирусных инфекций. Целью работы являлась разработка состава и технологии получения лекарственного препарата на основе аминокaproновой кислоты и сополимера *N*-винилпирролидона и 2-метил-5-винилпиридина в форме назального спрея для профилактики этих социально значимых заболеваний.

Методы. Для определения устойчивости лекарственной формы в зависимости от pH и температуры определяли прозрачность раствора сополимера с помощью метода турбидиметрии; значение pH определяли с помощью pH-метра со стеклянным комбинированным электродом. В дальнейшем наличие или отсутствие опалесценции раствора определяли визуально. Определение динамической вязкости раствора проводили при температуре 25.0 ± 0.5 °C методом ротационной вискозиметрии. В рамках разработки технологии подобраны оптимальные значения температуры и скорости перемешивания при растворении веществ. Количественное определение содержания активных веществ в полученном препарате проводили с помощью ранее разработанного способа с использованием ВЭЖХ. Предварительный срок годности полученного препарата устанавливали с помощью исследования стабильности методом ускоренного старения.

Результаты. Установлено, что необходимый диапазон pH разработанной лекарственной формы для обеспечения стабильности лекарственного препарата составляет 5.5–6.2. В ходе экспериментов было продемонстрировано, что добавление загустителя нецелесообразно вследствие его взаимодействия с активным веществом в процессе хранения, что недопустимо. Разработан состав лекарственного препарата в виде раствора для назального применения с содержанием 1 масс. % аминокaproновой кислоты и 0.5 масс. % сополимера 2-метил-5-винилпиридина и *N*-винилпирролидона в водном растворе. В качестве растворителя лекарственной формы выбрали фосфатный буферный раствор с значением pH 5.5 для обеспечения стабильности раствора препарата и комфортного применения без нарушения нормального функционирования ресничек в полости носа. Подобрана оптимальная технология получения лекарственного препарата, выделены контролируемые параметры для надлежащего проведения технологического процесса. В результате исследования стабильности спрея методом ускоренного старения установлен предполагаемый срок годности разработанного препарата, составляющий 2 года.

Выводы. Предложены новый состав и технология получения готового лекарственного препарата на основе аминокaproновой кислоты и сополимера *N*-винилпирролидона и 2-метил-5-винилпиридина в форме назального спрея для профилактики гриппа и ОРВИ.

Ключевые слова: аминокaproновая кислота, сополимер *N*-винилпирролидона и 2-метил-5-винилпиридина, назальный спрей, профилактика гриппа и ОРВИ.

Для цитирования: Карпова А.С. Создание назального спрея на основе аминокaproновой кислоты и сополимера *N*-винилпирролидона и 2-метил-5-винилпиридина для профилактики гриппа и ОРВИ. *Тонкие химические технологии.* 2020;15(1):67-75. <https://doi.org/10.32362/2410-6593-2020-15-1-67-75>

INTRODUCTION

Despite great efforts to prevent influenza and other viral respiratory infections (VRIs), the incidence rate of these infections has been increasing annually. Often, the global epidemic of these infections claims the lives of thousands of people [1]. The problem is exacerbated by the mixed nature of these infections, high transmission rate, and rapid onset of drug resistance [2]. The effectiveness of treatment options for influenza and other VRIs is largely determined by the rational selection of drugs that focus more on managing the causes of the disease rather than merely alleviating the symptoms [3]. The main goal of pharmaceutical technology is to create efficient, safe, and high-quality drugs aimed at combating the most dangerous and widespread diseases. According to the World Health Organization, influenza and other VRIs are both highly common and severe diseases; up to 500 mln people worldwide are infected annually, of whom around 650 000 die. In Russia, between 27.3 and 41.2 mln cases are registered each year¹. Despite these figures, only a small percentage of the global drug market for influenza and other VRIs are designed to have antiviral activity². Therefore, developing novel drugs aimed at preventing and eradicating influenza and other VRIs is a priority task for researchers globally.

Based on the mechanism by which the influenza virus penetrates human host cells [4], nasal route of drug administration is considered the most promising and effective means of prophylaxis [5, 6]. In this study, a combination of active components—aminocaproic acid (ACA) and a copolymer of *N*-vinylpyrrolidone and 2-methyl-5-vinylpyridine (hereafter referred to as the copolymer) – is proposed as a basis for creating an effective therapeutic agent. An aqueous solution of ACA and the copolymer at a molar ration of 2:1 showed significant antiviral activity when administered nasally to outbred mice [7, 8]. In this study, we aimed to optimize the formulation and the production conditions of a nasal spray based on aminocaproic acid and the copolymer of *N*-vinylpyrrolidone and 2-methyl-5-vinylpyridine.

MATERIALS AND METHODS

The active reagents of the nasal spray formulation were ACA (*Polisintez*, Russia) at a concentration of 1 wt % and the copolymer at a concentration of 0.5 wt % in aqueous solution. The copolymer was of medium viscosity with a molecular weight of 27 kDa and 32 mol % pyridine units (*Institute of Pharmaceutical Technology*, Russia). In the process of developing the model formulations for this nasal spray, the concentration of the excipients and the optimal conditions required for drug preparation were determined. The following reagents were used in the formulation: sorbitol (*Chimmed*, Russia), polyethylene glycol (PEG) 4000 (TU 20.16.40-008-71150986-2019; *Norchem*, Russia), carboxymethyl cellulose (Na-CMC), 7LF (*Ashland*, United States), glycerin (GOST 6259-57; *Chimmed Sintez*, Russia), polysorbate 80 (*Oleon*, Belgium), polyvinylpyrrolidone (*AK Sintvita*, Russia), Avicel® RC 591 (*FMC*, United States; United States Pharmacopeia), Vivapur® MCG 811 P (*JRS Pharma*, Finland), PEG 1500 (PEG-32; *Clariant*, Switzerland), benzalkonium chloride (CAS 63449-41-2; *Sigma-Aldrich*, United States), and purified water (Pharmacopeia Article 2.2.0020.18). Buffer solutions were prepared in accordance with the Russian State Pharmacopeia XIV³ by using the following components: potassium dihydrogen phosphate (CAS 7778-77-0; *Chimmed*, Russia), disodium hydrogen phosphate (CAS 7558-79-4; *Chimmed*, Russia), and sodium hydroxide (GOST 4328-77 Amend. 1, 2; *Chimmed Sintez*, Russia). Because the copolymer is both thermo- and pH-sensitive, the effects of pH and temperature on the transparency of the copolymer solution were studied using a WaterLiner WTM-86 turbidimeter (*Metronx*, Russia). The composition of the buffer system was also investigated. The pH of the solutions was measured using a pH meter (*Econix-Expert*, Russia) with an ESK-10601 combined glass electrode (*Izmeritelnaya Tekhnika*, Russia). Furthermore, when optimizing the conditions for producing the dosage form, the presence, or absence of opalescence in the solution was determined visually.

Studies were conducted on a selection of thickeners to determine the most effective distribution method for the drug in the nasal cavity and to increase the viscosity of the solution. The dynamic viscosity values were measured at 25.0±0.5°C using rotational viscometry with a Brookfield DV2T viscometer (*Brookfield Engineering Laboratories*, United States). Before

¹ The situation of influenza in Russia and the world. Ministry of Health of the Russian Federation. FSBI Research Institute of Influenza. D.I. Ivanovsky Research Institute of Virology. Available from: <http://www.influenza.spb.ru/system/> [Accessed September 22, 2019] (in Russ.).

² Pharmacological Management of Pandemic Influenza A (H1N1) 2009 Part I: Recommendations of World Health Organization. Available from: https://www.who.int/csr/disease/swineflu/notes/h1n1_use_antivirals_20090820/en/ [Accessed September 17, 2019].

³ The State Pharmacopeia of the Russian Federation. 14th ed. Moscow: Ministry of Health of the Russian Federation; 2018 (in Russ.).

the readings were noted, the temperature of the test sample was allowed to equilibrate for 15 min. The readings were conducted at shear rates ranging from 0.28 to 58.0 s⁻¹, which corresponded to 10–90% torque. The optimal dissolution time was determined, in addition to the ideal conditions for cooling and the influence exerted by the opalescence of the solution. The active substances in the prepared solution were monitored via high performance liquid chromatography [9] using a Dionex UltiMate 3000 (*Thermo Scientific*, Germany). For the analysis of the copolymer, a Luna column (150×4.60 mm); *Phenomenex*, United States) was filled with a C5 sorbent with a particle size of 5 µm and a pore diameter of 10 nm (mobile phase A: mixture of 0.1% phosphoric acid and acetonitrile in a volume ratio of 82:18 with the addition of 4.5 mM sodium pentanesulfonate solution; mobile phase B: acetonitrile). The ACA content was determined using a Nucleodur C18 Pyramid column (250×4.6 mm) filled with 5 µm spherical particles (mobile phase A: 30 parts by mass of methanol to 70 parts of a solution containing 1% H₃PO₄, 10 mM sodium pentanesulfonate, and 15 mM K₂HPO₄ in H₂O; mobile phase B: methanol). Sterility of the solution was ensured by filtration using a glass vacuum system (FilterSys AH0-1566 F; *Phenomenex*, UK) equipped with filters of pore sizes 0.45 and 0.22 µm (AF0-0514, AF0-0513; *Phenomenex*, UK). The shelf life of the drug was determined via the accelerated aging method using a climatic chamber (KK115; *Pol-Eko-Aparatura*, Poland); this investigation was conducted in accordance with the Russian State Pharmacopeia XIV (General Pharmacopeia Article 1.1.0009.15).

RESULTS AND DISCUSSION

Optimization of the pH values and the components of the buffer solution

The composition and conditions required to produce a nasal spray based on aminocaproic acid and the copolymer of *N*-vinylpyrrolidone and 2-methyl-5-vinylpyridine were developed after a comprehensive research. Phosphate buffered saline (PBS) was used as the base for the spray, and a series of buffer solutions with different pH values (5.0–6.6) was prepared in accordance with the Russian State

Pharmacopeia XIV (General Pharmacopeia Article 1.3.0003.15). The copolymer (0.5 wt %) was then added to each solution, and the stability of the solutions was determined at different temperatures (25–45°C) using turbidimetry. The effects of the pH value and temperature on the transparency of the copolymer solution in the buffer are presented in Table 1. The solutions were considered “transparent” when the turbidity index was up to 3.0 nephelometric turbidity units.

The results clearly showed that the turbidity of the copolymer solution at 30°C and pH 6.3 was high, implying instability of the formulation. Thus, the optimal pH range for the dosage form was determined to be between 5.5 and 6.2. For the PBS samples, the results of the pH optimization experiments are presented in Table 2 [10]. The most stable PBS samples had a pH value of 5.5.

Optimization of the excipients

Several studies were conducted to increase the viscosity of the spray solution through the use of an appropriate thickener, to prolong drug effectiveness. Afrin, a commercially available nasal spray [11], was chosen as the control sample as it contained thickeners with a measured viscosity of 500±50 mPa·s at 25°C. Samples with various concentrations of the excipients, all of which had been approved for medical use and were used in commercial nasal dosage forms, were used to determine the optimal characteristics (Table 3). The samples were compared on the basis of two parameters: the pH value and the viscosity of the solution at 25.0°C. The test was conducted at a shear rate of 22.4 s⁻¹.

As we can see from Table 3, the ideal pH and viscosity parameters were only observed in samples 4 and 5. When subsequent observations of these samples were conducted over the course of a month, sample 4 showed only a slight decrease in viscosity, whereas sample 5 exhibited a decrease in viscosity that was below the required threshold (see Figure).

From the results of the rheoviscometry experiments, it was clear that there was a noticeable decrease in the dynamic viscosity of the solution after prolonged storage with the thickener Vivapur®. In the absence of Vivapur®, however, the dynamic viscosity of the solution remained almost constant. This was

Table 1. Effect of pH and temperature on the transparency of the solutions

Temperature, °C	pH								
	5.0	5.5	6.0	6.1	6.2	6.3	6.4	6.5	6.6
25	2.9	0.8	0.9	0.9	0.8	0.8	0.8	1.4	14.3
30	2.3	1.1	1.0	1.0	0.9	3.4	157	685	–
40	2.4	1.3	1.7	1.0	2.0	326	609	678	–
45	2.6	1.3	4.4	14.8	280	742	817	–	–

indicative of pronounced intermolecular interaction between Vivapur® and the other components of the solution, which, in turn, disrupted the stability of the system during storage. Because the chemical interaction between the active components and the excipients was undesired, we decided to exclude Vivapur® from the final composition. Thus, the optimal distribution of the drug across the mucous membrane of the nasal cavity was accomplished by optimizing the spray nozzle rather than by lowering the viscosity of the solution.

The stability of the dosage form over the course of its entire shelf life was ensured by adding benzalkonium chloride (0.15 mg/mL), the commonly

used preservative in commercial nasal spray formulations. The optimal combination of reagents for the model mixture is shown in Table 4.

Next, the optimization of the laboratory conditions was conducted by the *Institute of Pharmaceutical Technologies*, Russia. The rapid dissolution of the copolymer was achieved only at low pH values and at low temperatures of the buffer solutions. The copolymer was dissolved in cold purified water with constant stirring, followed by refrigeration as part of the protocol for optimization process.

The preparation of a control form for the aforementioned samples was conducted visually (i.e., a transparent homogeneous solution was obtained without

Table 2. Change in pH values of 0.5% copolymer solutions during storage at 25°C depending on the initial pH value of the PBS

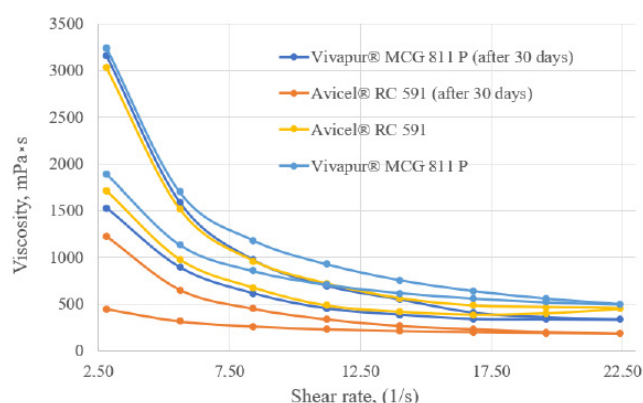
Shelf life, days	Samples PBS				
	pH 5.0	pH 5.2	pH 5.5	pH 5.8	pH 6.0
0	5.3	5.5	5.7	5.9	6.3
7	5.4	5.4	5.8	5.7	6.3
30	5.5	5.4	5.8	5.6	6.3

Table 3. Optimization of the excipients

Name of the component in the sample	Compositions of the nasal spray, with the content of substances, mg/mL								
	1	2	3	4	5	6	7	8	9
Sorbitol	50		–	–	20	10	5	–	–
PEG 4000	–	10	–	–	10	–	–	3	–
Na-CMC	–	–	25	–	–	30	–	15	–
Glycerin	1.5	1	–	–	–	–	1.2	–	0.5
Polysorbate 80	0.01	–	0.05	0.1	–	–	0.2	–	–
Povidone K29-32	–	5.5	–	–	4	–	10	5	5
Avicel® RC 591	10	–	–	–	20	–	–	–	15
Vivapur® MCG 811 P	–	–	–	20	–	–	–	10	–
PEG 1500	–	15	–	10	–	5	–	–	–
Parameters									
Viscosity, mPa·s at a shear rate of 22.4 s ⁻¹ and temperature of 25°C	374	275	1315	498	452	1117	989	2546	1245
pH	6.8	6.2	5.3	6.0	6.0	5.5	5.0	5.4	6.0

visible mechanical impurities and opalescence) as well as via quantitative analysis of the condition parameters for the active reagents. Based on the data shown in Table 5, the optimal process was set as follows:

1. Prepare the buffer solution with pH 5.5 from solutions 1 and 2 and then filter it through a 0.45 μm filter.
2. Cool the buffer solution to $15 \pm 2^\circ\text{C}$.
3. Fill the reactor with the buffer solution.
4. Add and dissolve the copolymer with subsequent sedimentation at $3\text{--}6^\circ\text{C}$ for 24 h.
5. Add and dissolve ACA and benzalkonium chloride.



Viscosity–velocity curves of samples 4 and 5 at 25°C .

6. Sterilize via filtration and then bottle the solution into 10 mL polymer bottles equipped with polymer based spray nozzles.

Thermal sterilization, in this case, was not possible because of the thermosensitivity of the copolymer. Additionally, sterilization using an autoclave resulted in precipitation within the solution. Therefore, filtration was selected as the preferred method of sterilization.

The shelf life of the nasal spray was determined by quantifying the stability of three series of spray samples (Table 6) in polymer based bottles with spray nozzles using the accelerated aging method at $40 \pm 2^\circ\text{C}$ and $75 \pm 5\%$ humidity for 180 days. This experiment was performed in accordance with the Russian State Pharmacopeia XIV, as these conditions were nearly similar to those of aging of the dosage form for 2 years under natural conditions. During this analysis, the pH, microbiological purity, and the quantitative content of the active substances were monitored [12].

From the results of the study, it was clear that the values of the controlled indicators remained within the reference range and that the deviation values corresponded to the measurement error calculations. The shelf life of the drug was estimated to be 2 years. As a confirmatory test, three series of drug samples were subjected to the same natural conditions.

Table 4. Composition of the solution of the nasal spray per 1 mL

Ingredient	Quality standard	Quantity, mg
Active substances		
Aminocaproic acid (ACA)	Pharmacopeia Article of the Manufacturer LS-000113-280909, Amend. 1, 2	10.00
Copolymer of 2-methyl-5-vinylpyridine and N-vinylpyrrolidone	Normative Documentation Project	5.00
Excipients		
Potassium dihydrogen phosphate	Russian State Pharmacopeia XIV	9.45
Disodium hydrogen phosphate	Russian State Pharmacopeia XIV	1.28
Benzalkonium chloride	European Pharmacopeia; Russian State Pharmacopeia XIV	0.15
Purified water	Russian State Pharmacopeia XIV	Up to 1.00

Table 5. Optimization of the production conditions

Parameter	Conditions				
Experiment number	E1	E2	E3	E4	E5
Temperature, °C	5	10	15	20	25
Dissolution time before opalescence, min	10	12	15	25	45

Conclusion: the optimal temperature for mixing is 5–15°C

Experiment number	E6	E7	E8	E9	E10
Mixer speed, rpm	30	40	50	80	100
Dissolution time before opalescence, min	>30	>30	13	>30	>30

Conclusion: the optimal mixing speed is 50 rpm

Experiment number	E11	E12	E13	E14	E15
Refrigeration until complete dissolution of the copolymer, h	12	15	20	24	30
The presence of opalescence, +/-	+	+	+	–	–
Copolymer content in the solution, mg/mL	4.68	4.80	4.97	5.04	5.01

Conclusion: the optimal storage time of the copolymer in the refrigerator is 24 h

Experiment number	E16	E17	E18	E19	E20
Dissolution of ACA and benzalkonium chloride at ambient temperature, °C	10	12	15	20	25
Dissolution time, min	3	3	3	3	3

Conclusion: ACA and benzalkonium chloride dissolve equally well between 10 to 25°C

Experiment number	E21	E22	E23	E24	E25
Dissolution of ACA and benzalkonium chloride with mixing, stirrer speed, rpm	50	80	100	150	300
Dissolution time, min	3	3	2	2	2

Conclusion: the rate of dissolution of ACA and benzalkonium chloride varies insignificantly

Table 6. Selected data on the stability of the nasal dosage form in polymer package

Specification	Standard	Shelf life, days	Batch		
			130318	210518	191118
pH	5.5–6.2	0	5.7	5.8	6.0
		180	5.8	5.8	5.9
Microbiological purity	Category 2	0	Complies	Complies	Complies
		180	Complies	Complies	Complies
Quantitative assay					
ACA, mg/mL	9.5–10.5	0	9.89	10.05	10.12
		180	9.89	10.05	10.11
Copolymer, mg/mL	4.75–5.25	0	5.03	5.15	4.96
		180	5.03	5.13	4.96

CONCLUSIONS

In this study, we developed the composition and conditions needed to produce a nasal spray for the prophylactic treatment of influenza and other VRIs. The nasal spray contains 1 wt % aminocaproic acid and

0.5 wt % copolymer of 2-methyl-5-vinylpyridine and *N*-vinylpyrrolidone. Accelerated aging studies showed that the estimated shelf life of the drug is 2 years.

The author declares no conflicts of interest.

REFERENCES

1. Svyatchenko S.V., Durymanov A.G., Kolosova N.P., Gudymo A.S., Goncharova N.I., Torzhkova P.Y., Bulanovich Y.A., Epanchintseva A.V., Danilenko A.V., Marchenko V.Y., Sysoeva A.V., Susloparov I.M., Tregubchak T.V., Ryzhikov A.B., Maksyutov R.A., Illicheva T.N. Severe cases of seasonal influenza in Russia in 2017–2018. *Journal of microbiology epidemiology immunobiology*. 2019;(4):58–64 (in Russ.). <https://doi.org/10.36233/0372-9311-2019-4-58-64>
2. Kiselev O.I., Marynich I.G., Somnina A.A. (eds.). *Gripp i drugie respiratornye virusnye infektsii: epidemiologiya, profilaktika, diagnostika i terapiya* (Influenza and other respiratory viral infections: epidemiology, prevention, diagnosis and therapy). Saint Petersburg: Borges; 2003. 245 p.
3. Dondurey E.A., Obratsova E.V., Semiletko Y.S., Ovchinnikova N.V., Golovacheva E.G., Osidak L.V., Afanasyeva O.I. ARVI antiviral therapy in children in modern clinical practice. *Meditinskiy sovet = Medical Council*. 2019;(2):183–187 (in Russ.). <https://doi.org/10.21518/2079-701X-2019-2-183-187>
4. Cheshik S.G. Influenza. *Detskie infektsii = Infant Infections*. 2005;(4):56–63 (in Russ.).
5. Ghorri M.U., Mahdi M.H., Smith A.M., Conway B.R. Nasal Drug Delivery Systems: An Overview. *Am. J. Pharm. Sci.* 2015;3(5):110–119.
6. Degenhard M.A., Gerallt W.U., Birkhoff M.S. Intranasal Drug Administration — An Attractive Delivery Route for Some Drugs. *Drug Discovery and Development – From Molecules to Medicine. IntechOpen*. 2015;(13):300–318. <http://dx.doi.org/10.5772/59468>

СПИСОК ЛИТЕРАТУРЫ

1. Святченко С.В., Дурьманов А.Г., Колосова Н.П., Гудымо А.С., Гончарова Н.И., Торжкова П.Ю., Буланович Ю.А., Епанчинцева А.В., Даниленко А.В., Марченко В.Ю., Сысоева А.В., Суслопаров И.М., Трегубчак Т.В., Рыжиков А.Б., Максюттов Р.А., Ильичева Т.Н. Тяжелые случаи заболевания гриппом на территории Российской Федерации в эпидемическом сезоне 2017–2018. *Журнал микробиологии, эпидемиологии и иммунобиологии (ЖМЭИ)*. 2019;(4):58–64. <https://doi.org/10.36233/0372-9311-2019-4-58-64>
2. Киселев О.И., Маринич И.Г., Сомнина А.А. (под ред.). *Грипп и другие респираторные вирусные инфекции: эпидемиология, профилактика, диагностика и терапия*. СПб.: Боргес; 2003. 245 с.
3. Дондурей Е.А., Образцова Е.В., Семилетко Ю.С., Овчинникова Н.В., Головачева Е.Г., Осидак Л.В., Афанасьева О.И. Противовирусная терапия ОРВИ у детей в современной клинической практике. *Медицинский Совет*. 2019;(2):183–187. <https://doi.org/10.21518/2079-701X-2019-2-183-187>
4. Чешик С.Г. Грипп. *Детские инфекции*. 2005;(4):56–63.
5. Ghorri M.U., Mahdi M.H., Smith A.M., Conway B.R. Nasal Drug Delivery Systems: An Overview. *Am. J. Pharm. Sci.* 2015;3(5):110–119.
6. Degenhard M.A., Gerallt W.U., Birkhoff M.S. Intranasal Drug Administration — An Attractive Delivery Route for Some Drugs. *Drug Discovery and Development – From Molecules to Medicine. IntechOpen*. 2015;(13):300–318. <http://dx.doi.org/10.5772/59468>

7. Karpova A.S., Kochkina Y.V., Kedik S.A. The antiviral activity study of complex drug with aminocaproic acid for prevention of influenza and ARVI. *Razrabotka i registratsiya lekarstvennykh sredstv* = *Drug Development & Registration*. 2019;8(2):22-26 (in Russ.).

<https://doi.org/10.33380/2305-2066-2019-8-2-22-26>

8. Evseeva A.S., Kochkina Yu.V., Krasilnikov I.V., Kedik S.A., Eremin D.V., Suslov V.V. Antiviral and immunomodulating combination based on aminocaproic acid and a copolymer of 2-methyl-5-vinylpyrrolidin and *N*-vinylpyrrolidone: patent 2669810 RF. Appl. 21.06.2017, publ. 16/10/2018. Bull. Number 29 (in Russ.).

9. Evseeva A.S., Vorfolomeeva E.V., Kochkina Yu.V., Kedik S.A., Vostrov I.A. A method for the quantitative determination of aminocaproic acid when it is combined with a copolymer of 2-methyl-5-vinylpyridine and *N*-vinylpyrrolidone by HPLC: patent 2700167 RF. Appl. 09/13/2018, publ. 09/13/2019. Bull. Number 26 (in Russ.).

10. Kravchenko I.A. *Sposoby vvedeniya lekarstvennykh preparatov v organizm. Intranasal'noe vvedenie lekarstvennykh preparatov* (Methods of introducing drugs into the body. Intranasal administration of drugs). Odessa: Astroprint; 2009. 164 p. ISBN 978-966-190-128-4 (in Russ.).

11. Kundoor, V., Dalby, R.N. Effect of Formulation- and Administration-Related Variables on Deposition Pattern of Nasal Spray Pumps Evaluated Using a Nasal Cast. *Pharm. Res.* 2011;28(8):1895-1904.

<https://doi.org/10.1007/s11095-011-0417-6>

12. Sakaeva I.V., Bunyatyan N.D., Kovaleva E.L., Sakanyan E.I., Mitkina L.I., Prokopov I.A., Shelekhina E.S., Mitkina Y.V. The main approaches to the study of drug stability: domestic and international experience. *Vedomosti Nauchnogo centra ekspertizy sredstv medicinskogo primeneniya* = *The Bulletin of the Scientific Centre for Expert Evaluation of Medicinal Products*. 2013;(3):8-11. (in Russ.).

7. Карпова А.С., Кочкина Ю.В., Кедик С.А. Изучение противовирусной активности комплексного препарата с аминакапроновой кислотой для профилактики гриппа и ОРВИ. *Разработка и регистрация лекарственных средств*. 2019;8(2):22-26.

<https://doi.org/10.33380/2305-2066-2019-8-2-22-26>

8. Евсеева А.С., Кочкина Ю.В., Красильников И.В., Кедик С.А., Еремин Д.В., Суслов В.В. Противовирусная и иммуномодулирующая комбинация на основе аминакапроновой кислоты и сополимера 2-метил-5-винилпиридина и *N*-винилпирролидона. Патент РФ № 2669810. Заявка от 21.06.2017, опублик. 16.10.2018 г. Бюлл. № 29.

9. Евсеева А.С., Ворфоломеева Е.В., Кочкина Ю.В., Кедик С.А., Востров И.А. Способ количественного определения аминакапроновой кислоты при её совместном присутствии с сополимером 2-метил-5-винилпиридина и *N*-винилпирролидона методом ВЭЖХ. Патент РФ № 2700167. Заявка от 13.09.2018; опублик. 13.09.2019 г. Бюлл. № 26

10. Кравченко И.А. Способы введения лекарственных препаратов в организм. Интраназальное введение лекарственных препаратов. Одесса: Астропринт; 2009. 164 с. ISBN 978-966-190-128-4

11. Kundoor, V., Dalby, R.N. Effect of formulation- and administration-related variables on deposition pattern of nasal spray pumps evaluated using a nasal cast. *Pharm. Res.* 2011;28(8):1895-1904.

<https://doi.org/10.1007/s11095-011-0417-6>

12. Сакаева И.В., Бунятян Н.Д., Ковалева Е.Л., Саканян Е.И., Митькина Л.И., Прокопов И.А., Шелехина Е.С., Митькина Ю.В. Основные подходы к изучению стабильности лекарственных средств: отечественный и международный опыт. *Ведомости Научного центра экспертизы средств медицинского применения*. 2013;(3):8-11.

About the author:

Anastasiya S. Karpova, Senior Quality Specialist, JSC "Institute of Pharmaceutical Technology" (of. 1, 21, Skolkovskoe shosse, Moscow, 121353, Russia). E-mail: karpova@ipt.ru.com.

Об авторе:

Карпова Анастасия Сергеевна, главный специалист по качеству Акционерного общества «Институт фармацевтических технологий» (121353, Россия, г. Москва, Сколковское ш., д. 21, оф. 1). E-mail: karpova@ipt.ru.com.

Submitted: October 25, 2019; Reviewed: November 26, 2019; Accepted: January 24, 2020.

Translated from Russian into English by H. Moshkov

Edited for English language and spelling by Enago, an editing brand of Crimson Interactive Inc.

ISSN 2686-7575 (Online)

<https://doi.org/10.32362/2410-6593-2020-15-1-76-83>



UDC 539.217.1

Application of the mercury porosimetry method in the analysis of sorption materials

Rashid K. Kostoev, Dzhabrail S. Tochiev, Eset I. Nilkho, Zakhirat H. Sultigova,
Raisa D. Archakova, Bagaudin A. Temirkhanov[@], Leyla Ya. Uzhakhova

Ingush State University, Republic of Ingushetia, Magas, 386001 Russia

[@]Corresponding author, e-mail: baga@inbox.ru

Objectives. This study aims to establish the available porosity of a sorbent based on carbonized rice husk and investigate its sorption properties for oil and oil products.

Methods. A rice-husk-based sorbent carbonized at 400°C for 30 min was selected as the subject. The porosity of this sorbent is analyzed with the help of mercury porosimeters, the Pascal 140 EVO and Pascal 240 EVO. The sorption properties of the sorbent are also studied when cleaning water containing oil and oil products.

Results. The test sample is a bulk porous material with a pore volume of 0.015 cm³/g; porosity higher than 15% was found, and the pore size distribution is shown. Studies were conducted on the sorption of oil and oil products as well as the possibility of using the aforementioned sorbent as a filtering material in the purification of water containing oil products. We investigated the sorption processes under dynamic and static conditions. The methodology for measuring the porous structure of solid materials on the mercury porosimeter, Pascal 140 EVO, was examined. The texture characteristics of the sorbent's porous structure were determined, which is primarily the total volume of pores, the values of the specific surface area, and the volume of the micropores and mesopores.

Conclusions. The materials studied can be used as sorbents with a developed porous structure for purification of water with dissolved and emulsified petroleum products.

Keywords: porosimetry, porosity, sorbent, sorption, pore volumes, oil, petroleum products, rice husks.

For citation: Kostoev R.K., Tochiev D.S., Nilkho E.I., Sultigova Z.H., Archakova R.D., Temirkhanov B.A., Uzhakhova L.Ya. Application of the mercury porosimetry method in the analysis of sorption materials. *Tonk. Khim. Tekhnol. = Fine Chem. Technol.* 2020;15(1):76-83. <https://doi.org/10.32362/2410-6593-2020-15-1-76-83>

Применение метода ртутной порозиметрии в анализе сорбционных материалов

Р.К. Костоев, Д.С. Точиев, Э.И. Нилхо, З.Х. Султыгова, Р.Д. Арчакова,
Б.А. Темирханов[@], Л.Я. Ужахова

Ингушский государственный университет, Республика Ингушетия, Магас, 386001 Россия
[@]Автор для переписки, e-mail: bada@inbox.ru

Цель. Целью данной работы явилось установление доступной пористости сорбента на основе карбонизированной рисовой шелухи и исследование его сорбционных свойств по отношению к нефти и нефтепродуктам.

Методы. В качестве объекта исследования был выбран сорбент на основе рисовой шелухи, карбонизированной при 400 °С в течение 30 мин. Для него проанализирована пористость с помощью ртутных порозиметров Pascal 140 EVO и Pascal 240 EVO, а также изучены сорбционные свойства сорбента в процессе очистки воды от нефти и нефтепродуктов.

Результаты. Показано, что образец сорбента на основе рисовой шелухи является объемно-пористым материалом с удельным объемом пор 0.015 см³/г. Представлено распределение пор по размерам. Установлено, что доступная пористость составляет более 15%. Проведены исследования по сорбции нефти и нефтепродуктов, а также показана возможность применения указанного сорбента в качестве фильтрующего материала при очистке воды от нефтепродуктов. Сорбционные процессы исследованы в динамических и статических условиях. Изучены методические аспекты измерения параметров пористой структуры твердых материалов на ртутном порозиметре Pascal 140 EVO. Определены текстурные характеристики пористой структуры анализируемого сорбента: общий объем пор, величина удельной поверхности пор, объем микро и мезопор.

Выводы. Исследуемые материалы могут быть применены в качестве сорбентов, обладающих развитой пористой структурой, для очистки воды от растворенных и эмульгированных нефтепродуктов.

Ключевые слова: порозиметрия, пористость, сорбент, сорбция, объемы пор, нефть, нефтепродукты, рисовая шелуха.

Для цитирования: Костоев Р.К., Точиев Д.С., Нилхо Э.И., Султыгова З.Х., Арчакова Р.Д., Темирханов Б.А., Ужахова Л.Я. Применение метода ртутной порозиметрии в анализе сорбционных материалов. *Тонкие химические технологии*. 2020;15(1):76-83. <https://doi.org/10.32362/2410-6593-2020-15-1-76-83>

INTRODUCTION

Currently, the use of raw plant material byproducts as sorption materials is critical. Studies of parameters, such as porosity, sorption capacity, mechanical strength, and others, provide information that allows us to predict the future use of raw plant material byproducts as sorption materials.

This work aims to establish the available porosity of a sorbent using carbonized rice husk (CRH) and study the sorption properties of oil as well as oil products.

Mercury porosimetry is one of the tools for studying the porous structure of a solid. It is very versatile because it provides information about a porous structure in a wide range of pore sizes, and its calculation equations are simple [1]. This method can

also be used to measure the specific surface of dispersed bodies under conditions when the highly concentrated particulate matter, e.g., a powder, has a relatively low surface energy. Mercury does not wet the surface of its particles when there are no one-side open pores, and the pressure in the porosimeter allows mercury to penetrate the smallest micropores of the sample [2].

The method for measuring porosity with mercury porosimetry consists of adding mercury to a previously evacuated vessel with a sample and increasing the pressure sequentially. The level of mercury in the vessel decreases as it penetrates the pores. If this level is measured accurately enough, we can plot the pressure of the volume of the pressed mercury as a function of pressure, calculate the diameters of the filled pores and, construct a program [3].

MATERIALS AND METHODS

Rice husk grown in the Krasnodar krai was crushed to a particle size of less than 1 mm and used as a raw material for the production of the sorbent; it was subjected to carbonization for 30 min at 400°C.

The porosity, as well as the bulk, apparent, and real (skeletal) density, of the material was measured on a Pascal 140 EVO mercury porosimeter and Pycnomatic ATC helium pycnometer from Thermo Scientific, according to the guidelines in the Pascal mercury porosimeter user manual¹.

The pore volume distribution was calculated by the amount of mercury that penetrated the pores of the samples and the equilibrium pressure at which the penetration phenomenon occurred. The calculations rely on assumptions such as the surface tension of the mercury and the wetting angle of the solid material must be constant during the analysis; the pressure during mercury penetration is the equilibrium pressure; the pores have a cylindrical shape; and solid materials are not subjected to deformation under the influence of high pressure.

The following parameters were recorded during the experiment: the experiment temperature, calculated mercury density, degassing time before filling the dilatometer, air pulse, degassing pressure, maximum pressure, maximum speed increase, maximum speed decrease, increase in pump speed, decrease in pump speed, distance between electrodes, dilatometer cone height, dilatometer rod radius, dilatometer number, empty dilatometer weight, sample weight, skeletal density of the sample, and contact angle of the mercury sample.

RESULTS AND DISCUSSION

The data were obtained from the porosimeter. The skeletal density of the material, 1.18 g/cm³, was measured with a helium pycnometer. We qualitatively determined the degree of compression; this could be adjusted using the SOLID software.

Figure 1 shows the intrusion curve (the dependence of the volume of depressed mercury on the applied pressure).

Figure 2 shows the pore size distribution data. Three peaks are clearly distinguished in Fig. 2, pores with a diameter of 9.1072, 36.1200, and 8.0432 μm. Based on the mercury intrusion data, the following material characteristics were calculated via the SOLID software:

- The total specific pore volume is 0.01578 cm³/g.
- The specific pore surface area is 0.001 m²/g

¹Mercury porosimeters of a PASCAL EVO series and SOLID software. User guide, P/N 31713070, Edition A, Italy, 2017.

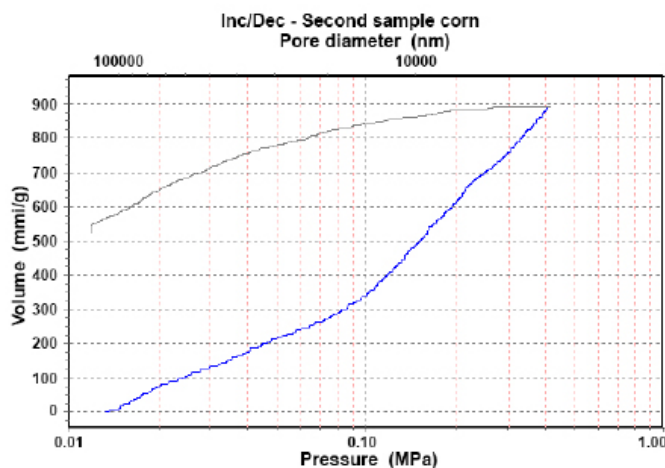


Fig. 1. Intrusion curve.

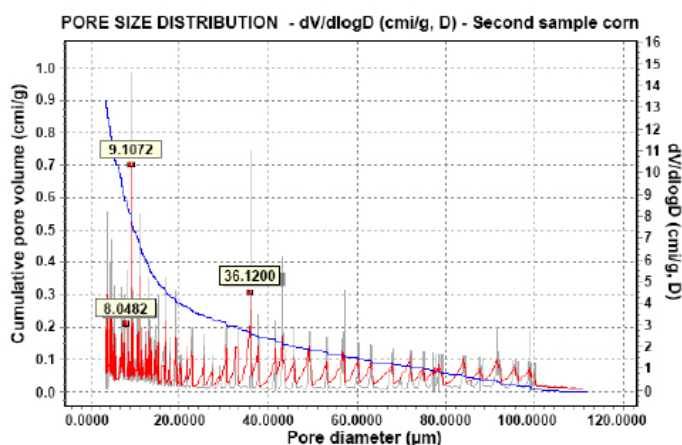


Fig. 2. Pore diameters of the carbonized rice husk.

(calculated according to the model of cylindrical and slit-like pores).

– The average pore diameter is 9.5113 μm (determined as four-fold pore volume divided by area. In this method, the pores are considered cylindrical).

– The median pore diameter is 10.9914 μm (defined as pore size calculated at 50% of the total pore volume).

– The most common pore diameter is 9.1072 μm (defined as the pore size at the maximum peak of the $dV/d\log D$ derivative).

We analyzed the pore size distribution of the test material. Figure 3 shows a histogram of the pore size distribution (information was obtained only on the Pascal 140 EVO device).

We constructed a histogram of the distribution of the specific surface area by pore size (Fig. 4) based on the model of cylindrical and slit-like pores.

As can be seen from the study, mercury porosimetry allows one to obtain information about the porous

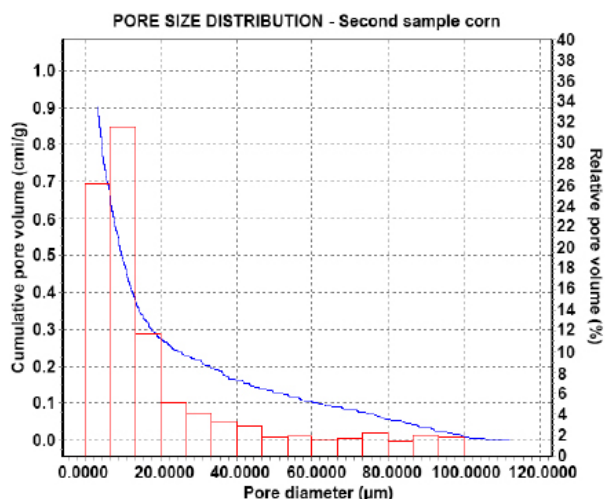


Fig. 3. Specific pore volume of the rice husk.

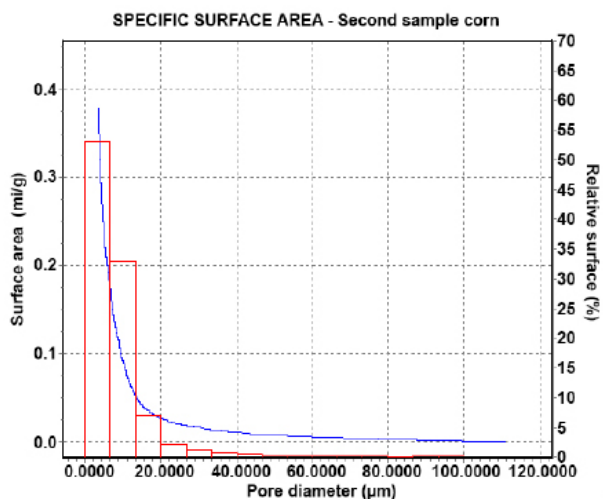


Fig. 4. Specific pore surface area of the carbonized rice husk.

structure of the studied sorbent, as well as its density and total surface.

Table 1 presents the results of the analysis of a sample of rice husk carbonized at 400°C.

After solving the main problem of determining the pore volume of the CRHs, we studied the sorption properties of this sorbent with oil and oil products in dynamic and static conditions. We used oil from

the Malgobekskoe field of the Republic of Ingushetia, AI-93 gasoline, and summer diesel fuel to determine the sorption capacity of the CRH. The characteristics of the oil are given in Table 2 [4].

It was previously established that the sorption of oil and oil products under static conditions by various sorbents depends not only on the pore volume of the sorbents but also on the viscosity of the absorbed substance and the duration of contact [5]. The sorption capacity of the CRH was determined gravimetrically, calculated as the ratio of the mass of the absorbed oil and oil products to the mass of the sorbent in the range from 5 to 120 min. The effectiveness assessment of the studied sorbents was determined according to TU 214-10942238-03-95 [6]. The results of the sorption capacity of the sorbent based on CRH for oil and petroleum products are summarized in Table 3 (average of three definitions).

From the data shown in Table 3, it is apparent that the full sorption capacity of the studied sorbent is low. However, carbonized carbon-containing substances can be effectively used for wastewater treatment.

The sorption characteristics of the CRH were studied under dynamic conditions by filtering the solution to be purified through a fixed adsorbent layer to determine the possibility of wastewater treatment of water with oil and oil products using the CRH. The equilibrium conditions were achieved at a constant temperature of 25°C and an oil concentration of 23.5 mg/l. The initial concentration of oil in the water was determined by the gravimetric method [7], based on the separation of oil products from water by extraction with hexane. This was followed by chromatographic separation of oil products from compounds of other classes in a column filled with aluminum oxide. The effectiveness of the sorbent was evaluated for distilled water contaminated with oil with a concentration of 23.5 mg/l.

A column with a height of 50 cm and a diameter of 3 cm was filled with a sorbent to a height of 20 cm; the total mass of the sorbent was 5 g. The solution was fed from above, and it passed by gravity through the sorbent layer. In this case, the water transmission rate (space velocity) was 6 ml/min.

Table 1. Results of the porosity analysis of the material studied

Helium pycnometer real density, g/cm ³	Apparent density, based on mercury porosimetry, g/cm ³	Available porosity, %	Closed cell porosity, %	Specific pore volume, cm ³ /g	Specific surface area of pores, m ² /g
1.18	0.3941	15.750	44.83	0.01575	0.001

Table 2. Physical and chemical parameters of the oil

№	Parameters	Experimental Method	Results of the Experiment
1	Density of the oil, kg/m ³ at 20°C	GOST 3900-85	833.7
2	Kinematic viscosity, cSt, at no higher than 20°C at no higher than 50°C	GOST 33-82	12.35 5.28
3	Dynamic viscosity, mPa·s, at 20 °C at 50 °C	GOST 33-82	10.3 4.40
4	Sulfur content, mass %, including: hydrogen sulfides mercaptans	GOST 1437-75 GOST 17323-71	0.31 Traces 0.0075
5	Chloride content, mass % (mg/dm ³)	GOST 21534-76	0.010 (82.03)
6	Silica gel resin content, mass %	GOST 11858-66	1.08
7	Paraffin content, mass %		2.1
8	Asphaltene content, mass %		0.03
9	Water content, mass %	GOST 2477-65	None
10	Mechanical impurity content, mass %	GOST 6370-83	0.001
11	Pour point, °C	GOST 20287-96	–20
12	Paraffin melting point, °C	GOST 4255-75	+54
13	Closed cup flash point, °C	GOST 4333-87	–17
14	Open cup flash point, °C		0
15	Flash point, °C		+11
16	Saturated steam pressure, kPa (mm Hg)	GOST 1756-52	24.4 (183)
17	Acidity, mg KOH/100 cm ³	GOST 5985-79	0.015
18	Ash content, %	GOST 1461-75	0.017
19	Molecular mass	GOST R 8.903-2015	213

Table 3. Sorption capacity of the carbonized rice husk (CRH) for oil and its products

Sorbent	Oil sorption capacity, g/g				
	5 min	10 min	30 min	60 min	120 min
CRH	4.3	4.7	4.9	5.1	5.2
	Sorption capacity for diesel fuel, g/g				
	4.4	4.6	4.8	5.0	5.0
	Sorption capacity for gasoline (AI-93), g/g				
	2.1	3.3	3.9	3.5	3.8

Table 4. Concentration of oil products in water before and after CRH filtration (sample volume is 250 ml)

Sorbent	Oil concentration, mg/l				
	Before filtration	After filtration			
		Sample 1	Sample 2	Sample 3	Sample 4
CRH	23.5	0.22	0.26	0.31	4.8

Purified water was collected in four 250 ml samples. At the exit from the column, the clear water obtained corresponds to RD 52.24.496-2005².

The maximum permissible concentration (MPC) of oil products in water, according to SanPiN 2.1.4.1074-01, "Drinking water. Hygienic requirements for water quality of centralized drinking water supply systems. Quality Control," is 0.1 mg/dm³. The MPC of oil products in wastewater is 0.3 mg/l.

The analysis of water for residual oil content was carried out by infrared spectroscopy using an InfraLUM FT-08 IR Fourier spectrometer. It indicated that the oil concentration in the water is below the MPC for wastewater. The determination of the petroleum products present in the samples was carried out according to the procedure, M-01-39-2010³.

Data on the concentration of petroleum products in purified water are given in Table 4.

As can be seen from Table 4, after the first three samples, that is, after 750 ml of contaminated water is filtered, oil products slip through the sorbent bed, pores begin to clog, and sorbent regeneration is required. The cleaning efficiency decreases from the

first sample to the last, and the concentration of oil in the first two samples remains below 0.3 mg/l.

CONCLUSIONS

Using mercury porosimetry via a Pascal 140 EVO device, we determined the main characteristics of a sorbent made from CRH. The studied sorbent samples are volume-porous materials. The studied materials can be used as sorbents with a developed porous structure.

We established the sorption capacity of the CRH for oil and oil products, which amounted to 2–5 g/g. We investigated the sorption process of oil products with a sorbent of rice husk in dynamic conditions. We showed that the CRH sorbent purifies water with dissolved and emulsified oil products.

Acknowledgments

The study was performed at the Engineering Center "Development of Modified Sorption Materials" of the Ingush State University with the support of the Ministry of Industry and Trade of the Russian Federation and the Ministry of Education and Science of the Russian Federation.

The authors declare no conflicts of interest.

² Guidance document RD 52.24.496-2005: *Temperatura, prozrachnost' i zapakh poverkhnostnykh vod sushi. Metodika vypolneniya izmerenii* (Temperature, transparency and smell of surface water of land. Methodology for making measurements) (approved by Roshydromet, May 15, 2005) (in Russ.).

³ M-01-39-2010. *Opredelenie nefteproduktov v probakh prirodnnykh, pit'evykh i stochnykh vod* (Determination of petroleum products in samples of natural, drinking and wastewater). GOST R 51797-2001 (in Russ.).

REFERENCES

1. Plachenov T. G., Kolosentsev S.D. *Porozimetriya* (Porosimetry). Leningrad: Khimiya; 1988. 176 p. (in Russ.).
2. Karnaukhov A.P. *Adsorbtsiya. Tekstura dispersnykh i poristykh materialov* (Adsorption. Texture of disperse and porous materials). Novosibirsk: Nauka. Sib. predpriyatie RAN; 1999. 470 p. (in Russ.).
3. Greg S., Sing K. *Adsorbtsiya, udel'naya poverkhnost', poristost'* (Adsorption, specific surface, porosity). M.: Mir; 1984. 310 p. (in Russ.).
4. Archakova R.D., Uzhakhova L.Ya. *Pererabotka nefi v regione (na primere Respubliki Ingushetiya)* (Oil Refining in the Region (Case Study of the Republic of Ingushetia)). Monograph, Magas: 2019. 152 p. (in Russ.).
5. Temirkhanov B. A., Temerdashev Z. A., Shpigun O. A. Evaluation of some properties of sorbents in the elimination of oil pollution. *Zaschita okruzhayushchei sredy v neftegazovom komplekse = Environmental Protection in the Oil and Gas Complex*. 2005;2:16 (in Russ.).
6. Kamenshchikov F.A., Bogomolny E.I. *Neftyanye sorbenty* (Oil sorbents). Moscow – Izhevsk. 2005. 268 p. (in Russ.).
7. *Sbornik metodik i instrukivnykh materialov po opredeleniyu vrednykh veshchestv dlya kontrolya istochnikov zagryazneniya okruzhayushchei sredy. Chast' 5.* (A collection of methods and guidance materials for the determination of harmful substances for controlling sources of environmental pollution. Part 5). Krasnodar: 1996. 128 p. (in Russ.).

About the authors:

Rashid K. Kostoev, Student, Chemical and Biological Faculty, Ingush State University (7, I.B. Zyazikova pr., Magas, Republic of Ingushetia, 386001, Russia). E-mail: kostoevrasid62@gmail.com. <https://orcid.org/0000-0002-2618-6099>

Dzhabrail S. Tochiev, Post-Graduate Student, Department of Chemistry, Ingush State University (7, I.B. Zyazikova pr., Magas, Republic of Ingushetia, 386001, Russia). E-mail: d.tochiev@mail.ru. <https://orcid.org/0000-0002-3340-8008>

Eset I. Niklho, Post-Graduate Student, Department of Chemistry, Ingush State University (7, I.B. Zyazikova pr., Magas, Republic of Ingushetia, 386001, Russia). E-mail: a.niklho@mail.ru. <https://orcid.org/0000-0003-0281-6356>

Zakhirat Kh. Sultygova, Dr. of Sci. (Chemistry), Professor, Vice-rector, Ingush State University (7, I.B. Zyazikova pr., Magas, Republic of Ingushetia, 386001, Russia). E-mail: sul-za@yandex.ru. Scopus Author ID 6503995007, <https://orcid.org/0000-0002-8730-4554>

Raisa D. Archakova, Cand. of Sci. (Engineering), Associate Professor, Professor of the Department of Chemistry, Ingush State University (7, I.B. Zyazikova pr., Magas, Republic of Ingushetia, 386001, Russia). E-mail: r_archakova@mail.ru. <https://orcid.org/0000-0002-6975-3612>

Bagaudin A. Temirkhanov, Cand. of Sci. (Chemistry), Associate Professor, Department of Chemistry, Ingush State University, (7, I.B. Zyazikova pr., Magas, Republic of Ingushetia, 386001, Russia). E-mail: бага@inbox.ru. <https://orcid.org/0000-0001-6710-8081>

Leyla Ya. Uzhakhova, Associate Professor, Department of Chemistry, Ingush State University, (7, I.B. Zyazikova pr., Magas, Republic of Ingushetia, 386001, Russia). E-mail: lenau62@yandex.ru. <https://orcid.org/0000-0003-1396-6456>

Об авторах:

Костоев Рашид Керимсултанович, студент химико-биологического факультета Ингушского государственного университета, (Россия, 386001, Республика Ингушетия, г. Магас, пр-кт И.Б. Зязикова, 7). E-mail: kostoevrasid62@gmail.com. <https://orcid.org/0000-0002-2618-6099>

Точиев Джабраил Салангиреевич, аспирант кафедры химии Ингушского государственного университета (Россия, 386001, Республика Ингушетия, г. Магас, пр-кт И.Б. Зязикова, 7). E-mail: d.tochiev@mail.ru. <https://orcid.org/0000-0002-3340-8008>

СПИСОК ЛИТЕРАТУРЫ

1. Плаченев Т.Г., Колосенцев С.Д. *Порозиметрия*. Л.: Химия; 1988. 176 с.
2. Карнауков А.П. *Адсорбция. Текстура дисперсных и пористых материалов*. Новосибирск: Наука. Сиб. предприятие РАН; 1999. 470 с.
3. Грег С., Синг К. *Адсорбция, удельная поверхность, пористость*. М.: Мир; 1984. 310 с.
4. Арчакова Р.Д., Ужахова Л.Я. *Переработка нефти в регионе (на примере Республики Ингушетия)*. Монография, Магас: 2019. 152 с.
5. Темирханов Б. А., Темердашев З. А., Шпигун О.А. Оценка некоторых свойств сорбентов при ликвидации нефтяных загрязнений. *Защита окружающей среды в нефтегазовом комплексе*. 2005;2:16.
6. Каменщиков Ф.А., Богомольный Е.И. *Нефтяные сорбенты*. Москва – Ижевск; Регулярная и хаотическая динамика; 2005. 268 с.
7. Сборник методик и инструктивных материалов по определению вредных веществ для контроля источников загрязнения окружающей среды. Часть 5. Краснодар: Сев. Кавказ; 1996. 128 с.

Нилхо Эсет Исаевна, аспирант кафедры химии Ингушского государственного университета (Россия, 386001, Республика Ингушетия, г. Магас, пр-кт И.Б. Зязикова, 7). E-mail: a.nilkho@mail.ru. <https://orcid.org/0000-0003-0281-6356>

Султыгова Захират Хасановна, доктор химических наук, профессор, проректор по научной работе Ингушского государственного университета (Россия, 386001, Республика Ингушетия, г. Магас, пр-кт И.Б. Зязикова, 7). E-mail: sul-za@yandex.ru. Scopus Author ID 6503995007, <https://orcid.org/0000-0002-8730-4554>

Арчакова Раиса Джабраиловна, кандидат технических наук, доцент, профессор кафедры химии Ингушского государственного университета (Россия, 386001, Республика Ингушетия, г. Магас, пр-кт И.Б. Зязикова, 7). E-mail: r_archakova@mail.ru. <https://orcid.org/0000-0002-6975-3612>

Темирханов Багаудин Ахметович, кандидат химических наук, доцент кафедры химии Ингушского государственного университета (Россия, 386001, Республика Ингушетия, г. Магас, пр-кт И.Б. Зязикова, 7). E-mail: бага@inbox.ru. <https://orcid.org/0000-0001-6710-8081>

Ужахова Лейла Яхьяевна, доцент кафедры химии Ингушского государственного университета (Россия, 386001, Республика Ингушетия, г. Магас, пр-кт И.Б. Зязикова, 7). E-mail: lenau62@yandex.ru. <https://orcid.org/0000-0003-1396-6456>

Submitted: September 09, 2019; Reviewed: December 03, 2019; Accepted: February 18, 2020.

Translated from Russian into English by H. Moshkov

Edited for English language and spelling by Enago, an editing brand of Crimson Interactive Inc.

MIREA – Russian Technological University
78, Vernadskogo pr., Moscow, 119454, Russian Federation.
Publication date February 28, 2020.
Not for sale

МИРЭА – Российском технологическом университет
119454, РФ, Москва, пр-кт Вернадского, д. 78.
Дата опубликования 28 февраля 2020 г.
Не для продажи

www.finechem-mirea.ru

